Anchoring Behavior of Chiral Liquid Crystal at Polymer Surface: In Polymer Dispersed Chiral Liquid Crystal Films

A Thesis
Presented to
The Academic Faculty

By

Haixia Wu

In Partial Fulfillment
Of the Requirements for the Degree
Master of Polymer in the
School of Polymer, Textile, and Fiber Engineering

Georgia Institute of Technology
April 2004

Anchoring Behavior of Chiral Liquid Crystal at Polymer Surface:
In Polymer Dispersed Chiral Liquid Crystal Films

Approved by:

Dr. Mohan Srinivasarao, Advisor

Dr. Anselm Griffin

Dr. Jung O. Park

April 8. 2004

ACKNOWLEDGMENTS

First, I must thank Professor Srinivasarao for his guidance, patience and persistent dedication during the course of this research. His support and friendship made the completion of this research possible. I must also thank Dr. Anselm Griffin and Dr. Jung O. Park for serving on my reading committee as well as providing technical support.

Special thanks are extended to fellow graduate students Jian Zhou, Lulu Song, and Vivek Shama. Their camaraderie made this struggle an enjoyable journey and the author will forever be indebted. I would also like to thank all the graduate students who assisted in this research and the PTFE and staff for providing a variety of supports. Last but not least, financial support from National Science Foundation is gratefully acknowledged through the grant DMR-0096240.

Finally, a special word of thanks is bestowed to the author's family for their never ending encouragement and confidence.

TABLE OF CONTENTS

LIST OF TABLES

LIST OF FIGURES

LIST OF ACRONYMS

Polymer Dispersed Chiral Liquid Crystal	PDCLC
Liquid Crystal	LC
Nematic Liquid Crystal	NLC
Chiral Liquid Crystal	CLC
Polymer Dispersed Liquid Crystal	PDLC
Polarized Optical Microscope	POM
Laser Scanning Confocal Microscopy	LSCM
Twisted Nematic Liquid Crystal Display	TN-LCD
Polymer Stabilized Cholesteric Liquid Crystal	PSCLC
Solvent-Induced Phase Separation	SIPS
Thermally-Induced Phase Separation	TIPS
Polymerization-Induced Phase Separation	PIPS
1-Methyl Heptyl Acrylate	1-MHA
2-Methyl Heptyl Acrylate	2-MHA

SUMMARY

Chiral liquid crystals/polymer composites are now widely proposed for color display application using electrical switching between selectively reflective (planar texture) and transparent state (focal conic texture). PDCLC uses cholesteric LC instead of the nematic LC used in PDLC. Cholesterics have a helical structure. Since LC with negative dielectric anisotropy is used, the applied field forces the director of LC to be always perpendicular to the field, with the helical axis parallel to the field. This texture selectively reflects the specific wavelength associated with the helical pitch of the cholesteric. The color display made with this composite has several advantages: 1. no polarizer is required; 2. no color filter is required; 3. color is easily managed. However, the reported results show long transition times between the states, say a few hundred milli-seconds, a high operating electric field, and low reflection intensity. Thus several improvements are required to commercialize this type of color displays.

This study was an investigation on factors affecting the anchoring behavior of CLC at the polymer surface in PDCLC films, understanding of which is critical to the application of this material in color displays. These factors include the chemical structure of monomers, the diameter of individual cells controlled by UV intensity, the thickness of

individual cells as mediated by spacer size, temperature, and surface treatment. The polarized optical microscope (POM) with a hot stage is used to observe the texture of PDCLC films. The laser scanning confocal microscopy (LSCM) is used to investigate the morphology of PDCLC films. The micro-spectrophotometer is applied to measure the transmission intensity of PDCLC films. We obtain PDCLC films that can selectively reflect light with a specific wavelength with neither prealignment of substrates nor application of external field. The normalized transmission intensity of these films is a little bit larger than that of pure CLC. These two results can solve part of the above reported problems. It is found that the chemical structure of monomers is the most important factor that controls the anchoring behavior of CLC at the polymer surface in PDCLC films.

CHAPTER 1

INTRODUCTION

Background

In the past three decades, material scientists have been exploring novel materials for applications in various electro-optical control and display devices such as optical shutters, switchable privacy windows, and reflective color displays. Polymer dispersed liquid crystal (PDLC) is a class of materials, normally prepared via polymerization-induced phase separation (PIPS) of an initially homogeneous solution of liquid crystal (LC) and polymer precursor. The PDLC display works based on an electric field controlled scattering mode, which is different from the traditional liquid crystal display (LCD), i.e., twisted nematic (TN) devices, and has a number of advantages over the conventional TN display: it requires no polarizers, no alignment layers, and no stringent thickness control. Although it (PDLC film) has these advantages, one problem still exists for this new material. In the field-on state, the materials are transparent only for a light beam normally incident and become hazy for obliquely incident light [1].

This problem was solved with an introduction of other new material, polymer stabilized cholesteric liquid crystals (PSCLCs), which are different from PDLCs in two aspects. One, the concentration of polymer in PSCLC composite is less than 10wt%. Two, nematic liquid crystal is replaced by chiral liquid crystal and the pitch of chiral liquid crystal is adjusted to reflect light in the infrared region. The operating mechanism for

PSCLC displays is based on the transition from the planar texture (transparent state) to the focal conic texture (translucent state) or from the focal conic state (translucent) to the homeotropic state (transparent). The former corresponds to the reverse-mode display and the latter to the normal-mode. This material is haz-free and transparent when viewed from all angles.

Another reason for the widespread investigation of chiral liquid crystals (CLC) in LC/polymer composites is due to their brilliant color reflection in the visible region. This property is utilized in the development of the flat panel color displays. The fabrication process for PDCLCs is similar to that of PDLCs. But the operating mechanism is totally different. Chiral nematic liquid crystal with negative dielectric anisotropy is utilized in PDCLCs. In the voltage-off state, the director configuration causes weak scattering of white incident light. When a large voltage is applied, the chiral liquid crystal is aligned from the scattering texture (focal conic texture) to a planar texture, where Bragg diffraction occurs and nearly monochromatic, circularly polarized light is reflected. The applied voltage controls the reflectivity of the display and the intrinsic pitch of the encapsulated chiral liquid crystals controls the color. There are several advantages of this color display over the conventional one (twisted or supertwisted nematic cells with color filters or ferroelectric LC with color filters): (1) no polarizers required; (2) no color filters required; (3) easy fabrication process.

But there are still some disadvantages that result from the right- or left-handed helical nature of the planar state of a PDCLC. The reflection peak is theoretically limited to 50% at the Bragg wavelength. Dr. Kato's group stacked left- and right-handed twist display together to increase the overall reflectivity of the PDCLC display [2]. In practice,

the theoretical 50% reflectivity of PDCLCs is not achievable. They usually reflect in the 10~20% range. Thus the high drive voltage and poor brightness limit the development of this new color displays. For its further application in color displays, we need to solve those problems and the objective of this thesis is to gain fundamental understanding toward this goal.

Objective of this research

The main purpose of this research is to fabricate the PDCLC film, which can reflect brilliant colors in the visible region without the prealignment of the substrates and without the drive from external fields. This research work has two purposes: to develop PDCLC films reflecting brilliant color as pure CLC does and to investigate the factors affecting the anchoring behavior of CLC at a photopolymerized polymer surface. Specifically, commercially available chiral dopant and nematic liquid crystals were carefully chosen to formulate the CLCs reflecting different colors in the visible region of the electromagnetic spectrum. These CLCs are mixed with various acrylate and methacrylate monomers respectively to form the homogeneous solutions by choosing the appropriate concentration of CLCs and monomers, and temperature. The homogeneous solution is UV cured at various conditions to obtain PDCLC films with large enough cells. The anchoring behavior of CLC at the photopolymerized polymer surface is characterized using polarized light optical microscopy and microscopic-spectrophotometry. The factors influencing the anchoring behavior of CLC at the polymer surface include chemical structure of the monomers, effective diameter of individual cells controlled by UV curing intensity, thickness of individual cells mediated

by spacer size, and the ratio of the pitch of CLC to the thickness of individual cells. The effect of temperature and surface treatment on the anchoring behavior of CLC in PDCLC films is also investigated. The morphology of the PDCLC film is characterized using a laser scanning confocal microscope (LSCM).

CHAPTER 2

BACKGROUND AND LITERATURE REVIEW

2.1 History And Nomenclature Of Liquid Crystal

2.1.1 Historical Development Of Liquid Crystal

The liquid crystal phase was first discovered by an Austrian botanist named Friedrich Reinitzer in cholesteryl benzoate, a chiral nematic liquid crystal derived from cholesterol found in both plants and animals [1]. After its discovery many German scientists began their research work in this field. Ludwig Gattermann and A. Ritschke, German chemists, synthesized first nematic liquid crystal not based on a natural substance [1]. With these synthesized liquid crystals, a German physicist named Otto Lehmann, observed that a solid surface in contact with a liquid crystalline substance causes the liquid crystal to orient in a certain direction, i.e., the liquid crystal molecules have the preferred aligning direction on the surface of the contacting solid substrate [1]. This phenomenon in liquid crystal is referred to as anchoring behavior of LC, which was found to be of paramount importance when modern scientists began to investigate the filed of liquid crystal display. The first practical application is the Twist Nematic Liquid Crystal Display (TN-LCD), made up of two bounding plates (usually glass slides), each with a transparent conductive coating (such as indium tin oxide) that acts as an electrode;

spacers to control the cell gap precisely; two crossed polarizers; and the nematic liquid crystal material. Its operating mechanism is schematically shown in Figure 2.1.

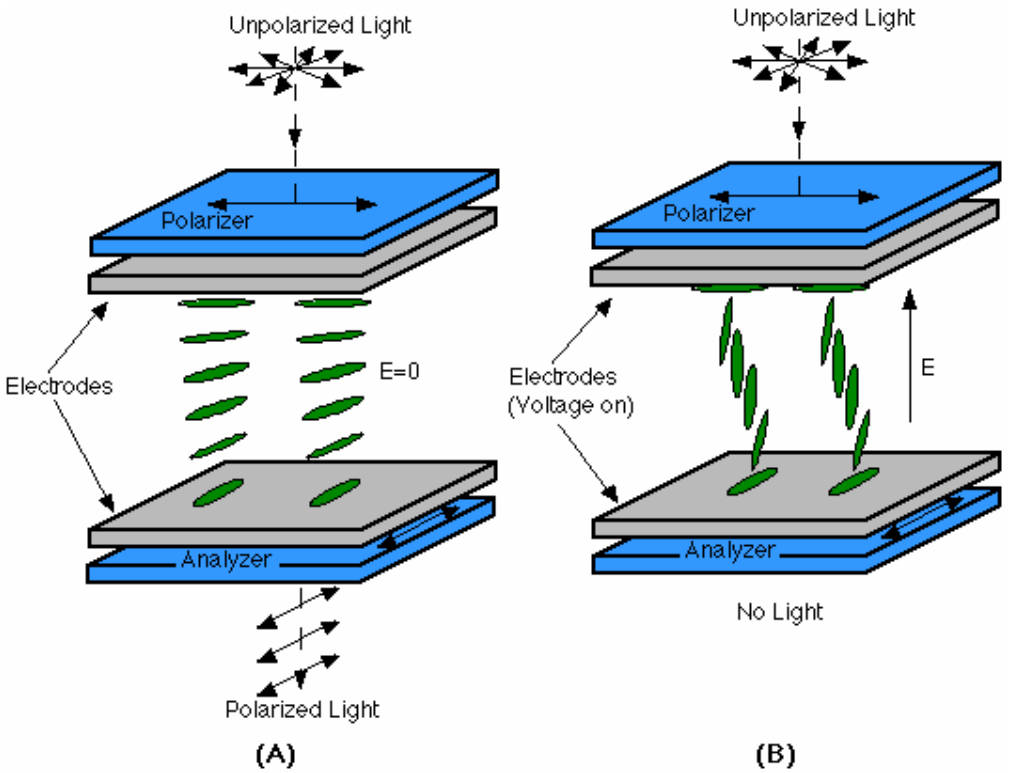

Figure 2.1. Twisted nematic device geometry. The polarizer and analyzer, which are arranged parallel to the director orientation at their adjacent glass plates, are oriented at 90° to each other. Refer to [3].

At the same time, another important contribution made was a complete theory of liquid crystals based on molecular structure. It became possible to identify what kinds of substances were likely to be liquid crystalline. In 1922, Georges Freidel described the different liquid crystal phases in his paper and proposed a classification scheme using the words nematic, smectic, and cholesteric [1]. He explained that the lines seen in liquid crystal phases under POM were defect structures, which represent drastic changes in the orientation direction of LC molecules. In addition, he made a great contribution to the

future development of liquid crystal displays that a liquid crystal could be oriented by an electric field. This effect of electric and magnetic fields on liquid crystals later became the subject of great attention.

In the period between 1922 and World War II scientists could explain why liquid crystals adopted various orientational configurations with new theoretical ideas, using the "continuum theory" [1]. Progress was made in understanding the light-scattering properties of liquid crystals that could explain for the first time why liquid crystals appear cloudy [1].

After World War II, there was a lack of interest in the research of liquid crystal. This situation began to change shortly before 1960. At this time a few individuals undertook a general reexamination of liquid crystals in the hope of learning more about their molecular structure, optical properties, and technical possibilities [4]. The combination of both basic scientific progress and new technological ideas caused an explosion in the number of researchers in the field. The area of LCD became one of the most exciting research fields. At least six different types of displays were developed, including some that used chiral nematic and smectic liquid crystals. A more recent development in LCD technology involves incorporating liquid crystal droplets in a solid polymer matrix (polymer dispersed liquid crystal or PDLC) or incorporating a polymer network in a bulk liquid crystal (polymer stabilized cholesteric liquid crystal or PSCLC). Both these schemes possess important advantages over conventional liquid crystal displays, such as TN-LCD, and are receiving considerable attention for commercial applications, primarily because these display elements do not require polarizers [1]. The review on these two research areas will be given later.

2.1.2 Nomenclature Used In liquid crystals

There are several different phases in liquid crystals, such as nematic, chiral, smectic A, and smectic C, etc. Here we mainly focus on the first two phases and introduce some nomenclature used to describe these two phases.

2.1.2.1 Nematic Liquid Crystal

The typical nematic liquid crystal molecule is composed of rigid rod-like and soft linear parts. This rigid part is necessary to make the interactions with the other molecules aniostropic and therefore favorable for the formation of liquid crystal phases. The soft part is responsible for the liquid-like appearance of LC. Molecules in liquid crystal possess some long-range orientational order, but no long-range positional order. The amount of orientational order is expressed as an order parameter, $S = \langle 3/2\cos^2\theta - 1/2 \rangle$, where θ is the angle between the molecular long axis and

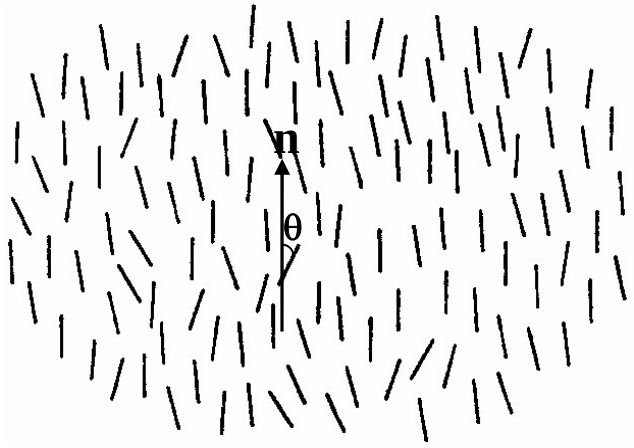

Figure 2.2. The director of nematic liquid crystal, **n,** is a unit vector in a direction where molecules are pointing in average. Refer to [5].

the nematic director **n** (Figure 2.2 [5]). It is very important to note that the parallel alignment in nematic liquid crystals is not connected with polar ordering, i.e., **n** and –**n**

are equivalent. This orientational order makes nematic liquid crytals possess anisotropic physical properties. The most obvious anisotropic property is their birefringence, $\Delta n = n_e - n_o$. The extraordinary refractive index, n_e, is effective for linearly polarized light with the plane parallel to the molecular axis and defined as $n_e^2 = \varepsilon_{||}$, which is the electric constant along the parallel direction to the optical axis. The ordinary refractive index, n_o is effective if the plane of polarization is perpendicular to the director and defined as $n_o^2 = \varepsilon_{\perp}$, which is electric constant along the perpendicular direction to the optical axis. A nonchiral nematic liquid crystal is optically uniaxial, and the optical axis is parallel to the director.

2.1.2.2 Chiral Liquid Crystal

Chiral (cholesteric) liquid crystal is chiral nematic liquid crystal. Locally it is very similar to a nematic liquid crystal: the elongated molecules are aligned, on an average, along the nematic director, **n**. However, chiral nematic liquid crystal has a helical structure: the director is uniformly twisted along an axis perpendicular to each molecule layer and this axis is defined as the helical axis of CLC. The distance along the helical axis for the director to rotate 2π is called the pitch, p, and the helical twist is defined as $q_0 = 2\pi/p$ (Figure 2.3) [6]. Chiral liquid crystal can be obtained by introducing chiral center or mixing nematic molecules with chiral dopants. When a chiral dopant is mixed with a nematic liquid crystal, the pitch of the mixture is related to the concentration of the chiral dopant. This relationship, given by De Gennes and Prost, is $1/P = (HTP)X_c$ [7], where HTP and X_c are the macroscopic helical twisting power and concentration of the chiral dopant, respectively. HTP is mainly a characteristic parameter of the chiral dopant and depends slightly on the nematic host [7].

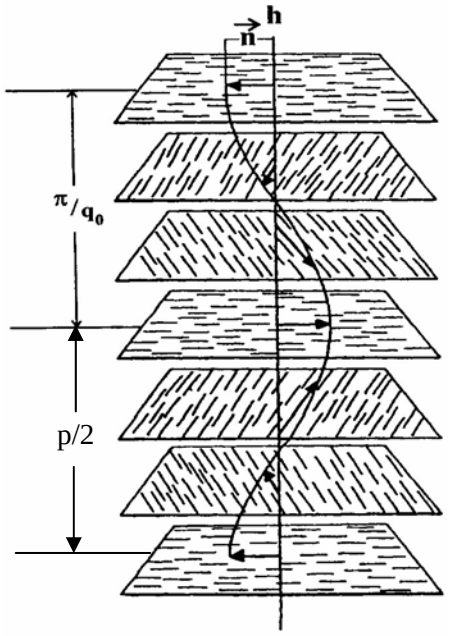

Figure 2.3. The helical structure of chiral liquid crystal, where **h** is helical axis, p is the pitch, **n** is the director, q_0 is the helical twist, and π/q_0 is the half pitch. Redrawn based on the reference [6].

The helical twisting structure makes chiral liquid crystals have many special optical properties. Two important optical properties of chiral liquid crystals that have been utilized in the LC displays are its reflective and scattering effects.

When a chiral liquid crystal (CLC) is sandwiched between two parallel plates, several types of electro-optic effects have been observed in CLCs, which depend on the surface treatment (boundary conditions), the helical pitch (p), the thickness-to-pitch ratio, the dielectric anisotropy ($\Delta\varepsilon$), and the frequency of the applied field.

At the zero-field with two parallelly prealigned substrates, the liquid crystal is in the planar state (also called planar texture or Grandjean texture), shown in Figure 2.4 (a), where the helical axis is perpendicular to the substrates. In this state, the refractive index of the material has a periodic structure along the direction normal to the surface of the

substrate and the maximum selective reflection occurs due to the first-order Bragg diffraction at a wavelength $\lambda = np$ (for normally incident light). The refractive index n is the average value between the ordinary and extraordinary indices and the wavelength λ corresponds to the center of the reflection peak. In reality, the Bragg reflection occurs in quite a large band of wavelengths defined by $pn_o < \lambda < pn_e$. The reflection peak width is determined by $\Delta\lambda = \Delta np$, where Δn is the birefringence of the material. If np is in the visible light region, the material reflects brilliant colored light. If np is in the infrared or ultra-violet regions, the cell is transparent for visible light.

When an electric field is applied normal to the plates, the director of chiral liquid crystal with positive dielectric constant ($\Delta\varepsilon>0$) tends to align along the field. A small field will switch the material into the fingerprint state or fingerprint texture, shown in Figure 2.4 (b), where the helical axis is parallel to the substrates. In practice, because of the anchoring effect of the surfaces of the cell, polydomains of fingerprint texture are formed, as shown in Figure 2.4 (c). The helical axes of the domains are more or less randomly oriented throughout the cell. This is called the focal-conic state and the material scatters because of the abrupt change of the refractive indices at the domain boundary [8]. When the applied field is above the threshold, calculated by De Gennes [7] as $E_c = 2\pi^2(\pi K_{22}/\Delta\varepsilon)^{1/2}/P$, where K_{22} is the twisting elastic constant of LC and P the unperturbed pitch, the liquid crystal switches into the homeotropic state, where the helical structure of the liquid crystal is untwisted with the director perpendicular to the plates, shown in Figure 2.4 (d), and the material becomes transparent.

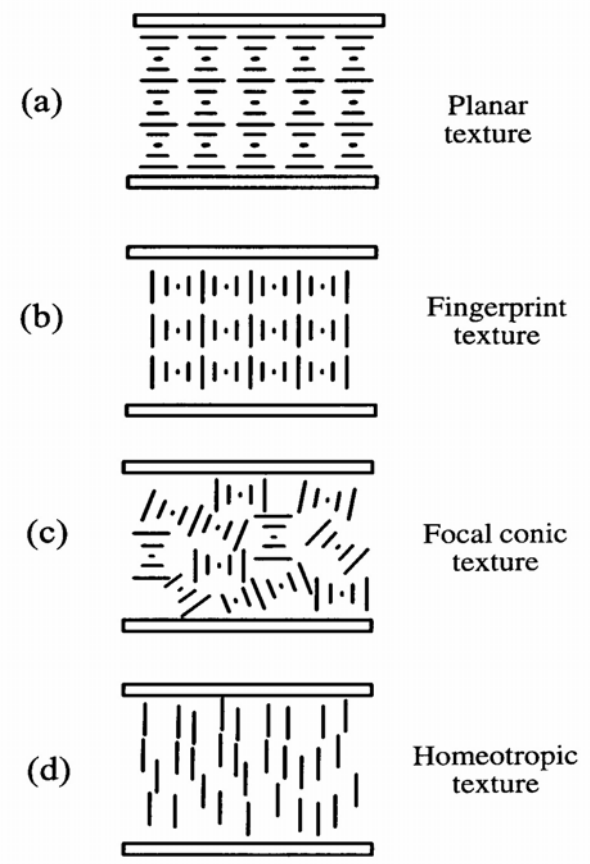

Figure 2.4. Different textures of a chiral liquid crystal sandwiched between two parallel substrates in the electric field. Refer to [8].

2.2 Anchoring Behavior Of LC At A Polymer Surface

Droplet configuration is a very important factor in developing the new display materials made of liquid crystal and polymer composites. There are a number of forces that interplay with each other to decide what kind of configuration will be adopted by the nematic director field within a droplet. The most important factors are the alignment properties of the liquid crystal at the polymer surface, the shape of the cavity containing the liquid crystal, the elastic constants of the bulk nematic, and the presence of external electric or magnetic field. Defect structures within the droplet can also be significant, as they may stabilize or destabilize a particular droplet configuration.

The most important factor in determining the droplet configuration is usually the preferred alignment of the nematic liquid crystal at the surface of the polymer binder. This anchoring energy is represented by the Rapini-Papolar free energy density [9], given by Equation (1)

$$F_{surface} = -g + \frac{1}{2}W_{\theta}\sin^2(\theta - \theta_0) + \frac{1}{2}W_{\varphi}\sin^2(\varphi - \varphi_0) \quad (1)$$

where θ_0 refers to the preferred zenithal (out of plane) angle of the director field at the cavity surface; the difference (θ - θ_0) reflects the deviation of the actual director field from this preferred angle; (φ - φ_0) represents the difference between the azimuthal (in plane) orientation of the director field and the preferred direction. The non-directional (isotropic) liquid crystal-interface interaction is given by g. The zenithal anchoring energy (W_θ), the azimuthal anchoring energy (W_φ), and g are proportional in magnitude to the order parameter S. Typically the anchoring energy which enforces this preferred alignment is quite strong compared to other elastic forces within the droplet. In the limit of strong anchoring, the nematic adopts a uniform tilt angle (either 0° or 90°) at all points on the droplet surface. In the case of weak anchoring, where the elastic free energy of the bulk nematic competes with the surface free energy of the droplet, the tilt angle of the nematic can vary spatially within the droplet in order to minimize curvature in the bulk of the droplet. Whether a system exhibits a strong or weak anchoring depends partly on the chemical nature of the polymer surface.

The balance of elastic forces within the droplet is the next most important factor in determining the director configuration. These elastic forces determine whether the structure within the droplet is simple or complex, the number and type of defect structures, etc. The elastic free energy density F [10], is given by Equation (2)

$$F_{elastic} = \frac{1}{2}[K_{11}(\nabla \bullet n)^2 + K_{22}(n \bullet \nabla \times n)^2 + K_{33}(n \times \nabla \times n)^2$$

$$- K_{24}\nabla \bullet (n \times \nabla \times n + n(\nabla \bullet n))] + \frac{3}{4}L(\nabla S)^2 \qquad (2)$$

where **n** is the director of liquid crystal; K_{11}, K_{22}, K_{33}, and K_{24} represent the splay, twist, bend, and saddle-splay elastic constants, respectively (Figure 2.5).

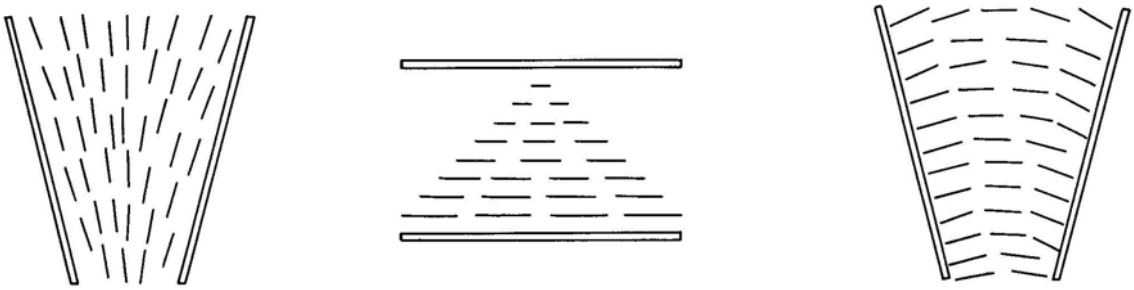

Figure 2.5 Basic types of deformation of LC. Refer to [11].

Several simplifications are applied for calculating this elastic free energy density. In supramicron droplets away from the nematic-isotropic clearing temperature, S is often treated as a constant ($\nabla S = 0$) and the last term in Equation (2) is neglected. K_{24} is often ignored in calculating director configuration. Equation (2) is simplified to Equation (3).

$$F_{elastic} = \frac{1}{2}[K_{11}(\nabla \bullet n)^2 + K_{22}(n \bullet \nabla \times n)^2 + K_{33}(n \times \nabla \times n)^2] \qquad (3)$$

However, in many cases the full form of Equation (3) is still too complex to be practical use – either because the relative values of the three elastic constants K_{ii} are unknown, or because the equilibrium equations derived from (3) are prohibitively difficult to solve. In such cases, K_{11}, K_{22}, and K_{33} are assumed to be the same [6]. With this simplification, Equation (2) becomes to Equation (4).

$$F_{elastic} = \frac{1}{2} K[(\nabla \bullet n)^2 + (\nabla \times n)^2] \quad (4)$$

The size of the droplet affects the droplet structure. The elastic (curvature) free energy scaling as curvature per unit length increases with decreasing droplet size. Curvature of the director field becomes more costly in energy in smaller droplets. The cavity shape can also be a critical factor in defining the nematic configuration in a droplet. Generally droplets are not spherical in the film formed by liquid crystals and polymer composites, but have some other irregular shape, such as cellular morphology. In these cases, the configuration adopted by the nematic droplet depends on the history of the local alignment as well as other forces like the electric or magnetic fields. External fields may simply influence the alignment direction of the nematic without changing the director configuration. But in some other cases, external fields can force the director configuration to change from one form to another.

The droplet configurations can be classified into two major cases. One is the parallel (or planar) anchoring, where the director within the droplet is parallel to the interface everywhere. The other is the homeotropic anchoring and the director here is perpendicular to the interface.

In the parallel case, the bipolar, concentric, and the twisted bipolar configurations are found for nematic droplets. For cholesteric droplets, the configuration depends on the ratio of the pitch of chiral liquid crystals and the droplet size. If this ratio is greater than 1, the star configuration can be observed. If it is much less than 1, a spiral shaped optical pattern with a radial disclination is observed [12]. According to the model given by Robinson and Ward [13], the optical pattern would look like a spiral or a series of concentric rings, depending on whether the radial disclination points out along the

direction of observation or in a plane perpendicular to it. The director field structures and the optical patterns of some configurations are shown in Figure 2.6.

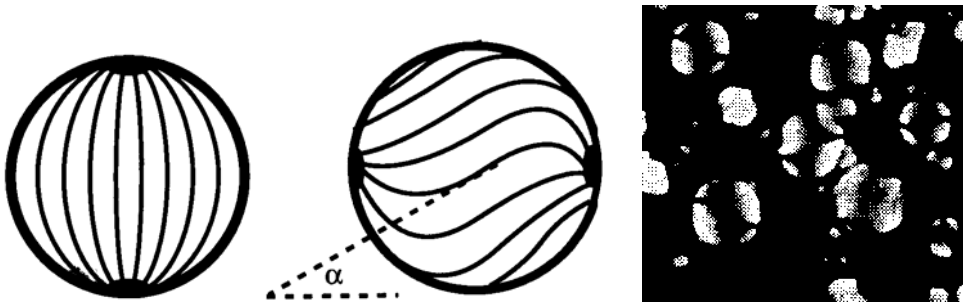

(a) (b) (c)

Figure 2.6. Schematic presentations of some configurations in parallel anchoring. (a) bipolar structure; (b) twist bipolar structure, α is the twisting angle of the director at the surface; (c) optical micrograph of bipolar droplets suspended in a polyvinyl alcohol film, viewed under crossed polarizers. Refer to [9].

In the perpendicular anchoring, the possible structures of nematic droplets are the radial, twisted radial, equatorial, and escaped radial (Figure 2.7). For cholesteric droplets, the director configurations also depend on the ratio of the pitch of the chiral liquid crystal and the droplet size. For cases the pitch is much smaller than the droplet size the fingerprint texture is formed. According to Lavrentovich and Kurik [14], the appearance of these droplets is similar to that seen in the parallel case. For larger layer spacings ($2\pi R/p < 5$, R is the droplet radius or the estimated radius for the irregular droplet, and p is the pitch), however, an equilateral line defect is observed and this line defect is similar to that observed in axial droplets. For very large pitch ($2\pi R/p < 1$), the line defect relaxes into a surface point defect. At infinite pitch (i. e., no twist) a radial droplet is observed.

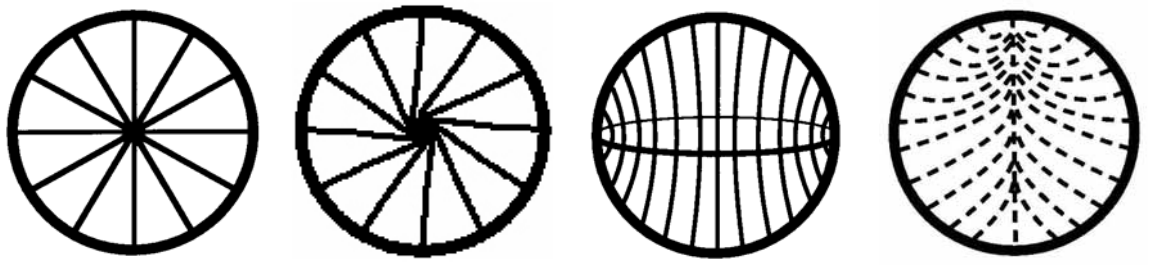

(a) (b) (c) (d)

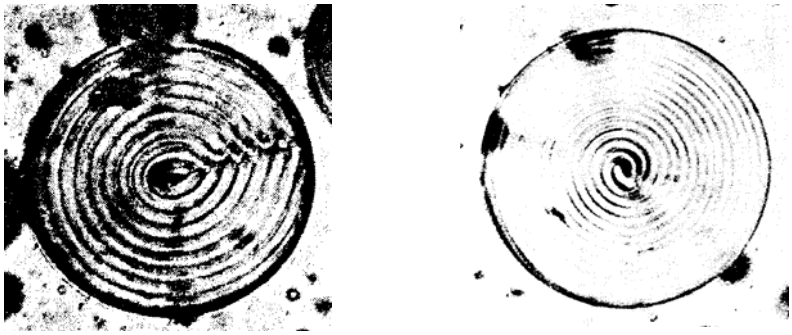

(e) (f)

Figure 2.7. Examples of some configurations in perpendicular wall alignment. (a) radial structure; (b) twist radial structure; (c) axial structure; (d) escaped radial structure (e) optical micrograph of the fingerprint texture with a spiral; (f) optical micrograph of the fingerprint texture with a series of concentric rings. Refer to [9].

These droplet configurations can transform from one to another under the influence of temperature, electric field, and magnetic field. For example, the temperature can drive transformation from the bipolar to radial structure, while the electric field drives from fingerprint texture to planar texture.

Dr. Srinivasarao's group has been doing research in the field of the dispersed liquid crystal materials, mainly on the anchoring behavior of nematic liquid crystal at a polymer interface. This PDLC material is formed by UV-curing the homogeneous mixture of nematic liquid crystal (TL205), monoacrylate, crosslinking agent (triacrylate), and photoinitiator. The cellular morphology in the PDLC films is formed to facilitate the investigation of the anchoring behavior of nematic liquid crystal [15]. It was found that

the concentration of both initiator and crosslinking agent, and the irradiance of UV beam are the most important curing parameters [16]. They focused on understanding the microscopic (and macroscopic) mechanism that is responsible for anchoring of nematic liquid crystal at the polyacrylates or polymethacrylate interfaces, and learning how to control the surface anchoring at the molecular level.

Several aspects involved in the research have been explored for the past 4 – 5 years [16]:

(1) Investigating the effect of the different chemical structures of polymers on the anchoring behavior of nematic LC at the interface, such as branching, copolymerization, and the difference between methacrylate and acryalte substituents. The position of methyl group in the side chain has the most striking effect on the anchoring transition temperature of the PDLC film when it is close to the backbone. The results are shown in Table 2.1. Poly(1-methylheptyl acrylate) (MHA) induces only planar anchoring within the experiment range (> –14 °C), while all other poly(MHAs) show homeotropic-to-planar anchoring transition at temperature between 71-78 °C. The experimental observations were explained based on an interfacial model. Van der Waal's interaction between the side chains of polyacrylates and the alkyl tails of LC molecules provides the enthalpic drive for homeotropoic anchoring at lower temperature. On the other hand, planar anchoring is driven by the entropy of the interfacial free energy, which is contributed by both the entropy-favored planar packing of the rod-like molecules on the surface and the order-disorder transition of the side chains at higher temperature. The two driving forces are competitive and reach a balance at T_t.

Table 2.1. Homeotropic-to-planar Anchoring transition temperature (T_t) of TL205 in PDLC

Acrylate side chain	Monomer structure	T_t (°C)
n-heptyl	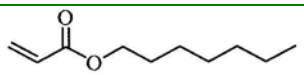	78
1-MHA	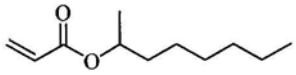	< -14
2-MHA	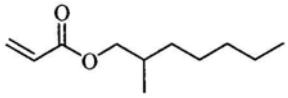	78
3-MHA	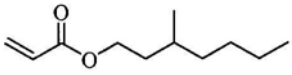	71
4-MHA	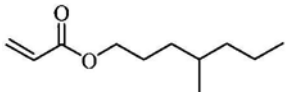	73
5-MHA	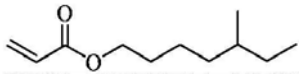	71

(2) Microscopic characterization of the Bloch walls, simulation of the Bloch walls, and estimation of anchoring energy (W_s). The Bloch wall can be created by quenching the film from the planar anchoring condition to the homeotropic anchoring condition. It was shown by the POM results that the homeotropic-to-planar anchoring transition actually initiates from the widening of the Bloch walls in the LC cell. It was shown that the anchoring energy could be estimated from the observation of the Bloch wall.

(3) Exploring the possibility of building novel LC-based devices by controlling the anchoring in PDLC materials. A LC-polymer composite system composed of a nematic fluid with negative dielectric anisotropy and a polymer network, and made by an in-situ photo polymerization, is proposed for potential application for flexible LC displays. The switching voltages, contrast ratio and response times of these composite films are

measured and the approaches to improve the contrast ratio and response times are discussed. The proposed LC display based on this system has advantages such as ease of manufacturing (rub-free, one-step photo polymerization), high contrast ratio, low switching voltages, fast switching, and compatible with flexible LC displays.

(4) Demonstrating a facile and operationally simple method to prepare electrically switchable diffraction gratings with periodic spatial alignment of LC. The method is based on polymerization-induced phase separation with the formation of a cellular structure, which affords control over the anchoring behavior of the encapsulated LC domains. The effects of electric field, polarization of the incident light, and temperature on the diffraction efficiency of the gratings are discussed. The advantages of the LC gratings are ease of manufacturing (rubbing-free, one-step photo polymerization), low switching voltages, and structure stability offered by polymer matrix. The method should also fit plastic substrates for making flexible devices.

2.3 LC Display

2.3.1 Display From PDLC

Polymer dispersed liquid crystal material has gained widespread attention from researchers and scientists for its scattering, reflective, and bistable display applications in recent twenty years. In 1985, James Fergason first developed a system in which a liquid crystal is dispersed in a waterborne polymer to form an emulsion [17]. The liquid crystal is encapsulated to form micrometer-size droplets. The emulsion is then sandwiched between two parallel plates. Another more popularly used system, polymer dispersed liquid crystal (PDLC) was invented by J. W. Doane's group at Kent State University in 1986 [18, 19]. This system is formed by dispersing liquid crystal in polymer matrix. In

fabrication of PDLC, a liquid crystal is mixed with a prepolymer, or a polymer or a mixture of polymer and solvent to form a homogeneous solution. Then the liquid crystal is phase separated from the polymer by one of the following several methods; solvent-induced phase separation (SIPS), thermally induced phase separation (TIPS), and polymerization-induced phase separation (PIPS).

The operating mechanism of PDLC display is described in Figure 2.7 [17]. The rigid polymer matrix permanently supports the liquid crystal droplets. The director inside a droplet is more or less along one direction (called the director of the droplet). When no field is applied, the droplet directors are randomly oriented throughout the sample. The droplets shown in Figure 2.8 are well-known bipolar configuration, which is the most common configuration in nematic liquid crystal and polymer systems. This randomly oriented droplet system scatters light because of the mismatch between the average refractive index of liquid crystal and the polymer matrix. When a field is applied, the droplet directors are aligned along the applied field for liquid crystal with positive dielectric anisotropy. If the ordinary refractive index (n_o) approximately matches that of the polymer (n_p), the material is optically homogeneous and the cell appears transparent.

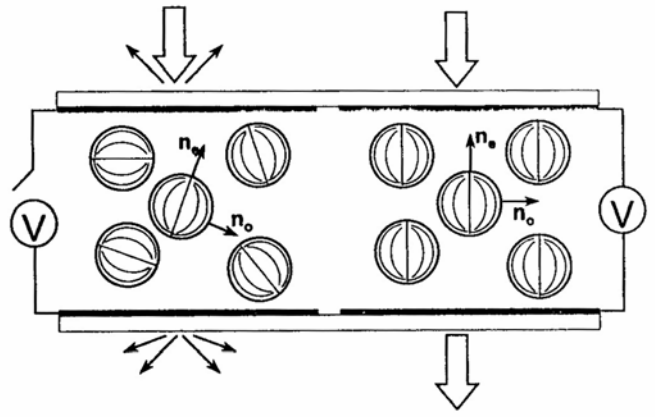

Figure 2.8. The schematic representation of the operating mechanism of PDLC display. n_e and n_o are extraordinary and ordinary refractive indices of nematic liquid crystal, respectively. Refer to [9].

The performance of PDLC devices greatly depends on electro-optic properties of PDLC film, which is determined by the final morphology of PDLC films. For phase-separation PDLC films, the morphology often shows a great dependence on the nature of polymerization chemistry, the concentration of liquid crystal, and the curing conditions, which include curing temperature, curing intensity, and curing time. In these studies using acrylate-based PIPS system, Noh et al. [20] noted several general trends.

(1). The starting mixture must show good solubility between the liquid crystal and polymer-forming components.

(2). A multifunctional acrylate can increase the rate of cure and phase separation in the system, which affects both the droplet size and the film morphology.

(3). Mixtures with good solubility between the liquid crystal and polymer, when cured at a slow polymerization rate, tend to give films with isolated droplets. On the other hand, low solubility between the polymerizing acrylate and liquid crystal with a fast curing rate, tends to produce a film with highly interconnected liquid crystalline domain.

Amundson et al. [21] investigated the relationship between the liquid crystal fraction and temperature during curing, on the morphology and electro-optic properties of a photopolymerized PDLC film made from the acrylate systems. It was found that there is a strikingly strong dependence of properties on the liquid crystal fraction, which was explained by consideration of phase separation process. In this process, the distance between the temperature-composition coordinate and the coexistence curve is an important parameter, and this parameter changes rapidly for small changes in liquid crystal fraction in the vicinity of the coexistence curve.

In order to make the photopolymerized PDLC films with excellent performance, there are several variations one can make in photo cured PDLC systems:

(1). Align the nematic liquid crystal during the cure process. Several examples have been reported in which aligning liquid crystal during the cure process imposes a preferential alignment direction on the liquid crystal in the PDLC film and this alignment persists even after the field is removed. Margerum et al. [22] demonstrated that the presence of an electric field perpendicular to the cell plates during cure results in partial alignment of the liquid crystal along the applied field direction. Magnetic field and surface treatment of the cell substrates can also play the same function.

(2). Replace the liquid crystal fluid within the cured PDLC film. Takatsu et al. [23] reported such a system. After cure, one substrate was removed, the liquid crystal was washed away with a solvent, and a new liquid crystal was imbibed into the film. The counterplate is replaced to form the final device. It is possible to place an alignment layer on the counterplate prior to lamination. In some cases, the presence of an alignment layer affected the properties of the PDLC device, indicating that the alignment force of the substrate propagated some distance into the liquid crystal/polymer composite. In principle, such a procedure allows a selective modification of the surface of the polymer without the usual change in polymer morphology that is seen when the ingredients in a phase separation PDLC are varied.

(3). Spatially varying PIPS structures can be formed by modulating the light intensity across the film during cure. For example, a mask can be used to expose different portions of a PDLC film to different curing intensities. Since these different portions of the film will require different voltages for orientation, the mask pattern can be made to appear or

disappear in the film by controlling the voltage across the sample. Another example of this strategy is to use the interference of laser beams to form sinusoidal intensity pattern in the film [24]. The formed film has the periodic pattern, i.e. the density of the liquid crystal droplets follows the intensity of the laser used to cure the film. Such films, often called holographic PDLC (HPDLC) films, act as an electrically controllable diffraction grating for light.

Although the modified PDLC displays have some advantages over the conventional TN-LCD, there are still some problems in PDLC displays. In a field-on situation, the display is transparent only for a light beam incident normally and becomes hazy for obliquely incident light [25]. Doane et al. [26] solved this problem by substituting a liquid crystal polymer for an isotropic polymer in PDLC, where the refractive indices, n_{p11} and $n_{p\perp}$, of the liquid crystal polymer match those of liquid crystal, respectively. In such a case, the liquid crystal polymer and the liquid crystal are all aligned along the applied field in the field-on condition. Then the refractive indices are matched for light incident at all angles and therefore the cell is transparent in all directions. Unfortunately, another problem arises for this system.

In order for the refractive indices of the liquid crystal polymer and the liquid crystal to be matched, the mesogenic moieties of the liquid crystal polymer must have a similar structure to that of the liquid crystal. Then obviously phase separation becomes difficult for such a system. In order to solve this problem, Yang's group [27] introduced a new method: dispersing a small amount of polymer in liquid crystal, less than 10wt%. This new system is called polymer-stabilized liquid crystal (PSLC) or polymer-modified liquid crystal (PMLC). The refractive index mismatch problem is eliminated due to the

low concentration of polymer. Particularly when the polymer is a mesogenic network, the scattering caused by the refractive index mismatch between the liquid crystal and the polymer network is very small and negligible. For this system the mixture of the liquid crystal and the monomer is usually in a liquid crystal phase because of the low concentration of the monomer. When the monomer is being polymerized, a surface alignment layer or external field can be used to control the orientation of the liquid crystal, and consequently the direction of the polymer network. In this way the polymer formed is anisotropic and has an aligning effect on the liquid crystal. After polymerization, the polymer network can be used in turn to control the orientation of the liquid crystal. Later, the electro-optic performance of this composite has been investigating by many other researchers. They try to understand the effects of curing temperature and other UV-curing conditions on the properties of these special composites [28 - 32].

2.3.2 Display From PDCLC

The chiral liquid crystal is the most promising in the display industry and has received the most attention [33 - 35]. Yang's group [36, 37] was the first to utilize polymer dispersed cholesteric liquid crystal (PDCLC) materials to make color displays. In this work, the PDCLC film was made from the mixture of ZLI-2806, which has negative dielectric anisotropy, CE2, chiral dopant with a short pitch, and thermosetting plastic polyvinyl butyral (PVB) by the temperature induced phase separation. The operating mechanism for this display is depicted in Figure 2.9. In the field-off state, the configuration of the liquid crystal in the droplet is determined by the polymer-liquid crystal boundary conditions. The resulting director configuration causes incident light to

be weakly scattered. Consequently, white light incident on the cell is randomly scattered. When a field is applied, the helical axes are aligned perpendicular to the substrate if the dielectric anisotropy of the chiral liquid crystal is negative, and the planar texture is obtained. At this state, selective reflection occurs according to the Bragg diffraction law (discussed in chiral liquid crystal above) as in bulk. Upon the removal of the field, the planar texture relaxes back to the state with the helical axes randomly oriented.

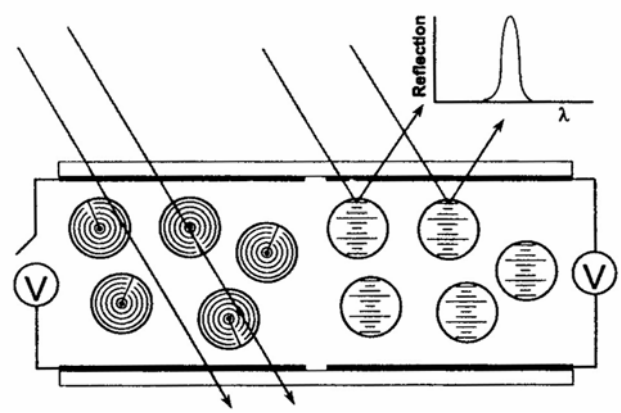

Figure 2.9. The schematic representation of the operating mechanism of PDCLC display. The peak in the small insert graph is where the Bragg reflection occurs. Refer to [36].

But there is some problem in PDCLC films made by TIPS. The miscibilities of liquid crystal with negative dielectric anisotropies in various polymers have been found to be quite different from those with positive dielectric anisotropies [38 - 42]. For this reason, many of the polymers, such as poly(methyl methacrylate), used for nematic PDLC displays (where dielectric anisotropy is positive), do not work for PDCLCs. While success has been achieved with PVB, the lack of suitable polymers for the TIPS process has motivated a search for other techniques.

Kitzerow's group [43 - 45] successfully made the PDCLC display by utilizing polymerization induced phase separation process with materials of UV-curable polymer adhesive NOA-65 (Norland), several commercial nematic liquid crystals with negative dielectric anisotropies (EN18, EN38, ZLI-2585, and ZLI-4788-000), and the chiral dopant (S811). They obtained good results with EN18 and ZLI-4788-000. They found that large droplet sizes (obtained by low UV intensities and long curing times) lead to high contrast and low threshold voltages, whereas small droplet sizes are required for fast switching.

Compared with TIPS-prepared PDCLC films [36], these PIPS-prepared PDCLC films have several advantages: they are easier to prepare, are operable at room temperature, and have fast switching time. Times constants (switching time) down to a few ms are found. This is a great improvement over the minimum values of about 0.1 s which have been found for cholesteric droplets in TIPS-prepared thermoplastic polymer films

It is well known that the color of the selectively reflected light can be controlled by adjusting the concentration of the chiral dopant. Kitzerow and Crook [46] adjusted the chiral concentrations to tune the peak wavelength of PDCLCs for the red, green, and blue primary colors of a full-color display. Kato and coworkers [2, 48, and 49] achieved full-color by integrating red, green, and blue stacked devices. In this work electric-field-assisted thermal process is used to form a color image. The originally fabricated PDCLC is almost transparent due to the refraction index match of the liquid crystal and polymer. The state of the PDCLC film is determined by whether or not an electric field is applied during the cooling process. Figure 2.10 schematically shows such a process for PDCLCs.

After heating, an electric field applied during cooling makes the PDCLC selectively reflective, and the absence of the field allows recovery of the transparent state. The selectively reflective state can be changed back to the original transparent state by reheating and recooling without the field. This change of states is repeatable. The transparent state can also be converted to reflective state, but much higher electric field is required. Therefore, a low electric field, which does not change the state of the PDCLC unless heating is used, can be used for the electric-field-assisted thermal process. Figure 2.11 shows the color image made in this way.

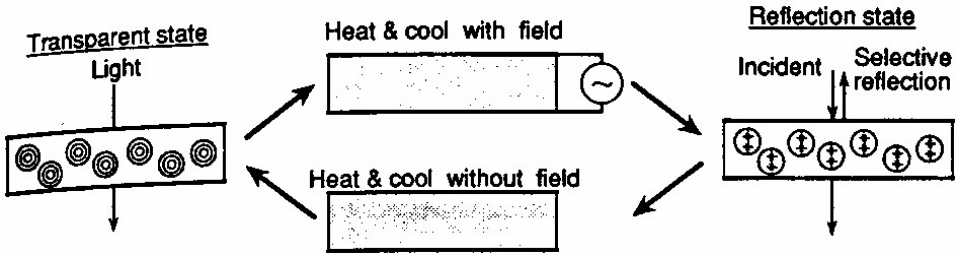

Figure 2.10. Schematic of electric-field-assisted thermal process for PDCLCs. Refer to [48].

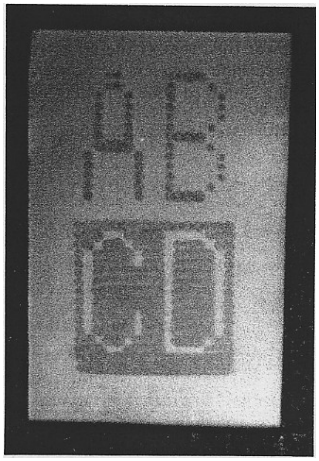

Figure 2.11. Color image on a stack consisting of two PDCLC films with different chiralities. Refer to [2].

Because of the right- or left- handed helical nature of the planar state of a PDCLC, the reflection peak is theoretically limited to 50% at the Bragg wavelength. The simplest explanation of this phenomenon has been proposed by De Gennes. If the incident wave is analyzed into two components of opposite circular polarizations, only one component is strongly reflected – i.e. the component for which the instantaneous electric pattern is identical in shape to the cholesteric helix of CLC. The other component is transmitted without any significant reflection through the sample. This explanation is well displayed in Figure 2.12.

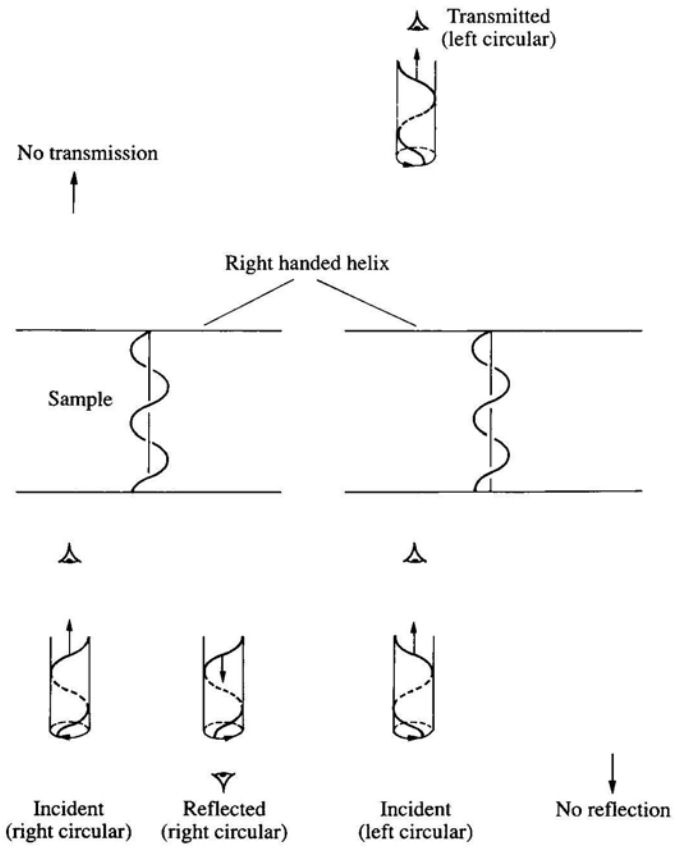

Figure 2.12. Bragg reflection and transmission by CLC sample in the planar texture. The cylinders with S represent 'snapshots' of the electric field **E** associated with one wave. The vertical arrows give the direction of propagation. The circles C show the rotation of **E** as seen by an observer at one fixed point in space. The reflected wave emitted by the sample is an image of the cholesteric helix, translated downwards. Examination of the corresponding projected path C shows that it is right circular. Refer to [7].

In practice, the reflectivity is often much less, usually just 10~20%. In addition to this, there is another problem. These PDCLC materials do have high drive voltages (~ 50 V) [37]. Thus poor brightness and a high drive voltage limit the usefulness of this type color display. For further development of the application of chiral liquid crystals in color display, these two limitations have to be solved, which is the motivation of our research work.

Yang et. al. [26] developed another new system with chiral liquid crystal and polymer composites that could effectively scatter white incident light. The concentration of polymer is very small (~2 wt%) and the pitch of the chiral liquid crystal is selected such that the cholesteric liquid crystal material reflects light in the infrared region. This type of chiral technology is optically reminiscent of the conventional PDLC, except it can be tailored to operate in the reverse and normal mode, and is essentially haze-free. In the reverse mode display, the glass substrates are treated with polyimide and rubbed and assembled in a uniform homogeneous configuration. The chiral liquid crystal is doped with a low reactive monomer (~1-2 wt%) and assumes a planar configuration with helical axis normal to the substrates. The display is irradiated with UV light and the network polymerizes within the planar configuration. After the polymerization, the planar texture remains stable. As shown in Figure 2.13, in the off state, the cell appears totally transparent to visible light because the pitch is adjusted in the IR region.

When an electric field is applied across the cell, the planar texture transforms into the focal conic texture, and the material is opaque for all polarizations of the incident light. Upon the removal of the field, the focal conic texture relaxes back to the planar texture. The function of the polymer in the reverse mode is to create focal conic domains

that scatter light and force the chiral liquid crystal to return to the planar state after the field is removed. In the normal mode no surface treatment is required. However the polymerization is carried out with an *in situ* electric field enforcing chiral nematic to unwind and align homeotropically. When the field is removed after photo-polymerization, the liquid crystal is influenced by the aligned polymer to stay locally aligned along the polymer network and perpendicular to the surface, while in other areas it relaxes back to the helical structure. A focal conic structure is formed as a result of the competition between intrinsic chirality of the liquid crystal and the frustrating effect of the polymer. The normal mode is illustrated in Figure 2.14. In the field-off state, the material is strongly scattering for all polarizations of incident light and the cell takes on an opaque appearance. When an electric field is applied, the focal conic state transforms into the homeotropic state and the display is transparent. The underlying function of the polymer in the normal mode display is to create poly-domain focal conic texture and control the domain size.

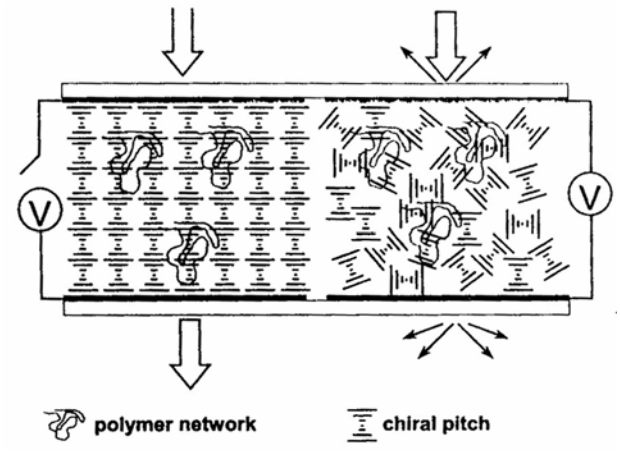

Figure 2.13. A schematic illustration of a reverse-mode polymer-stabilized cholesteric display. The display scatters white light in the voltage-on state (right) and is transparent in the off state (left). Refer to [6].

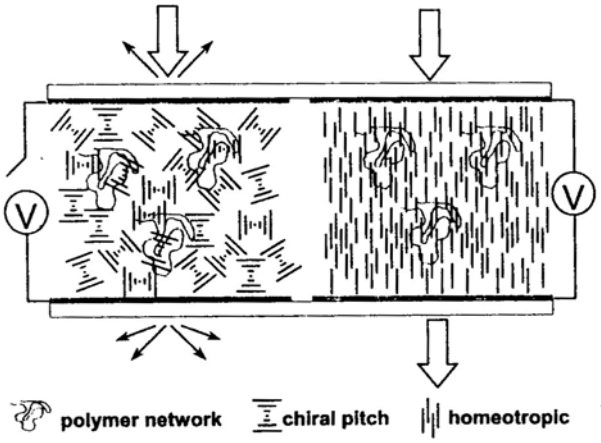

Figure 2.14. A schematic illustration of a normal-mode polymer-stabilized cholesteric display. In the zero-voltage state the display scatters light (left), while in the homeortopic texture the display is transparent. Refer to [6].

CHAPTER 3

EXPERIMENT DETAILS

PDCLC films were made by photo polymerization-induced phase separation using UV-curable polymer precursor and chiral nematic liquid crystal. Several factors, i.e. UV intensity, concentration of chiral nematic liquid crystal, pitch of chiral nematic liquid crystal, chemical structure of monomers, and the size of the spacer, were adjusted to obtain the film which can reflect brilliant color. The effects on the anchoring behavior of CLC at a polymer surface in PDCLC films, including the chemical structure of the polymer precursor, the approximate diameter of individual cells in PDCLC films, the thickness of individual cells in PDCLC films, the ratio of the diameter of individual cells to the pitch of CLC, temperature, and surface prealignment were investigated with POM and the micro-spectrophotometer. The three dimensional structure of the PDCLC film doped with dye was imaged by the laser scanning confocal microscopy (LSCM).

3.1 Preparation Of PDCLC

3.1.1 The Procedures Of Preparing The Sample To Be Cured

The empty glass cell was first prepared in the following way. A tiny droplet of methanol solution of spacers (listed in Table 3.2) was put on the center of a glass slide and was covered by a cover glass. Norland optical adhesive (Nov 68) was applied to seal the two edges of the glass slide. The sealed glass slide was put under the mercury lamp

with high intensity (around 0.5 mW/cm^2) to solidify Nov 68. After methanol evaporated, a glass cell with the fixed thickness was ready to use. A tiny droplet of homogeneous solution containing chiral nematic liquid crystal, alkyl acrylates or methacrylate, crosslinking agent, and photoinitiator (~ 0.2 wt%) was put at one unsealed edge of this glass cell by a pipette and it automatically flowed into the glass cell due to capillary effect. After the droplet completely filled the glass cell, the two unsealed edges were sealed by Teflon tap. The schematic of the process for the sample preparation is shown in Figure 3.1. This sample was ready to be irradiated by the mercury lamp.

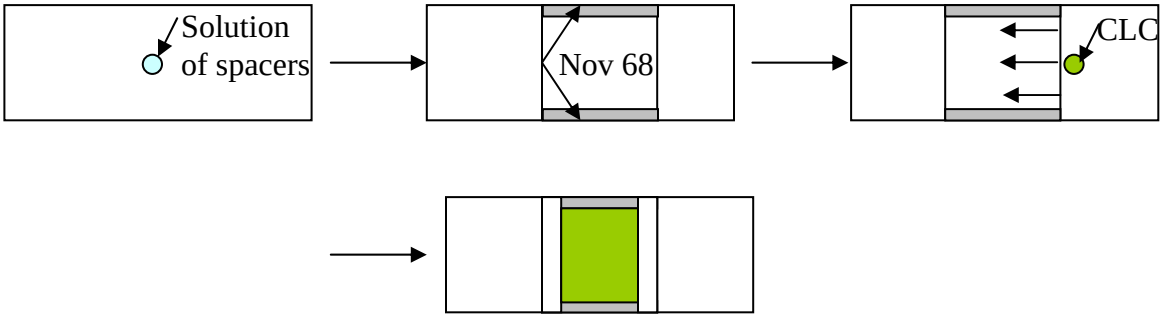

Figure 3.1. The schematic process of the POM sample preparation

3.1.2 Materials

3.1.2.1 CLC

Chiral liquid crystals with different pitches were obtained from the mixture of nematic liquid crystal (TL213) and chiral dopant (CB15). TL213 (EM Chemicals) with positive dielectric anisotropy is a mixture of halogenated bi- and terphenyls with aliphatic tails of two to five carbons, averaging between three and four carbons. Its general physical properties are listed in Table 3.1 [50]. It was chosen because it permits the nematic phase in the broad temperature range. CB15 (EM Chemicals) is a pure chiral

compound. The pitch length p of the resulting cholesteric liquid crystal is adjusted by varying the concentration of CB15.

Table 3.1. General physical properties of nematic liquid crystal TL213

Clearing point (°C)		88
Flow viscosity at 20 °C		49 mm^2s^{-1}
Dielectric anisotropy (20 °C, 1 KHz)	$\Delta\varepsilon$	+ 5.7
	ε_{11}	10.0
	$\varepsilon_{\perp}$	4.3
Optical anisotropy (20 °C, 589 nm)	Birefringence Δn	0.2388
	Extraordinary refractive index n_e	1.7659
	Ordinary refractive index n_o	1.5271
	Average refractive index n	1.6465
Elastic constants (20 °C)	Elastic constant for splay deformation K_{11}	16.8 pN
	Elastic constant for bend K_{33}	22.0 pN
	K_{33}/K_{11}	1.31

3.1.2.2 UV Curable Matrix And Other Additives

The polymer matrix of PDCLC films was made from various acrylate monomers or methacrylate monomers, crosslinking agent, and photoinitiator. In the experiment, sixteen commercial acrylate monomers and methacrylate monomers were used to investigate the effect of chemical structure of monomers on the anchoring behavior of CLC at a polymer interface. In order to observe the morphology of PDCLC films and

investigate the anchoring behavior of CLC at a polymer interface, Pyromethene 546 dye was added into the homogeneous mixture. Chemical structures of these materials are listed in Table 3.2.

Table 3.2 UV curing materials

Materials	Name	Chemical Structure	Sources
Monomer	1-methylheptyl acrylate	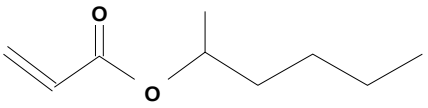	Sigma-Aldrich
	2-methylheptyl acrylate	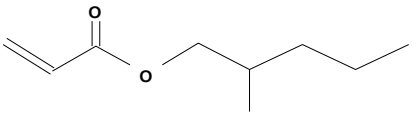	Sigma-Aldrich
	Isobornyl acrylate	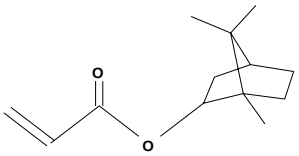	Sigma-Aldrich
	Isobutyl acrylate	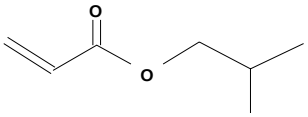	Sigma-Aldrich
	n-butyl acrylate	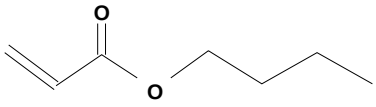	Sigma-Aldrich
	n-hexyl acrylate	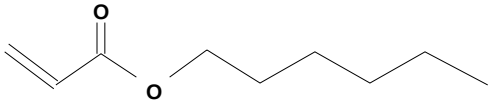	Sigma-Aldrich
	Isooctyl acrylate	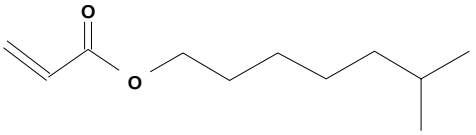	Sigma-Aldrich
	n-decyl acrylate	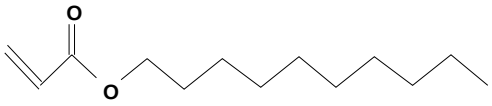	Sigma-Aldrich

Table 3.2 UV curing materials (Continued)

	n-lauryl acrylate	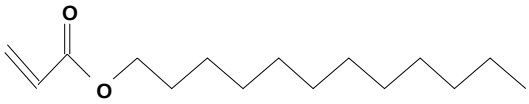	Sigma-Aldrich
	Isobutyl methacrylate	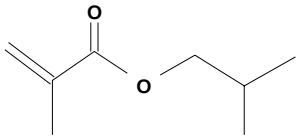	Sigma-Aldrich
	n-butyl methacrylate	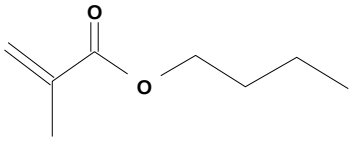	Sigma-Aldrich
	n-hexyl methacrylate	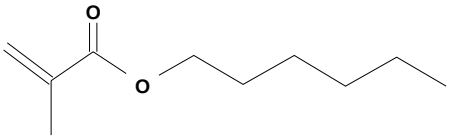	Sigma-Aldrich
	n-octyl methacrylate	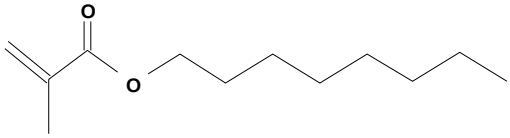	Sigma-Aldrich
	n-decyl methacrylate	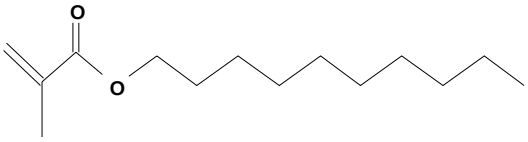	Sigma-Aldrich
	2-ethylhexyl methacrylate	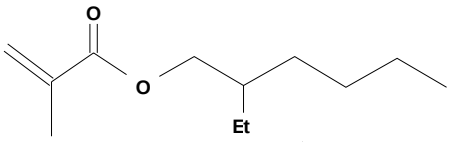	Sigma-Aldrich
	isobornyl methacrylate	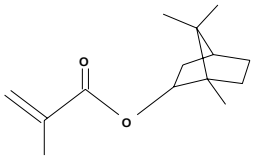	Sigma-Aldrich
Crosslink agent	Trimethylolpropane triacrylate	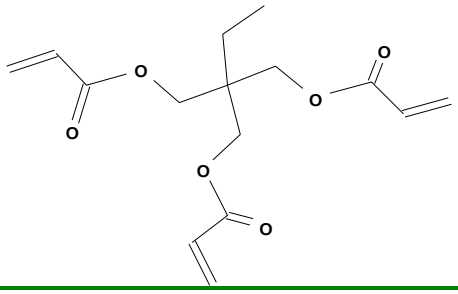	Sigma-Aldrich

Table 3.2 UV curing materials (Continued)

Photo initiator	Darocur 1173 (2-hydroxy-2methyl-1-phenyl-1-propanone)	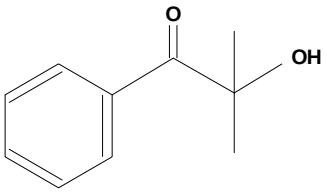	Ciba
Dye	Pyrromethene 546	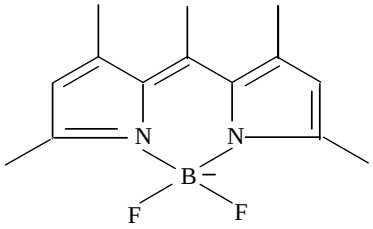	Exciton
Spacers	Borosilicate glass	-	Duke

3.1.3 Equipment And Process

3.1.3.1 UV Curing Process

The glass cells containing reaction mixtures were irradiated by the mercury lamp (DRIEL 66902). The power provided by this mercury lamp ranges from 50 W to 200 W. Films were made by a two-step photo polymerization, a slow polymerization process induced by a UV irradiation with low intensity for several hours, followed by curing at higher intensity (~ 0.5 mW/ cm^2) for about 10 min [15]. The output (listed in Table 3.3) of the mercury lamp was measured by using a radiometer under the UV exposure lamp in each experiment. The measurement wavelength was set at 365 nm in the radiometer. The diameter of the detector is 1.1 cm. The UV curing intensity used in the experiment was calculated as following:

UV curing intensity ($\mu W / cm^2$) = measured output of mercury lamp (μW) / the surface area of the detector (cm^2)

e. g. UV Intensity = 40 μW / ($\pi \cdot 0.055^2$) = 42 ($\mu W / cm^2$)

Table 3.3 The measured output of the mercury lamp and the calculated intensity

Measured output of the mercury lamp (μW)	Calculated UV intensity (μW / cm^2)
40	42
70	74
130	137

Four factors were adjusted to obtain films that can reflect brilliant color, varying one, while keeping others fixed. The UV curing intensities are listed in Table 3.3. The variation of other factors in UV curing process is summarized in Table 3.4.

Table 3.4. The variations of the curing conditions

Curing intensity (μW/cm^2)	Concentration of CLC (wt%)	Weight ratio of CB15 and TL213	Size of spacer (μm)
42	80	30 / 70	3
74	85	35 / 65	5
137	90	40 / 60	10
-	95	45 / 55	15
-	-	50 / 50	-

3.1.3.2 Surface Treatment

In order to compare the normalized transmission intensity of PDCLC films without surface treatment with that of films with surface treatment, two glass substrates were coated with polyimide by using the desktop spinner. The coating solution is the mixure of PI2556 (HD MicroSystems) and the reducer T-9039 (HD MicroSystems) with the weight ratio of 4:1. The thickness of the coated polyimide film measured with DEKTAK ST surface profiler (Floan Technology) is related with the rotating speed of the spinner (Figure 3.2). According to this relationship, we chose the speed to be 6900 rpm to obtain the film with the thickness of 0.1 μm. The coated substrates were rubbed in the antiparallel direction to form a planar texture that reflects colored light.

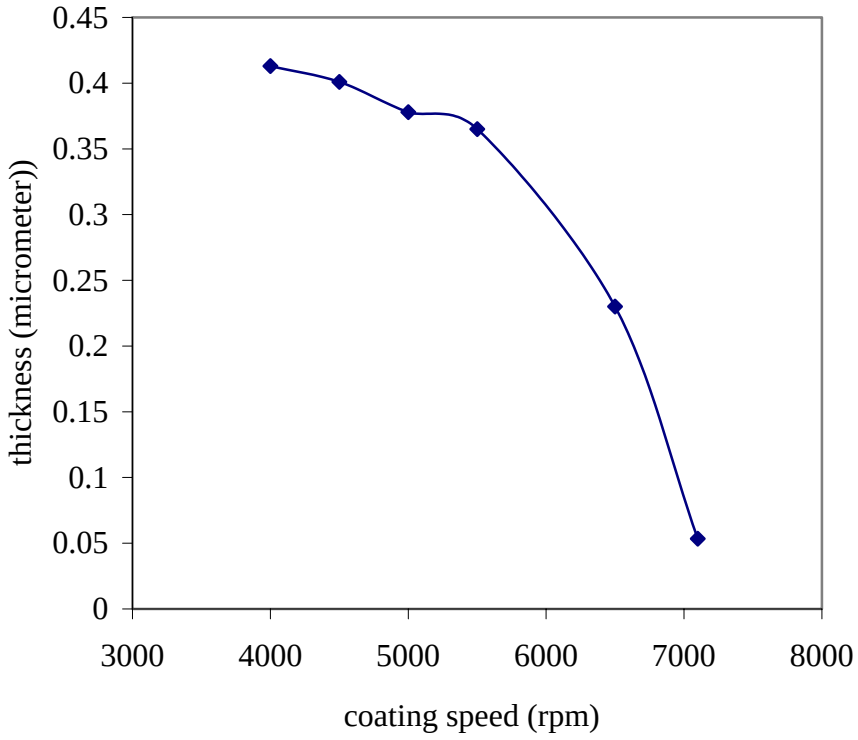

Figure 3.2. The relationship of the coating film thickness and the coating speed

3.2 Characterization Of CLC And PDCLC

3.2.1 Pitch Measurement

The maximum wavelength of the selective reflection for different chiral nematic liquid crystals was measured by the micro-spectrophotometer (SEE 1000). The pitch length, p, was calculated according the Bragg law, $\lambda = np$, where n is the average refractive index of TL213, which is listed in Table 3.1. With this instrument, we can verify whether the anchoring behavior of CLC at a polymer surface is planar or not.

3.2.2 Texture Observation Under Polarized Optical Microscopy (POM)

PDCLC films and CLC samples were observed with POM (LEICA DMRX) in the transmission mode. The nonpolarized light from the lamp house is polarized by the polarizer. When the polarized light passes through the anisotropic sample, the polarized direction of exiting light from the sample will be changed due to the interaction between the electric fields of the polarized light and the anisotropic sample. The analyzer only lets some part of this coming light pass through. If the polarizer and the analyzer are perpendicular with each other, the observed texture of the sample will be different with different orientation direction of the optical axis of an anisotropic sample. Therefore, from the observed texture, we can get the anchoring behavior of CLC at a polymer surface in PDCLC films. The scheme of POM was shown in Figure 3.3.

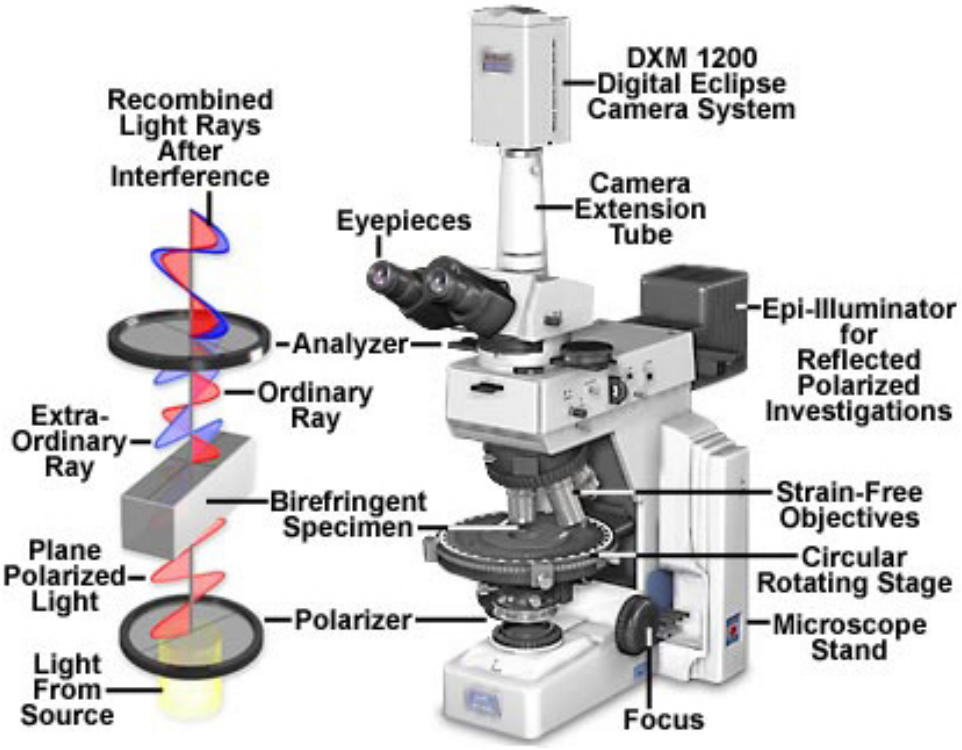

Figure 3.3. The scheme of polarized optical microscopy. Refer to [51].

3.2.3 Laser Scanning Confocal Microscopy (LSCM)

The PDCLC films were observed by LSCM (LEICA DMRXE). The schema of LSCM principle was shown in Figure 3.4. A laser ($\lambda \sim 488$ nm) spot, focused in a defined image plane, was used to excite fluorescence. This spot is scanned in lines accross the field of view resembling image formation by an electron beam in a TV-screen. The fluorescence is detected by a photomultiplier with high sensitivity. Out-of-focus-light is excluded by the pinhole and the intensity of the laser beam decreases with the third potency above and below the focal plane. Thus the observation of thin optical secitons in thick, intact specimens is obtained.

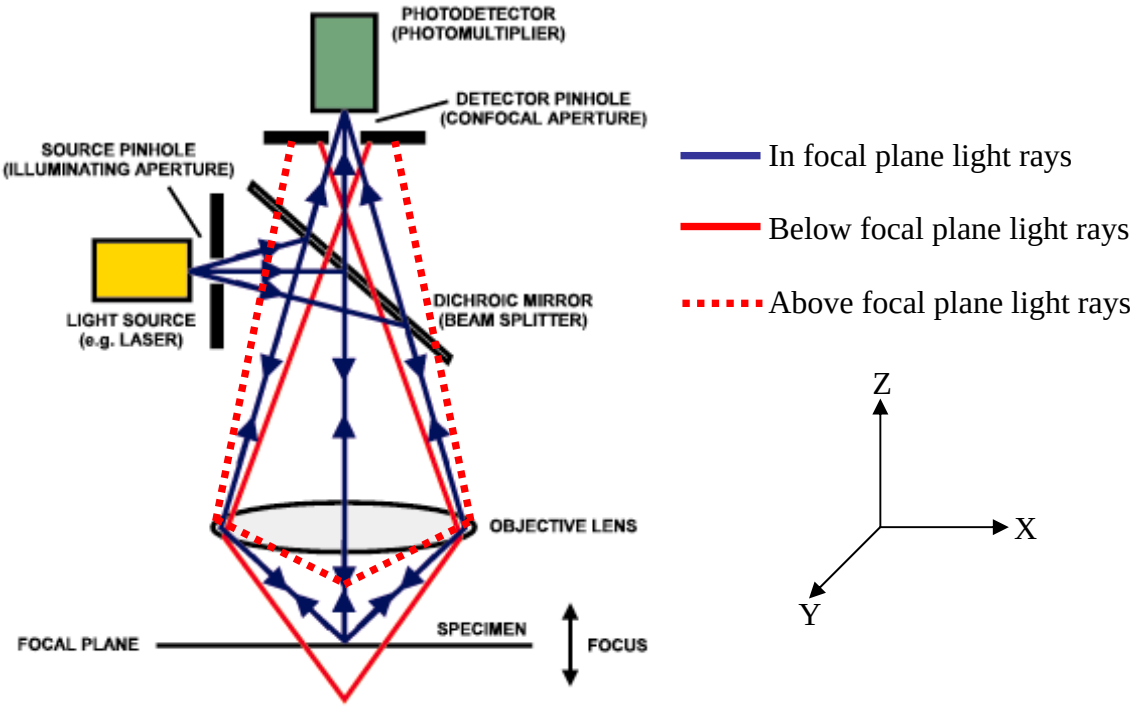

Figure 3.4. The schema of the principle of LSCM. Redrawn based on the reference [52].

CHAPTER 4

RESULTS AND DISCUSSIONS

4.1 Analysis Of Properties Of Pure CLC

The director structure of chiral liquid crystals is very complex and difficult to study due to its rotation along the optical direction of the system, called helical axis of CLC. But this director structure of CLC is important for its application in the display field. Normally this is determined by the balance two important factors, elastic energy and anchoring energy. Before using CLC to fabricate PDCLC films, we should first know what the properties of CLC are, for example, its chirality, its pitch, and its POM texture.

4.1.1 Properties Of CLC Investigated With POM

In the experiment, five CLC samples with different weight ratio of CB15 and TL213, i.e. 30/70, 35/65, 40/60, 45/55, and 50/50, were prepared. When CLC sample was sandwiched between two glass-slides as described in the experimental part, the planar texture (or Grandjen texture), where the helical axis is perpendicular to the substrate, was observed under POM for each prepared sample. In Figure 4.1, the uniform area was separated by several edges, which is a network of disclinations. These disclinations are called oily streaks and may be caused by inhomogenieties in dispersing spacers used to

control the distance of the bound glass slide and the glass cover. The color shown under POM is determined by the relationships between the birefringence (Δn) of CLC and the thickness of the sample (d), and can be inferred from to the Michel – Levy Chart (Figure 4.2).

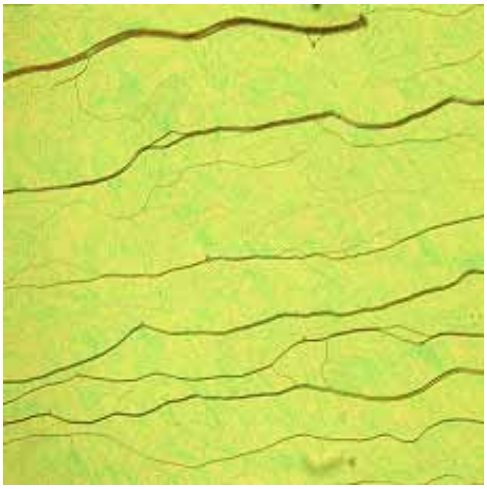

a. CB15/TL213 = 30 / 70

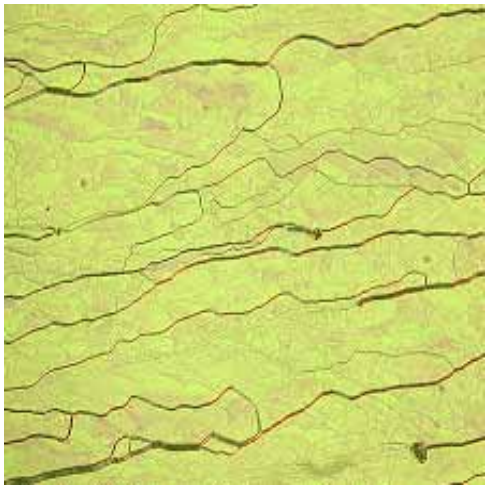

b. CB15/TL213 = 35 / 65

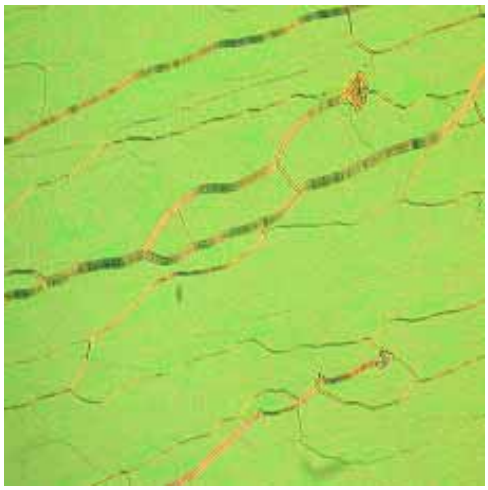

c. CB15/TL213 = 40 / 60

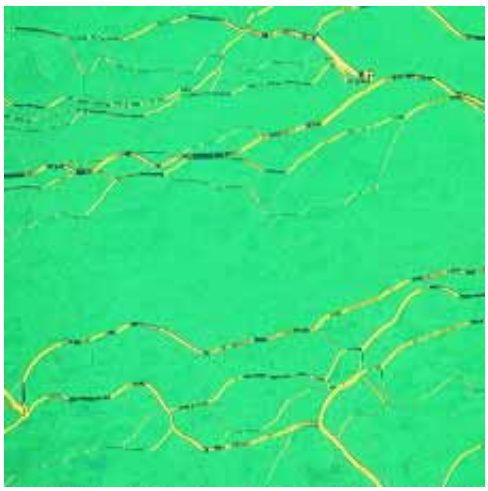

d. CB15/TL213 = 45 / 55

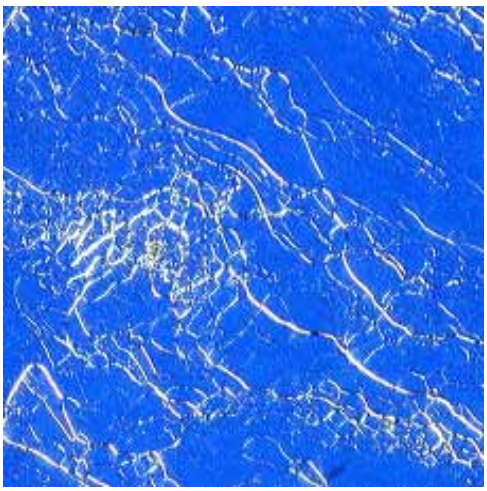

e. CB15/TL213 = 50 / 50

Figure 4.1. The texture of pure CLC with different concentration of CB15 under POM.

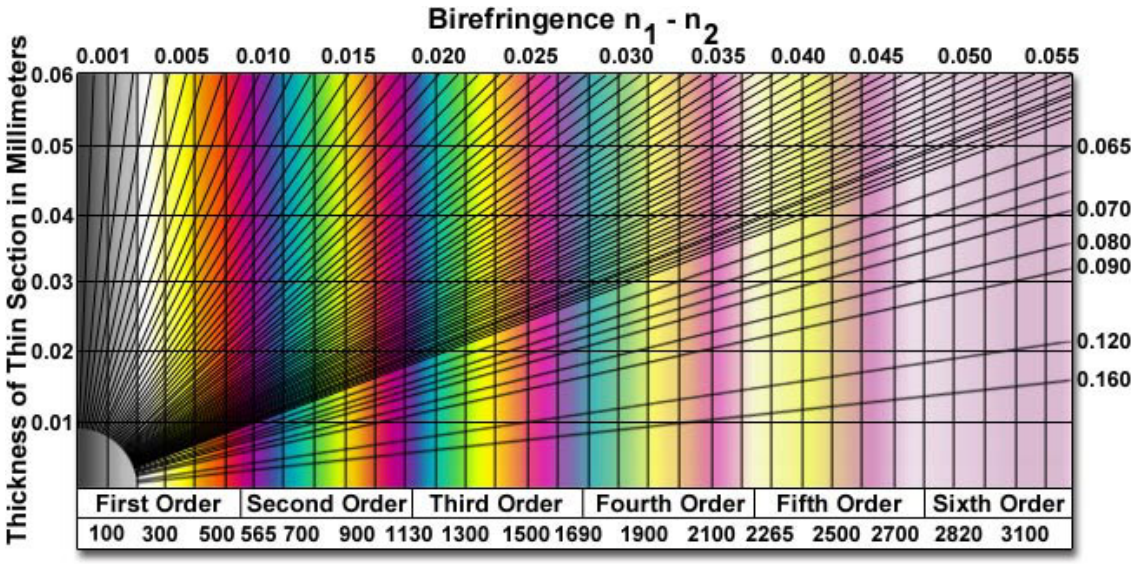

Figure 4.2. Michel – Levy Interference Color Chart. Refer to [53].

4.1.2 Selective Reflection Of CLC

The maximum wavelength of the selective reflection was measured by the micro-spectrophotometer. The transmission spectrum for each sample is shown in Figure

4.3. The transmission peak shifted to the lower wavelength with the concentration of CB15. In fact, the selective reflection light is not a single wavelength, but has a range of wavelengths (Table 4.1), $\Delta\lambda$, which is product of the birefringence and the pitch of CLC. There are several reasons for the broad transmission peak. The main reason is that the liquid crystal is anisotropic material. According to the first-order

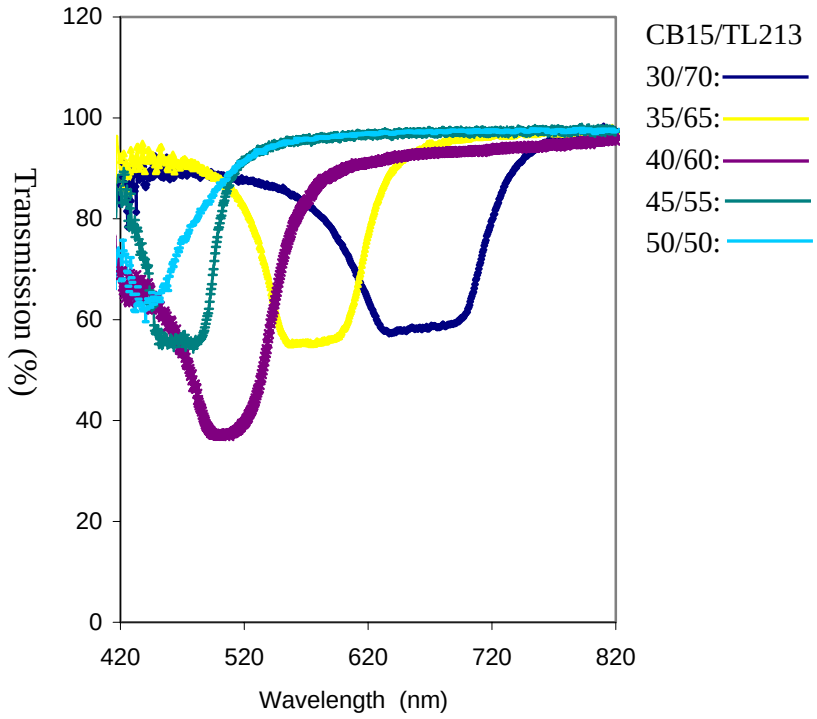

Figure 4.3. Transmission spectrum of chiral nematic liquid crystal (CB15 and TL213).

Table 4.1 The experimental and theoretical parameters of CLC samples

Weight ratio of CB15 and TL213	λ (nm)	Normalized Transmission intensity (%)	Pitch p (μm)	Δλe (nm)	Δλt (nm)	Deviation ε
30 / 70	670.4	33.8	0.44	120	105.1	0.14
35 / 65	580.3	38.2	0.36	88	86.0	0.023
40 / 60	508.4	46.2	0.33	80	78.8	0.015
45 / 55	476.3	35.3	0.31	73	74.0	0.013
50 / 50	444.8	14.7	0.29	34	69.3	0.51

Bragg diffraction equation and the refractive index along the direction at the angle, θ' (Figure 4.4), with the optical axis of CLC, and θ is equal to π/2 - θ' [54], the relationship between λ^2 and θ can be deduced as follows:

$$\lambda = np\cos\theta$$

$$n^2 = n_o^2 n_e^2 / (n_e^2 \sin^2\theta + n_o^2 \cos^2\theta)$$

$$\lambda^2 = 2n_o^2 n_e^2 p^2 \cos^2\theta / (n_e^2 \sin^2\theta + n_o^2 \cos^2\theta)$$

let $\lambda = f(\theta)$, then $\Delta\lambda = \lambda_{\theta=0} - \lambda_\theta = \int f'(\theta)\, d\theta$, thus

$$\Delta\lambda = \int \{pn_o n_e^3 / [n_e^2 + (n_e^2 - n_o^2)\cos^2\theta]^{3/2}\}\, d\theta, \text{ integrating from 0 to } \theta$$

where

n_o is the ordinary refractive index of CLC;

n_e is the extraordinary refractive index of CLC;

p is the pitch of CLC;

θ’ is the angle between the incident beam and the optical axis of CLC;

n is the refractive index of CLC along this angle.

From this equation, it is obvious that the width of the peak is related to the angle between the incident direction and the optical axis and the pitch of CLC. Since the incident beam on the sample is not collimated, there is always some collection angle existing between the beam and the sample, which is larger for the objective with the larger magnification. For the detected area, the sample in this area is not that uniform even though this area is small, about several μm^2. These two reasons result in broad transmission peaks in Figure 4.3.

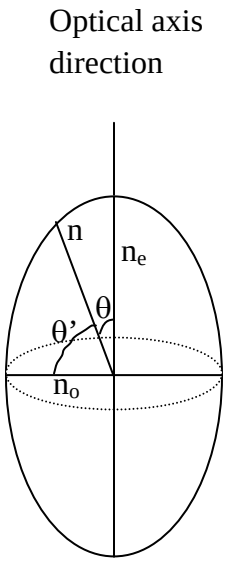

Figure 4.4. The uniaxial indicatrix.

Compared with the experimental value of $\Delta\lambda$ with the calculated value (Table 4.1), for the first four samples, the deviations are very small, but for the last sample, where the ratio of CLC is 50 / 50, this deviation is very big. This is due to the inaccuracy of the

transmission spectrum for this sample. This inaccuracy occurs as the transmission peak is close to the ultraviolet range, which is at the limit of what can be detected by the detector of the used micro-spectrometer and there is some noises as shown in Figure 4.3.

For the sample with the weight ratio of 40 / 60, the normalized maximum transmission intensity is a little bit larger than that of other samples. That's because this sample is more uniform in the detected area of the detector than that of other samples. Meanwhile, as the concentration of CB15 increased, the pitch of the sample decreased. According to the equation, $\Delta\lambda = \Delta np$, the width of the peak increased, which maybe also the reason causing the higher normalized transmission intensity for CLC with weight ratio of 40/60.

The pitch for each sample is calculated according to $\lambda = np$, which is a function of the concentration of CB15 (Figure 4.5). The dotted line shows the trend of the experiment data. According to the theoretical equation, $1/p = (HTP)Xc$ [7], the HTP for this CLC is calculated to be +0.056. The positive sign means that CB15 is right-handed. For CB15, this small HTP value indicates that the twisting power of CB15 is weak, i.e. much more amount of CB15 is needed to add into the nematic host, TL213, to obtain the CLC with small pitch when compared with the chiral dopant that has the strong twisting power.

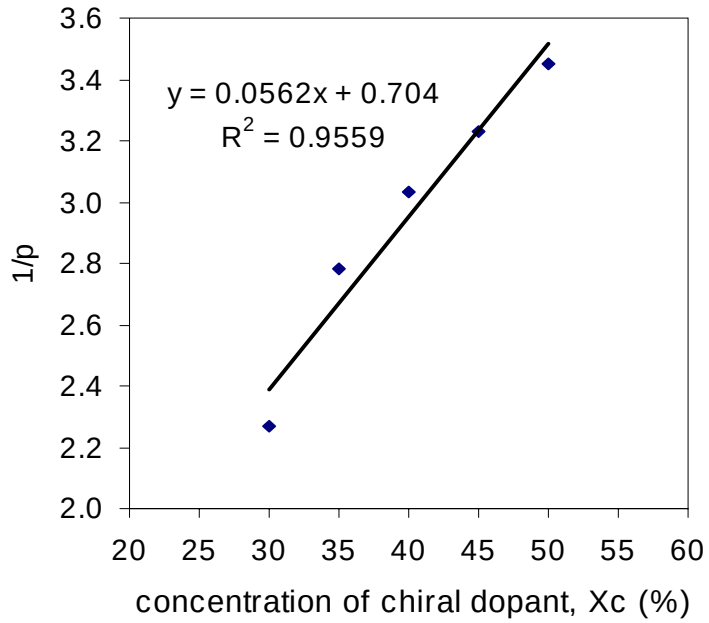

Figure 4.5. The pitch of CB15 / TL213 as a function of the concentration of CB15.

Meanwhile pitch is also a function of temperature. In most cholesteric derivatives p is a decreasing function of temperature, i.e. $dp(T)/dT < 0$, and the order of magnitude of dp/dT is often surprisingly large [7]. The increasing in p when T is decreased may be due to the onset of a short-range order of the smectic type; most of the compounds at hand have smectic phase at lower temperatures, and the smectic stacking in equidistant planes is incompatible with twist [7]. For the sample made from the mixture of CB15 and TL213, as shown in Figure 4.6, the pitch of CLC increases with temperature. As temperature increases, chiral liquid crystal changes to the nematic phase, which causes the pitch to increase. The order of magnitude of dp/dT is small when T is less than 45 °C and large when T is greater than 50 °C, which indicates that chiral liquid crystal begins to change to nematic liquid crystal when temperature is greater than 50 °C.

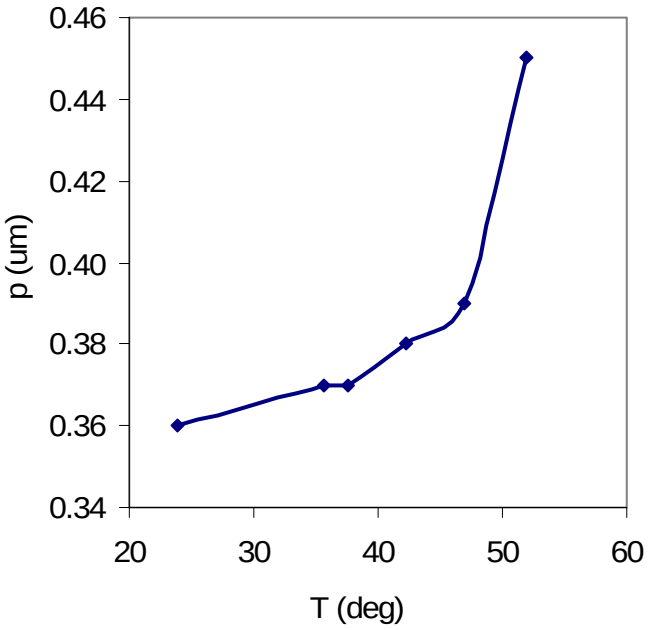

Figure 4.6. The pitch of CB15 / TL213 as a function of temperature.

4.2 Anchoring Behavior Of TL213 At A Polymer Surface In PDLC Films

To understand and compare the anchoring behavior of TL213 at different polymer surfaces, eight PDLC films were made first. The mole ratio of monomer and TMPTA, and the average functionality of the samples are listed in Table 4.2. The composition of the homogeneous mixture is fixed as following;

Monomer: 17.8 wt%;

Crosslinking agent (TMPTA): 2 wt%;

Photoinitiator: 0.2 wt%;

Nematic liquid crystal, TL213: 80 wt%;

Sample thickness: 15 μm

Table 4.2 Mole ratio of monomer and TMPTA, and the average functionality of PDLC films

Monomer	Molecular Formula	Molecular Weight	Mole ratio of monomer and TMPTA	Average Functionality
n-hexyl acrylate	$C_9H_{16}O_2$	156.2	16.9 : 1	2.22
isobornyl acrylate	$C_{13}H_{20}O_2$	208.3	12.7 : 1	2.29
1-MHA	$C_{11}H_{20}O_2$	184.0	14.3 : 1	2.26
2-MHA	$C_{11}H_{20}O_2$	184.0	14.3 : 1	2.26
isobutyl acrylate	$C_7H_{12}O_2$	128.2	20.6 : 1	2.18
n-butyl acrylate	$C_7H_{12}O_2$	128.2	20.6 : 1	2.18
n-butyl methacrylate	$C_8H_{14}O_2$	142.2	18.5 : 1	2.20
isobutyl methacrylate	$C_8H_{14}O_2$	142.2	18.5 : 1	2.20
2-ethylhexyl methacrylate	$C_{12}H_{22}O_2$	198.3	13.3 : 1	2.28
n-octyl methacrylate	$C_{13}H_{24}O_2$	212.0	12.4 : 1	2.30

Most of these monomers, except n-hexyl acrylate, can induce the planar anchoring behavior of TL213 at the polymer interface in PDLC films, i.e. the director of TL213 is parallel to polymer walls everywhere, which is indicated by the textures observed under POM (Figure 4.7 a - h). For n-hexyl acrylate, the anchoring behavior of TL213 is homeotropic at this polymer surface. The centers of the cells remain dark as the

sample was rotated, indicating no in-plane birefringence and a director field that is perpendicular to the film substrates. For n-octyl methacrylate, the anchoring behavior of TL213 at the polymer wall is not typically planar or homeotropic. There are four-crossed dark arms in some individual cells, which may due to a slight tilt of the director of TL213 at the polymer wall in these cells. And the color of this sample changed with temperature as shown in Figure 4.8 a – f. This may due to the variation of the tilt angle with temperature, or due to the variation of refractive index of TL213 with temperature, or both factors contribute to this phenomenon.

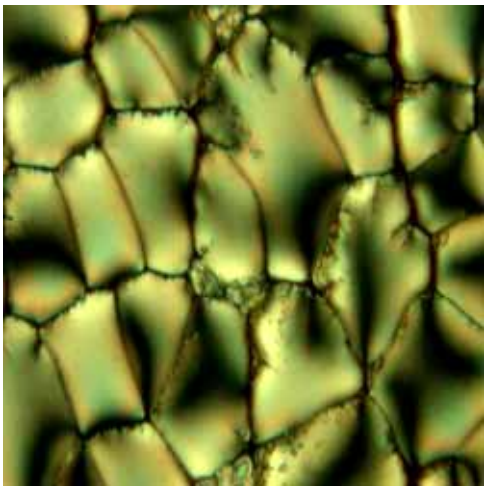

a. monomer: isobutyl acrylate

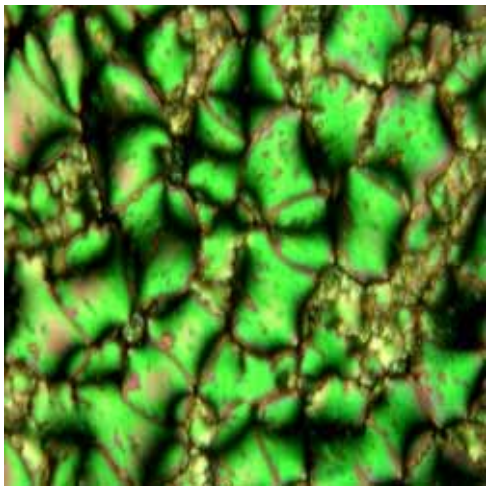

b. n-butyl acrylate

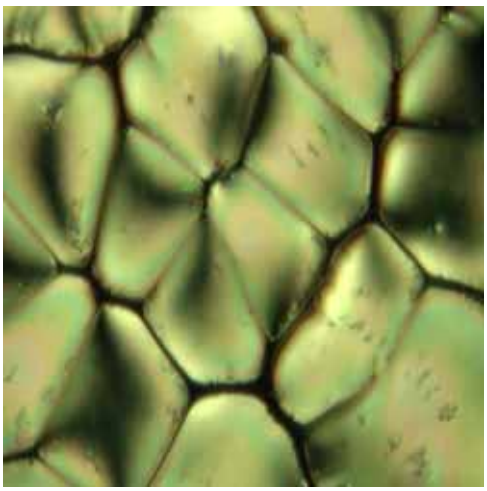

c. n-butyl methacrylate

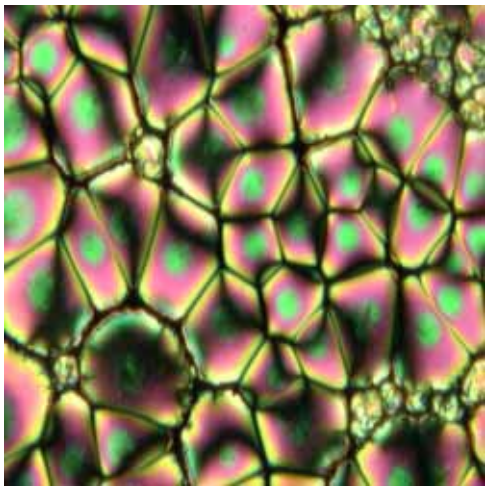

d. isobutyl methacrylate

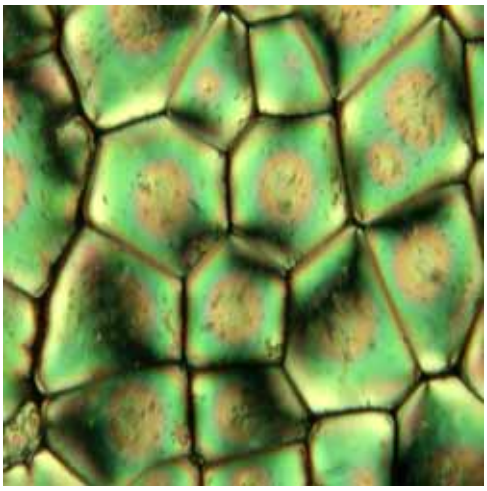

e. 2-ethylhexyl methacrylate

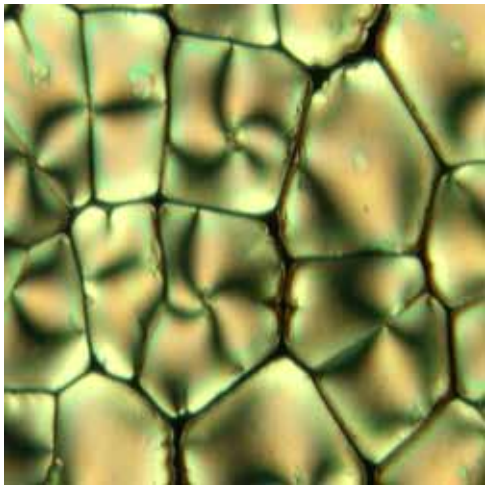

f. n-octyl methacrylate

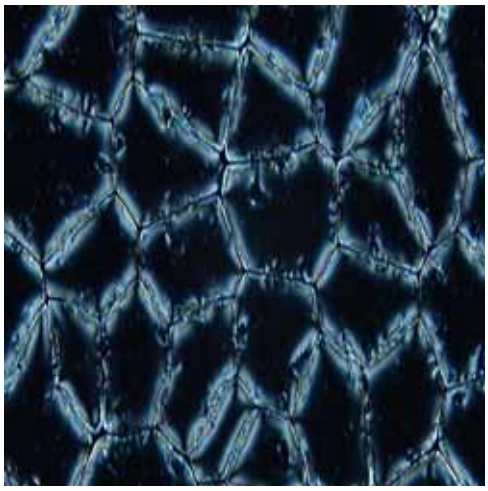

g. n-hexyl acrylate

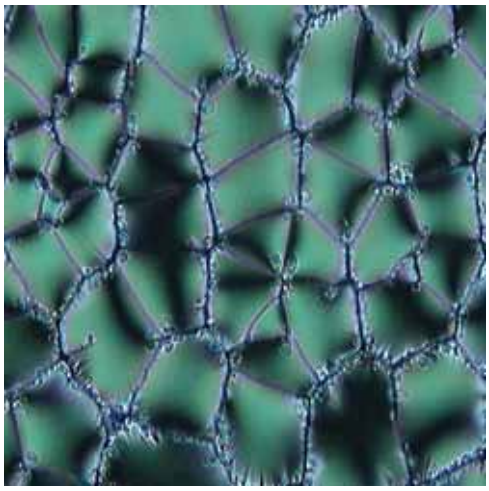

h. isobornyl acrylate

Figure 4.7. The POM texture of PDLC made with different acrylates and methacrylates.

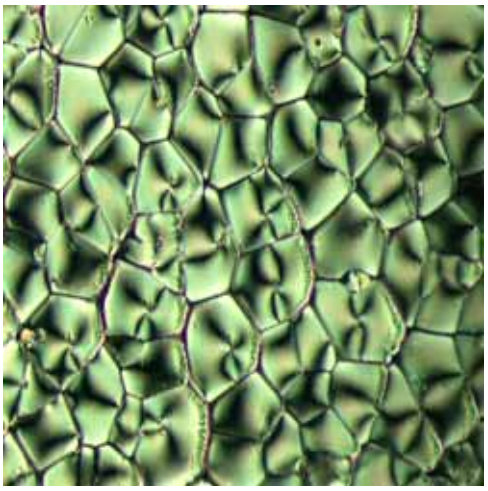

a. T_1 = 47.7 °C

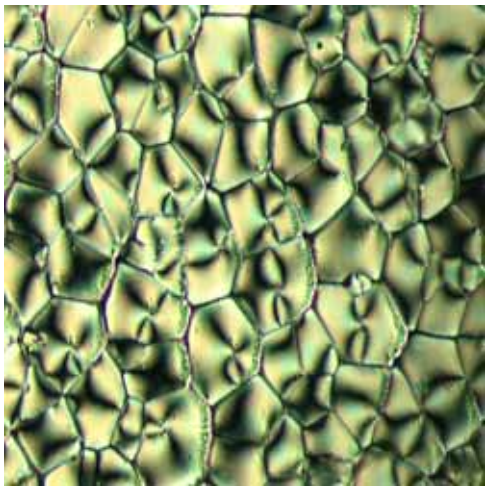

b. T_2 = 68.0 °C

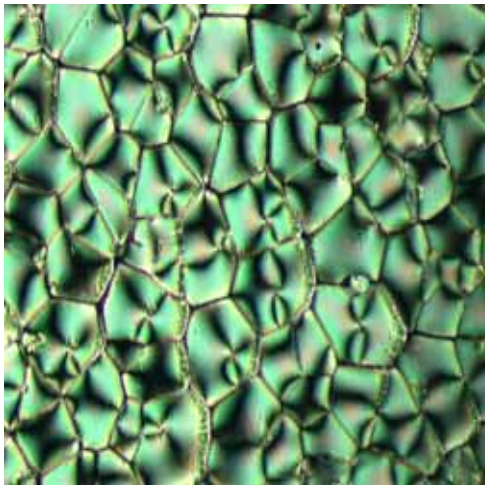

c. T_3 = 75.6 °C

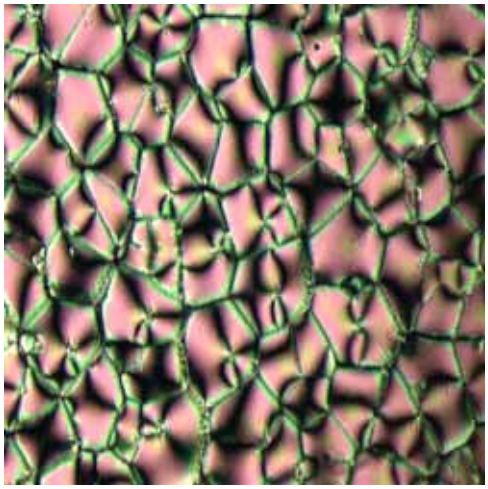

d. T_4 = 79.4 °C

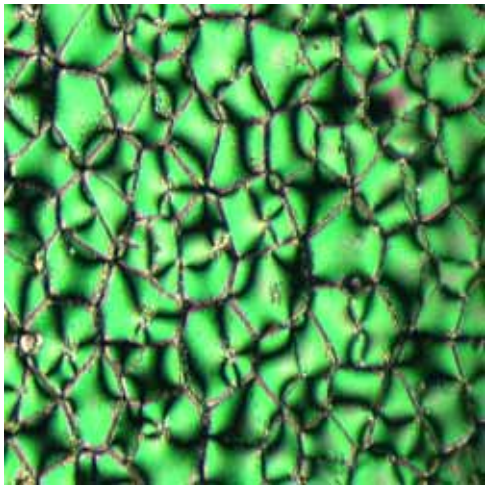

e. T_5 = 80.4 °C

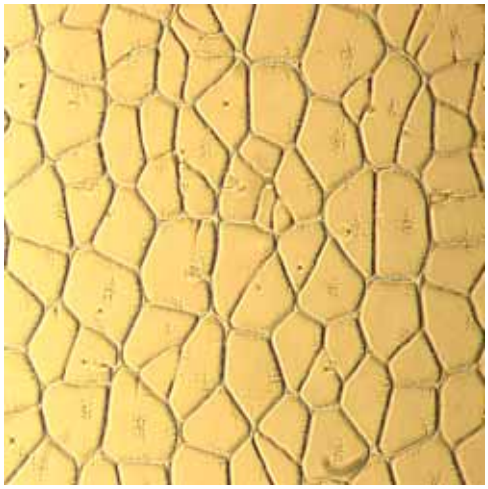

f. T_6 = 81.3 °C

Figure 4.8. The color change of POM texture with temperature for the PDLC film: monomer, n-octyl methacrylate.

The difference in anchoring behavior of TL213 at the different polymer interface was explained by the suggested interfacial model [16]. Van der Waal's interaction between the side chains of polyacrylates and the alkyl tails of nematic LC molecules provides the enthalpic drive for homeotropic anchoring [55, 56]. NMR investigation has shown that the alkyl side chains of polyacrylate contacting the nematic molecules at the interface are partially ordered under homeotropic anchoring condition. On the other hand, planar anchoring is driven by the entropy of the interfacial free energy, which is contributed by both the entropy-favored planar packing of the rod-like molecules on the surface [57] and the order-disorder transition. For example, in poly(1-MHA), where the methyl substituent is the closest to the polymer backbone, the side chain is likely to adopt a "tilted" conformation with respect to the interface normal such that an ordered packing of the side chains at the interface is impossible. Planar anchoring is thus preferred even at temperatures as low as –14 °C.

4.3 Better UV Curing Conditions For Making PDCLC Films With Large Cells

To investigate the anchoring behavior of CLC at the polymer surface, we have to obtain the PDCLC film such that the size of cells in the film is large enough to be observed. But when chiral dopant CB15 is added into the homogeneous mixture, the UV curing conditions have to be varied to get such PDCLC films. In order to find the best UV curing conditions, we vary all possible factors one by one. As shown in Table 4.2, the average functionality for acrylate monomers and methacrylate monomers is around 2.5, which means that they have the similar photo polymerization rate. Therefore, we only

need to choose one monomer to get the result and 1-MHA was chosen. Other UV curing conditions, i.e. weight ratio of CB15 and TL213 in CLC, UV curing intensity, and PDCLC film thickness, were varied. Sixty samples were prepared and listed in Table 4.3 – 4.7. The composition of homogeneous mixture to make PDCLC films is the same as that of making PDLC films described above.

Table 4.3 PDCLC films with weight ratio of CB15 and TL213 as 30 / 70

Samples Name	UV curing intensity ($\mu W/cm^2$)	Spacer size (μm)	Morphology observable
1-MHA_80%_30/70_42_3	42	3	Yes
1-MHA_80%_30/70_42_5	42	5	No
1-MHA_80%_30/70_42_10	42	10	Yes
1-MHA_80%_30/70_42_15	42	15	No
1-MHA_80%_30/70_74_3	74	3	No
1-MHA_80%_30/70_74_5	74	5	No
1-MHA_80%_30/70_74_10	74	10	No
1-MHA_80%_30/70_74_15	74	15	No
1-MHA_80%_30/70_137_3	137	3	No
1-MHA_80%_30/70_137_5	137	5	No
1-MHA_80%_30/70_137_10	137	10	Yes
1-MHA_80%_30/70_137_15	137	15	No

Table 4.4 PDCLC films with weight ratio of CB15 and TL213 as 35 / 65

Samples Name	UV curing intensity ($\mu W/cm^2$)	Spacer size (μm)	Morphology observable
1-MHA_80%_35/65_42_3	42	3	No
1-MHA_80%_35/65_42_5	42	5	Yes
1-MHA_80%_35/65_42_10	42	10	No
1-MHA_80%_35/65_42_15	42	15	Yes
1-MHA_80%_35/65_74_3	74	3	Yes
1-MHA_80%_35/65_74_5	74	5	Yes
1-MHA_80%_35/65_74_10	74	10	Yes
1-MHA_80%_35/65_74_15	74	15	Yes
1-MHA_80%_35/65_137_3	137	3	Yes
1-MHA_80%_35/65_137_5	137	5	Yes
1-MHA_80%_35/65_137_10	137	10	Yes
1-MHA_80%_35/65_137_15	137	15	Yes

Table 4.5 PDCLC films with weight ratio of CB15 and TL213 as 40 / 60

Samples Name	UV curing intensity ($\mu W/cm^2$)	Spacer size (μm)	Morphology observable
1-MHA_80%_40/60_42_3	42	3	No
1-MHA_80%_40/60_42_5	42	5	No
1-MHA_80%_40/60_42_10	42	10	No
1-MHA_80%_40/60_42_15	42	15	No
1-MHA_80%_40/60_74_3	74	3	No
1-MHA_80%_40/60_74_5	74	5	No
1-MHA_80%_40/60_74_10	74	10	No
1-MHA_80%_40/60_74_15	74	15	No
1-MHA_80%_40/60_137_3	137	3	No
1-MHA_80%_40/60_137_5	137	5	No
1-MHA_80%_40/60_137_10	137	10	No
1-MHA_80%_40/60_137_15	137	15	No

Table 4.6 PDCLC films with weight ratio of CB15 and TL213 as 45 / 55

Samples Name	UV curing intensity ($\mu W/cm^2$)	Spacer size (μm)	Morphology observable
1-MHA_80%_45/55_42_3	42	3	No
1-MHA_80%_45/55_42_5	42	5	No
1-MHA_80%_45/55_42_10	42	10	No
1-MHA_80%_45/55_42_15	42	15	No
1-MHA_80%_45/55_74_3	74	3	No
1-MHA_80%_45/55_74_5	74	5	No
1-MHA_80%_45/55_74_10	74	10	No
1-MHA_80%_45/55_74_15	74	15	No
1-MHA_80%_45/55_137_3	137	3	Yes
1-MHA_80%_45/55_137_5	137	5	No
1-MHA_80%_45/55_137_10	137	10	No
1-MHA_80%_45/55_137_15	137	15	No

Table 4.7 PDCLC films with weight ratio of CB15 and TL213 as 50 / 50

Samples Name	UV curing intensity ($\mu W/cm^2$)	Spacer size (μm)	Morphology observable
1-MHA_80%_50/50_42_3	42	3	No
1-MHA_80%_50/50_42_5	42	5	No
1-MHA_80%_50/50_42_10	42	10	No
1-MHA_80%_50/50_42_15	42	15	No
1-MHA_80%_50/50_74_3	74	3	No
1-MHA_80%_50/50_74_5	74	5	No
1-MHA_80%_50/50_74_10	74	10	No
1-MHA_80%_50/50_74_15	74	15	No
1-MHA_80%_50/50_137_3	137	3	Yes
1-MHA_80%_50/50_137_5	137	5	No
1-MHA_80%_50/50_137_10	137	10	No
1-MHA_80%_50/50_137_15	137	15	No

For the PDCLCs films made under the prementioned conditions, cells can be observed clearly only at the edges. Cells at the center are too small to be observed under POM where the resolution is 1 μm. Since the bigger the original concentration of CLC in homogeneous mixture, the more CLC will be encapsulated by polymer matrix in PDCLC films and the bigger the size of individual cells. Therefore we decide to increase the concentration of CLC in the homogeneous mixture. It was found that when the

concentration of CLC is 85 wt% and 95 wt%, no such film can be obtained. Only when it is 90 wt%, good films where cells are large enough to be observed can be obtained. According to the observability of the morphology of PDCLC films made in Table 4.3 – 4.7, we just select optimum UV curing conditions in the experiment for the concentration of 1-MHA to be 90 wt%, as listed in Table 4.8.

Table 4.8 PDCLC films with the concentration of 1-MHA as 90 wt%

Samples name	Weight ratio of CB15 and TL213	UV curing intensity ($\mu W/cm^2$)	Spacer size (μm)
1-MHA_90%_35/65_42_3	35 / 65	42	3
1-MHA_90%_35/65_42_5	35 / 65	42	5
1-MHA_90%_35/65_42_10	35 / 65	42	10
1-MHA_90%_35/65_74_3	35 / 65	74	10
1-MHA_90%_35/65_137_3	35 / 65	137	3
1-MHA_90%_30/70_42_3	30 / 70	42	3

According to the results from POM and micro-spectrophotometer for PDCLC films made under the conditions listed in Table 4.8, it was found that the following three conditions (Table 4.9) are the best for making PDCLC films with large enough cells to be observed and preference for planar texture.

Table 4.9 Better UV curing conditions

Samples name	Weight ratio of CB15 and TL213	UV curing intensity ($\mu W/cm^2$)	Spacer size (μm)
1-MHA_90%_35/65_42_3	35 / 65	42	3
1-MHA_90%_35/65_42_10	35 / 65	42	10
1-MHA_90%_35/65_74_10	35 / 65	74	10

We investigate the effect of UV curing conditions, UV curing conditions, including UV curing intensity, weight ratio of CB15 and TL213, spacer size, and chemical structure of monomers, are varied by varying systematically on the anchoring behavior of CLC at the polymer interface in PDCLC films in the following, we choose the UV curing intensity in the range of 42 ~ 137 $\mu W/cm^2$), and set the weight ratio of CB15 and TL213 to be 35 / 65, and vary spacer size from 3 μm to 15 μm.

4.4 Effect Of UV Curing Conditions On The Anchoring Behavior Of CLC At A Polymer Interface In PDCLC Films

The morphology of the polymer walls in PDCLC films is same as that in PDLC films. The slow polymerization process leads to a polygonal morphology. The film contains only one layer of close-packed polygonal LC cells between two glass substrates. Each CLC cell is completely encapsulated by polymeric matrix, with thin vertical polymer walls extending from the top substrate to the bottom. The morphology of PDCLC films is verified by the pseudo-3D and cross-section images obtained from

LSCM (Figure 4.9). The texture of the confined CLC depends on chemical structure of monomers, the fraction of CLC in the homogeneous mixture, the pitch of CLC, the spacer size, and the UV curing intensity. UV curing intensity is the most important factor to control the rate of phase separation. The concentration of initiator and crosslinking agent is also important to the rate of phase separation. Here we concentrate only on the effect of UV curing intensity, keeping the concentration of the initiator and the crosslinking agent constant.

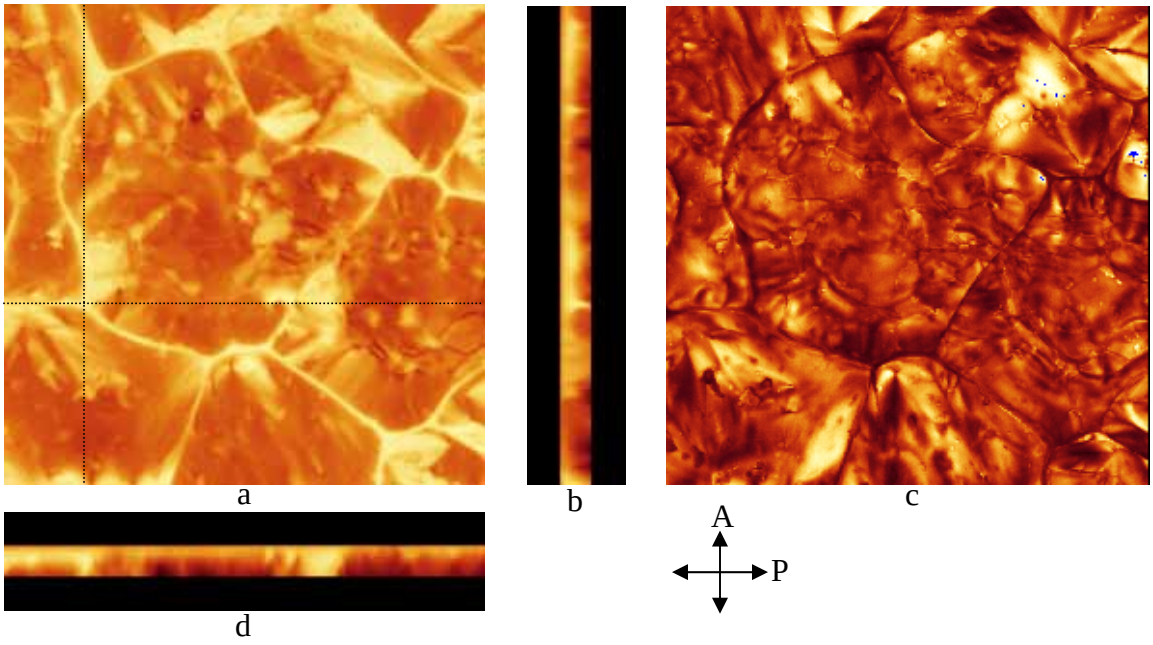

Figure 4.9. The confocal microscopic sections of a PDCLC film with polygonal polymer walls. a is the fluorescent image of 'xy' section, b is the fluorescent image 'yz' section taken along the vertical dotted line in a, d is the fluorescent image of 'xz' section taken along the horizontal dotted line in a, and c is the traditional transmission image of 'xy'section.

In PDCLC films, CLC has the preferential orientation at a polymer surface as NLC does in PDLC films. Simultaneously CLC rotates perpendicularly around its helix, which means that CLC molecules are always perpendicular to its helix. We use half pitch of its helical structure to represent CLC as shown in Figure 4.10 (e) and call this structure as a small reflector. Since CLC are perpendicular to its helix, we can use the orientation of the helix with respect to a polymer surface to represent the anchoring behavior of CLC at the polymer surface. As shown in Figure 4.10, if CLC molecules are parallel to a polymer surface, all helices orient perpendicular to this surface. This orientation state will give the planar texture of CLC in PDCLC films. If CLC molecules are perpendicular to a polymer surface, then all helices are parallel to this surface. The fingerprint texture of CLC in PDCLC films will be observed under POM. When all helices orient randomly with respect to a polymer surface, the focal conic texture is formed. This state is called random orientation. In the following investigation of anchoring behavior of CLC at a polymer surface in PDCLC films, the texture and transmission spectra were used to indicate the anchoring behavior of CLC in PDCLC films.

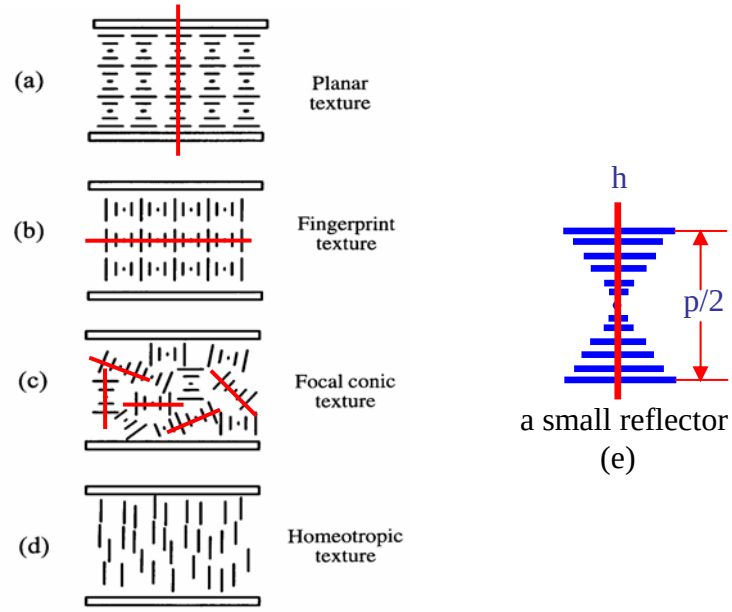

Figure 4.10. Different orientation states of helices of CLC in PDCLC films, and red lines represent helical axes. Redrawn based on the reference [8].

4.4.1 Effect Of Chemical Structure Of Monomers

Several different acrylate and methacrylate monomers were chosen to make PDCLC films. When chiral dopant, CB15, was added, the director of CLC molecules rotated along the helical axis. We anticipate that the following results may be obtained. If the anchoring behavior of TL213 is planar at a polymer surface in PDLC films, in PDCLC films it may still be parallel to the polymer surface with all helices perpendicular to the polymer surface and the planar texture would be observed for this PDCLC film (Figure 4.11). If the anchoring behavior of TL213 is homeotropic at a polymer surface in PDLC films, it may still be perpendicular to the polymer surface with all helices parallel to the polymer surface and the fingerprint texture would be observed for this PDCLC film (Figure 4.11). However our experimental results did not match this simple expectation

well. Some cells have the planar texture, some show the focal conic texture, and others have the fingerprint texture. The observed texture depends on several curing conditions, such as chemical structure of monomers, UV curing intensity, and spacer size. The first part of this study is focused on studying the effect of chemical structure of monomers. Two types of monomers were chosen, acrylate monomers and methacrylate monomers.

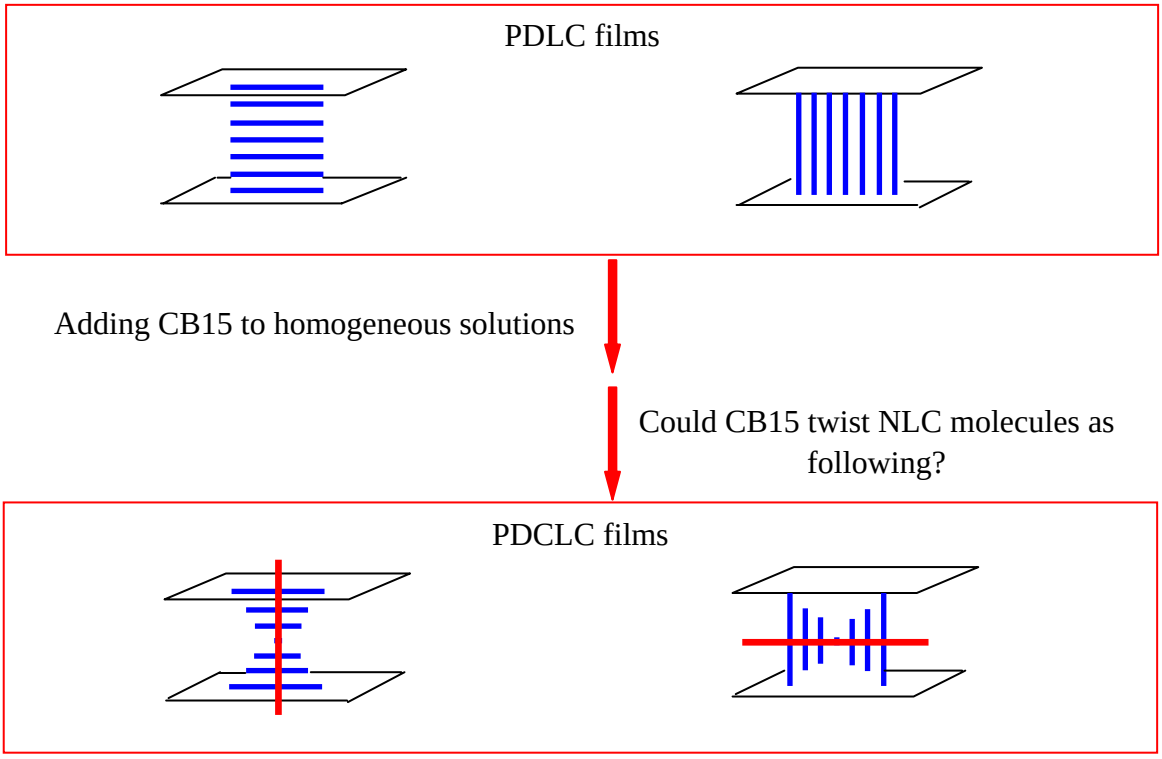

Figure 4.11. The anticipation of anchoring result for CLC in PDCLC films.

4.4.1.1 Acrylate Monomers With Linear Alkyl Tails

For acrylate monomers with linear alkyl tail, when the number of carbon atoms in alkyl linear tails increase from 4 to 12, the anchoring behavior of TL213 at the polymer surface in PDLC films changes from the planar anchoring to homeotropic anchoring. In PDCLC films, POM images of these PDCLC films do not show the corresponding change from the planar texture to the fingerprint texture, but in all these PDCLC films (Table 4.10) CLC has focal conic textures. However observation of their transmission spectra (Figure 4.12 a - d) shows some differences among these PDCLC films. As shown in Figure 4.10 c and d, there is no transmission peak, which indicates that the orientation of helices of CLC encapsulated by poly(n-decyl acrylate) and poly(n-lauryl acrylate) matrices is random. But for n-butyl acrylate and n-hexyl acrylate, their transmission spectra (Figure 4.12 a and b) do have obvious transmission peaks located at some specific wavelengths. This implies that in some part of individual cells, helices of CLC encapsulated between these polymer matrices are oriented perpendicular to the polymer surface in these PDCLC films. In these transmission spectra, the transmission intensity never reaches 100%, due to the light scattering from these films, because the refractive indices of CLC and the polymer matrix are not matched with each other. The existence of light scattering shows that the helix of CLC is not perfectly perpendicular to the substrates and they have some tilt angle with respect to the substrates, i.e. CLC at these two polymer surfaces has the tendency to form the planar texture. In order to compare this tendency for the two PDCLC films, the transmission intensity of PDCLC films is normalized using the following equation:

$$Normalized \quad transmission = \frac{I_{tran(a^*)} - I_{tran(b^*)}}{I_{tran(a^*)}} \times 100\%$$

where "*trans*" represents transmission and "*I*" represents intensity, and point a* and point b* are shown in Figure 4.10 a. From the comparison of their normalized transmission intensity (Figure 4.13), it is found that the tendency to have the planar texture of CLC in PDCLC films decreases with the number of carbon atoms in the alkyl linear tail of acrylates. Meanwhile the maximum refection wavelength shifts to the higher value compared with that of pure CLC (Figure 4.14). This is caused by the phase separation of components in originally homogeneous solutions, i.e. the weight ratio of CLC in the polygonal domain is different from that of original homogeneous solutions.

Table 4.10. Acrylate monomers with linear alkyl tails

Monomer Name	Chemical Structure	Anchoring in PDLC films	POM texture of PDCLC films
n-butyl acrylate	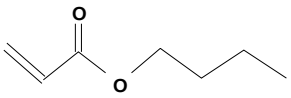	planar	
n-hexyl acrylate	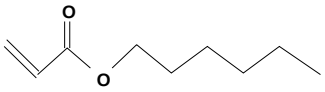	homeotropic	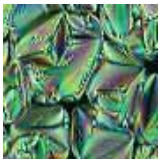
n-decyl acrylate	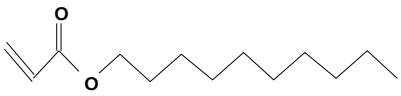	homeotropic	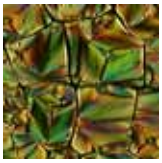
n-lauryl acrylate	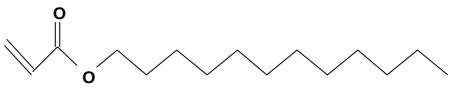	homeotropic	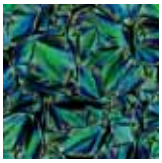

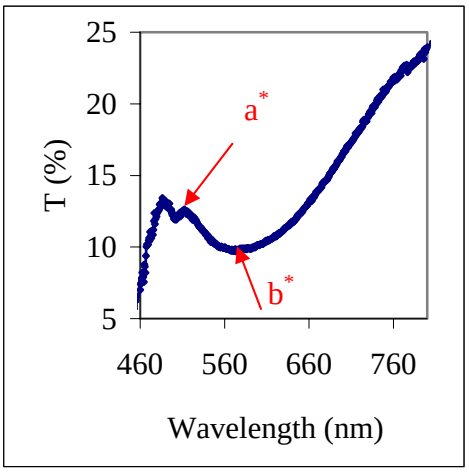

a. monomer: n-butyl acrylate

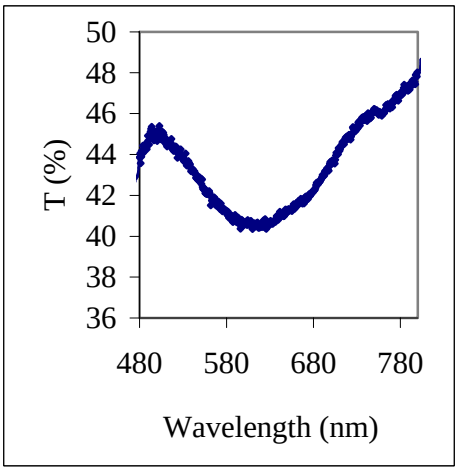

b. monomer: n-hexyl acrylate

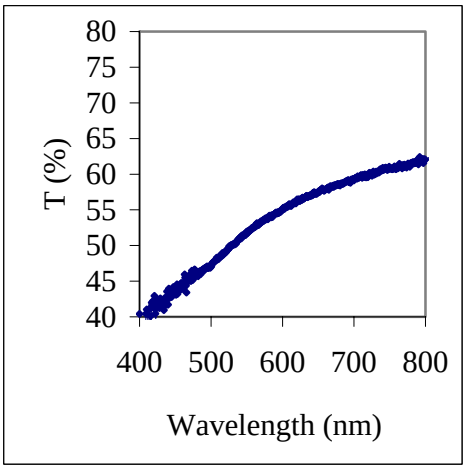

c. monomer: n-decyl acrylate

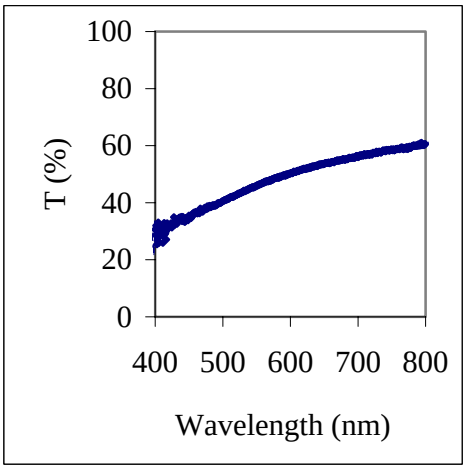

d. monomer: n-lauryl acrylate

Figure 4.12. Transmission spectra of PDCLC films made with different linear acrylate

Note: other UV-curing conditions for above PDCLC films: curing intensity, 74 μW/cm^2; concentration of CLC, 90 wt%; pitch of CLC, 0.36 μm (CB15 / TL213 = 35 / 65, weight ratio); spacer size, 10 μm.

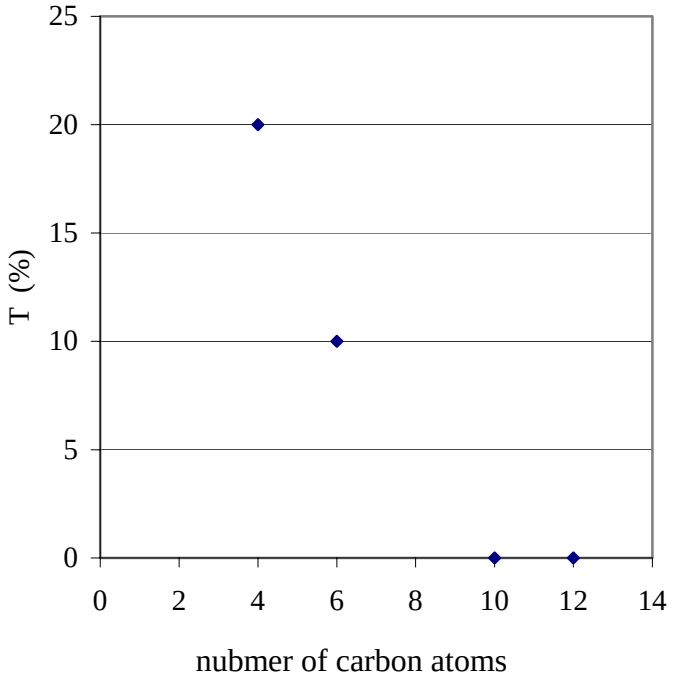

Figure 4.13. Comparison of normalized transmission intensity of PDCLC films made with linear acrylate monomers.

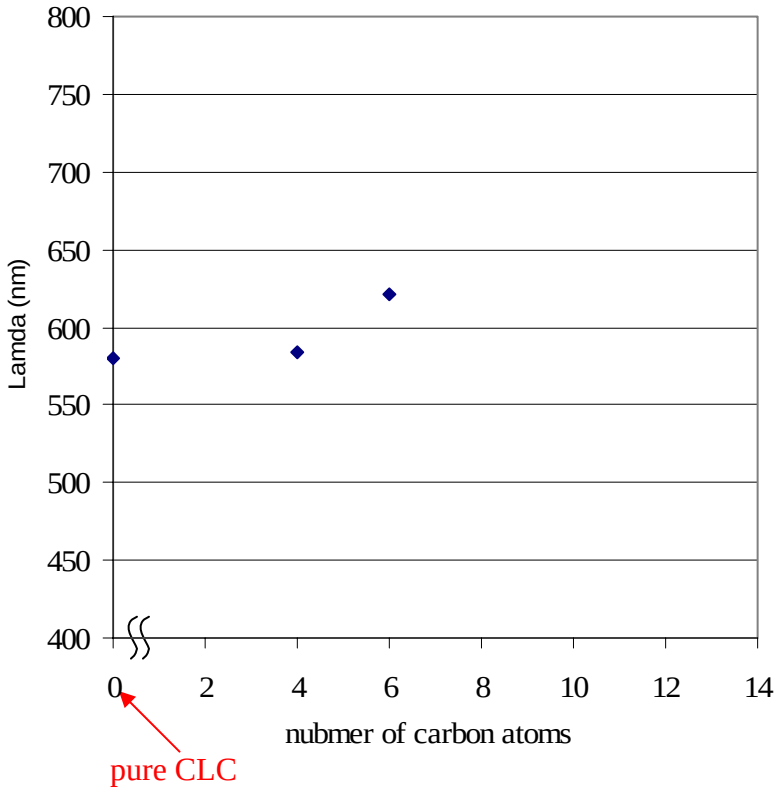

Figure 4.14. The maximum selective reflection wavelength of PDCLC films compared to that of pure CLC.

4.4.1.2 Acrylate Monomers With Branched Alkyl Tails

If acrylate monomers with branched alkyl tails are chosen to fabricate PDLC and PDCLC films, changing the position and type of side group of alkyl tails changes, the anchoring behavior of TL213 at the polymer surface in PDLC films varies. For 1-position and bulky side groups in alkyl tails, planar anchoring of TL213 is obtained, while others have homeotropic anchoring [16]. But for their corresponding PDCLC films, no planar texture of CLC in PDCLC films is observed even if TL213 has planar anchoring at the polymer surface except poly(isobornyl acrylate). In this PDCLC film, some individual cells have the planar texture of CLC, which means that helices of CLC are perpendicular to the polymer surface. No fingerprint texture of CLC is observed even when TL213 has homeotropic anchoring at the polymer surface. All other PDCLC films have the focal conic texture (Table 4.11). However further observation of their corresponding transmission spectra (Figure 4.15 a - e) shows that CLC tends to have the planar texture in the PDCLC films made with 1-MHA and isooctyl acryalte since there is a transmission peak in Figure 4.15 c and d. Meanwhile the transmission spectra of the PDCLC film made with isobornyl acrylate do have a transmission peak in Figure 4.15 e, which is consistent with its POM texture. By comparison of normalized transmission intensities of these films in Figure 4.16, it can be found that branched acrylates with 1-position side group and bulky side group tend to induce the planar texture of CLC in PDCLC films. For the similar reason, the maximum selective reflection wavelength for PDCLC films shifts to higher value compared to that of pure CLC.

Table 4.11. Acrylate monomers with branched alkyl tails

Monomer Name	Chemical Structure	Anchoring in PDLC films	POM texture of PDCLC films
isobutyl acrylate	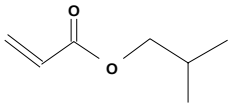	planar	
2-methyl-heptyl acrylate	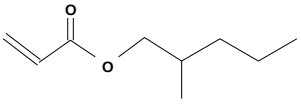	homeotropic	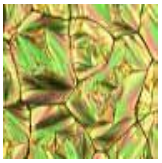
1-methyl-heptyl acrylate	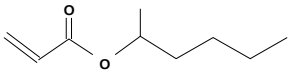	planar	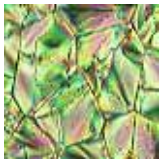
isooctyl acrylate	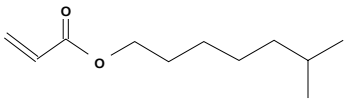	homeotropic	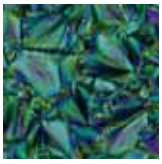
Isobornyl acrylate	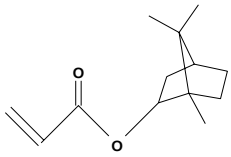	planar	

Note: other UV-curing conditions for above PDCLC films: curing intensity, 74 μW/cm^2; concentration of CLC, 90 wt%; pitch of CLC, 0.36 μm (CB15 / TL213 = 35 / 65, weight ratio); spacer size, 10 μm.

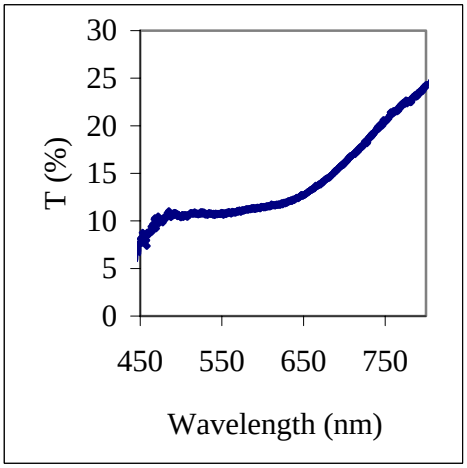

a. monomer: isobutyl acrylate

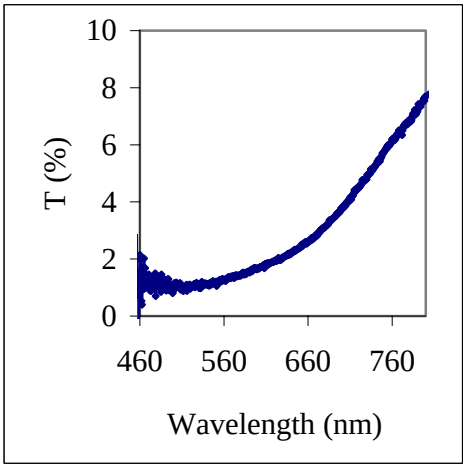

b. monomer: 2-MHA

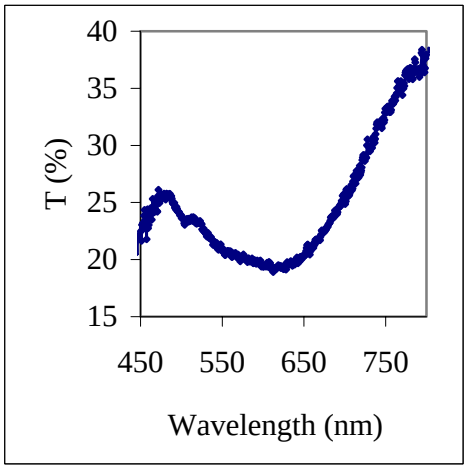

c. monomer: 1-MHA

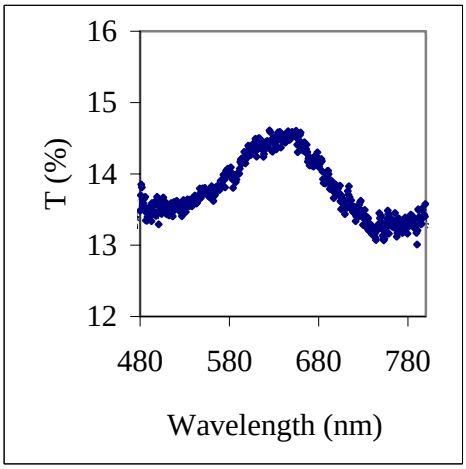

d. monomer: isooctyl acrylate

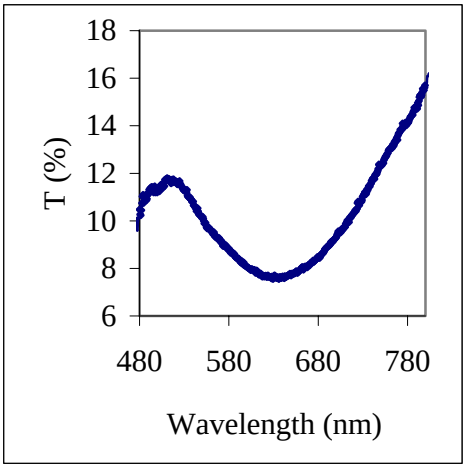

e. monomer: isobornyl acrylate

Figure 4.15. Transmission spectra of PDCLC films made of branched acrylate monomers.

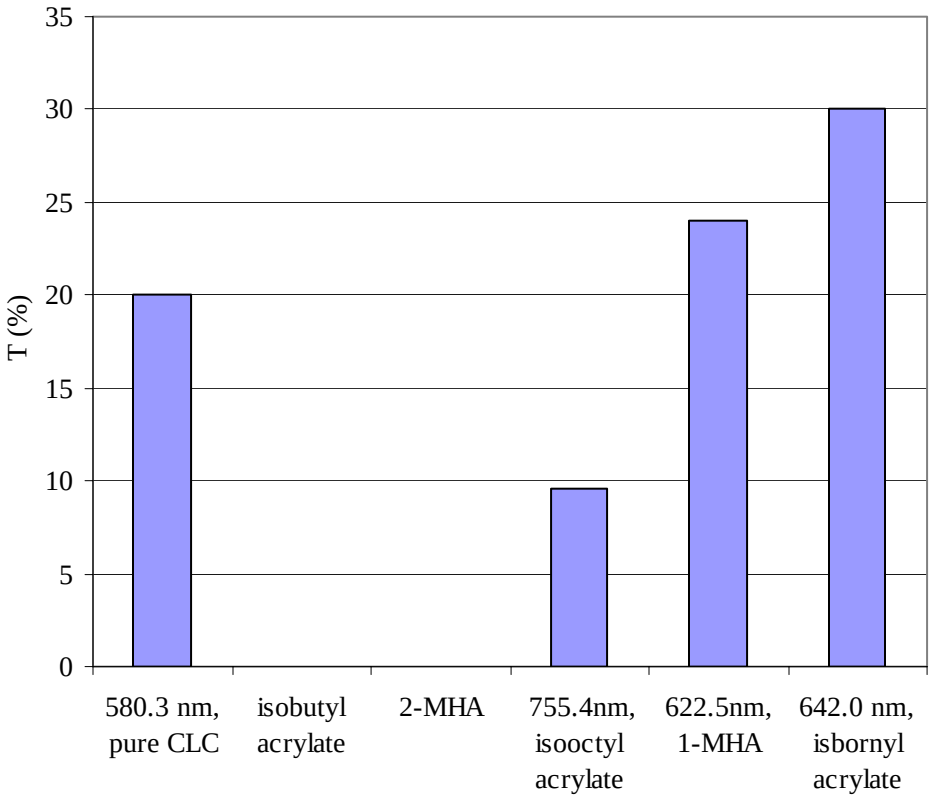

Figure 4.16. Comparison of normalized transmission intensity of PDCLC films made with branched acrylates.

4.4.1.3 Methacrylate Monomers With Linear Alkyl Tails

For methacrylate monomers with linear alkyl tails, the anchoring behavior of TL213 at a polymer surface in PDLC films is planar except for n-decyl methacrylate. TL213 molecules are tilted with respect to the polymer surface and the tilt increases as the number of carbon atoms increases from 4 to 10. For n-hexyl methacrylate, CLC in this PDCLC film has the perfect planar texture (Table 4.12) as anticipated, which means that all helices in individual cells are perpendicular to the polymer surface in these PDCLC films. But for other methacrylates, CLC has the focal conic textures in their PDCLC films. However, a detailed examination of their corresponding transmission spectra (Figure 4.17 a - e) shows that CLC tends to have the planar texture in the PDCLC films made with n-octyl methacrylate and n-decyl methacrylate since there is a

transmission peak in Figure 4.17 d and e. Meanwhile the transmission spectrum of the PDCLC film made with n-hexyl methacrylate does have a transmission peak in Figure 4.17 e, which is consistent with its POM texture. By comparison of normalized transmission intensities of these films in Figure 4.18, it is found that when the number of carbon atoms in linear alkyl tails of methacrylate monomers is increased to 6, CLC can have the perfect planar texture. This tendency decreases as the number of carbon atoms continues increasing to 8 and 10. Meanwhile the maximum selective reflection wavelength shifts to higher value compared to that of pure CLC with the same weight ratio of CB15 and Tl213.

Table 4.12. Methacrylate monomers with linear alkyl tails

Monomer Name	Chemical Structure	Anchoring in PDLC films	POM texture of PDCLC films
butyl methacrylate	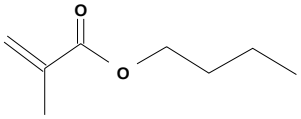	planar	
amyl methacrylate	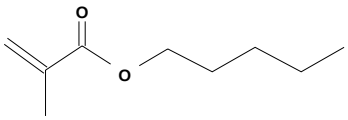	planar	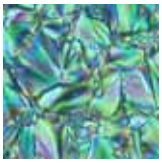
hexyl methacrylate	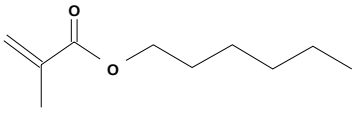	planar	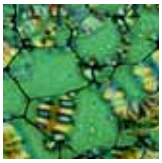
octyl methacrylate	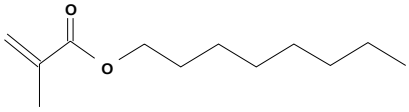	planar	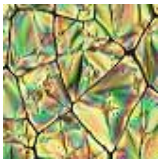

Table 4.12. Methacrylate monomers with linear alkyl tails (Continued)

decyl methacrylate	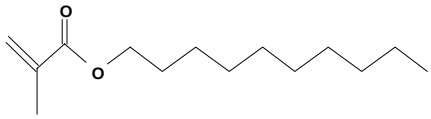	tilt	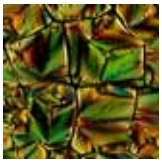

Note: other UV-curing conditions for above PDCLC films: curing intensity, 74 μW/cm^2; concentration of CLC, 90 wt%; pitch of CLC, 0.36 μm (CB15 / TL213 = 35 / 65, weight ratio); spacer size, 10 μm.

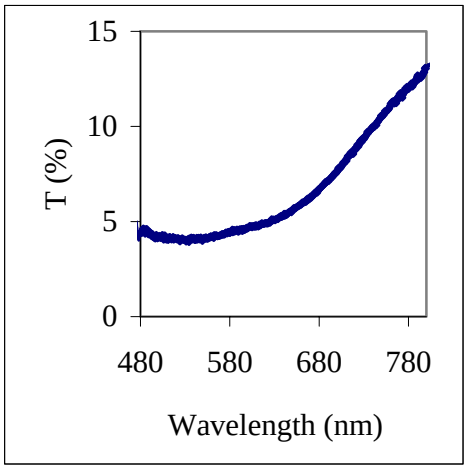

a. n-butyl methacrylate

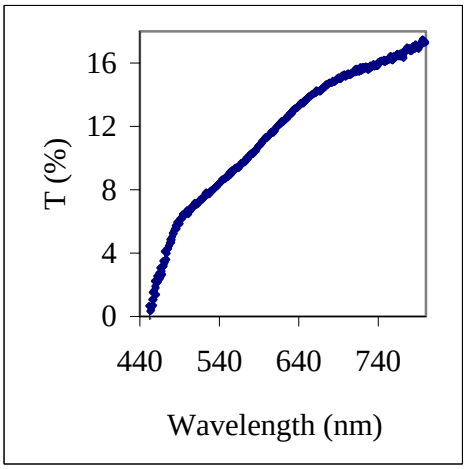

b. n-amyl methacrylate

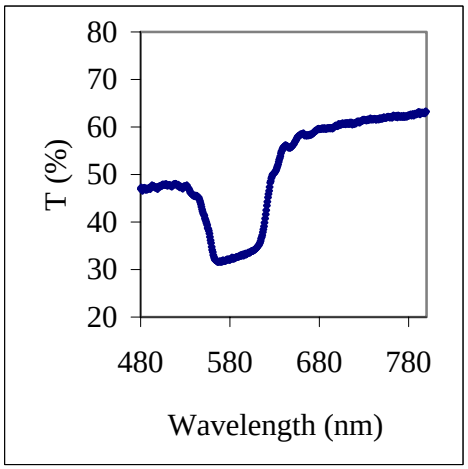

c. n-hexyl methacrylate

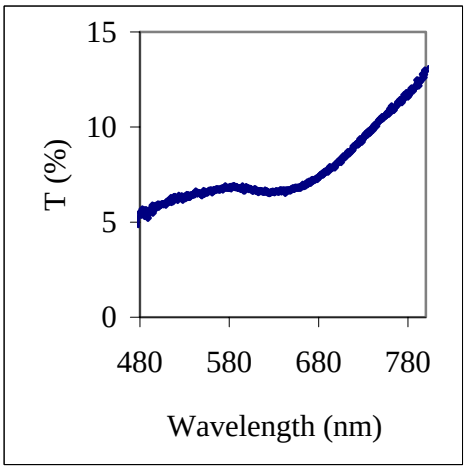

d. n-octyl methacrylate

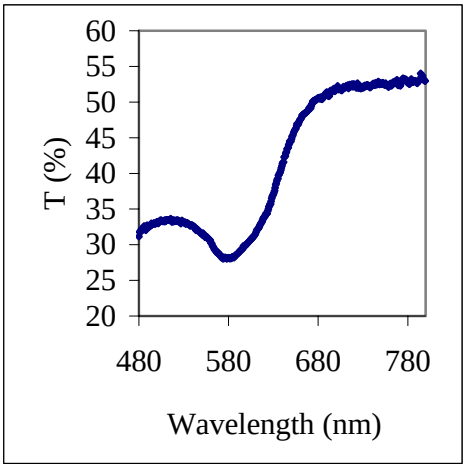

e. n-decyl methacrylate

Figure 4.17. Transmission spectrum of PDCLC films made of linear methacrylates.

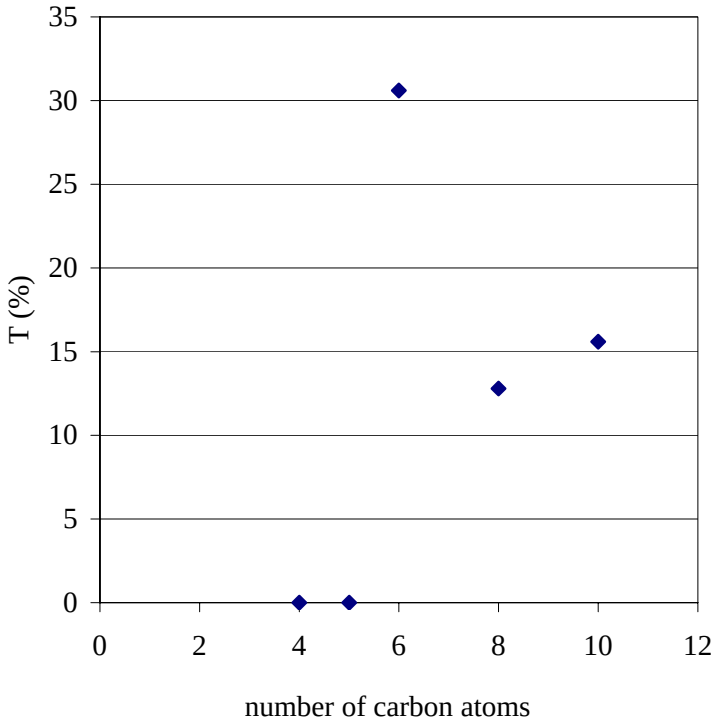

Figure 4.18. Comparison of normalized transmission intensity of PDCLC films made with linear methacrylates.

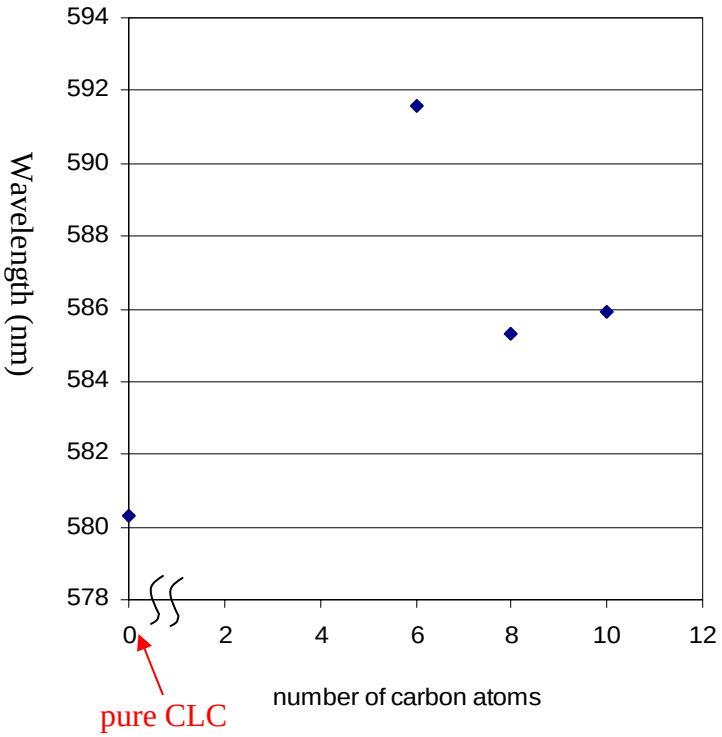

Figure 4.19. Comparison of maximum selective reflection wavelengths of PDCLC films and that of pure CLC.

4.4.1.4 Methacrylate Monomers With Branched Alkyl Tails

The position and type of side groups in alkyl tails of methacrylate monomers were varied as shown in Table 4.13. The anchoring behavior of TL213 in these PDLC films is planar except for isobornyl methacrylate which shows homeotropic. Totally opposite to our anticipation that CLC in the PDCLC film made with isobornyl methacrylate should have the fingerprint texture since NLC at poly(isobornyl methacrylate) surface has the homeotropic anchoring, CLC in this PDCLC film has the planar texture of CLC in some individual cells. The PDCLC films made with isobutyl methacrylate and 2-ethylhexyl methacrylate have the focal conic texture of CLC, which means that helices of CLC in these two PDCLC films orient randomly. However again the corresponding transmission

spectra (Figure 4.20 a - c) show that CLC tends to have the planar texture at the polymer surface in the PDCLC film made with isobutyl methacrylate since there is a transmission peak in Figure 4.20 a. Meanwhile the transmission spectrum of the PDCLC film made with isbornyl methacrylate does have a transmission peak in Figure 4.20 c, which is consistent with its POM texture. By comparison of normalized transmission intensities of these PDCLC films in Figure 4.21, it is found that the texture of CLC at the polymer surface in these films is determined by the position and type of the substituents in the branched tail of methacrylates. The short branched tail and the bulky side group of the branched methacrylate monomer tend to make CLC have the planar texture in these PDCLC films.

Table 4.13 Methacrylate monomers with branched alkyl tails

Name	Chemical Structure	Anchoring in PDLC films	POM texture of PDCLC films
isobutyl methacrylate	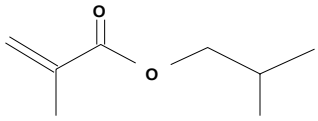	planar	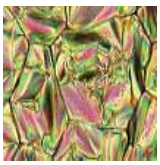
2-ethylhexyl methacrylate	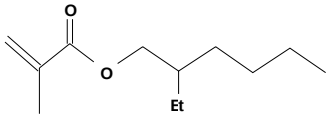	planar	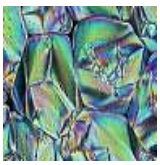
isobornyl methacrylate	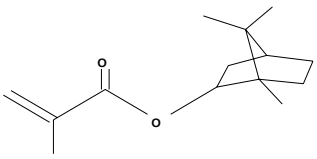	homeotropic	

Note: Other UV-curing conditions for above PDCLC films: curing intensity, 74 μW/cm^2; concentration of CLC, 90 wt%; pitch of CLC, 0.36 μm (CB15 / TL213 = 35 / 65, weight ratio); spacer size, 10 μm.

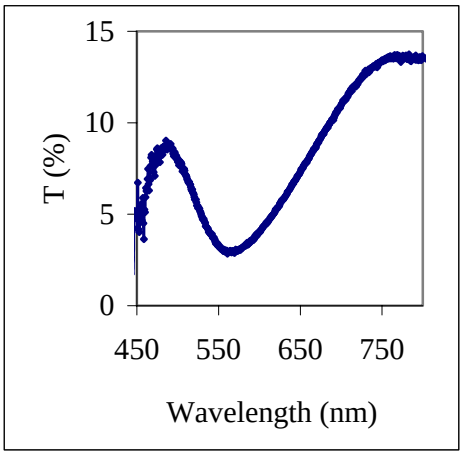

a. isobutyl methacrylate

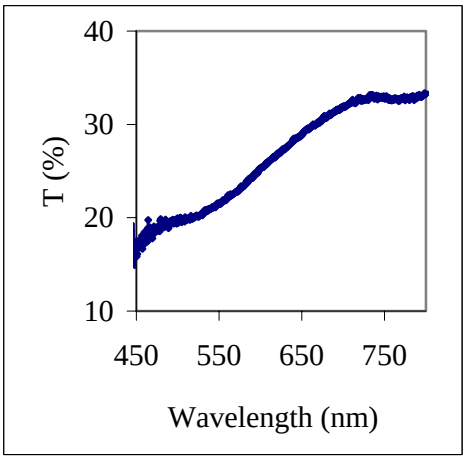

b. 2-ethylhexyl methacrylate

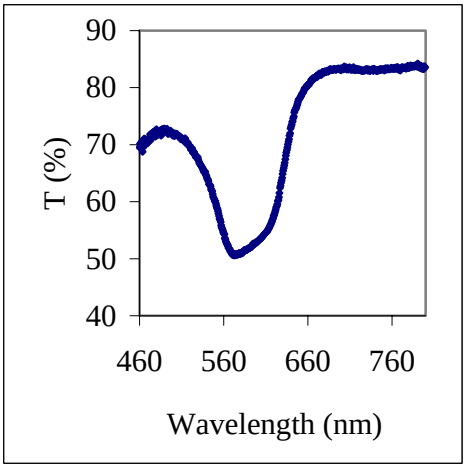

c. isobornyl methacrylate

Figure 4.20. Transmission spectrum of PDCLC films made of branched methacrylates.

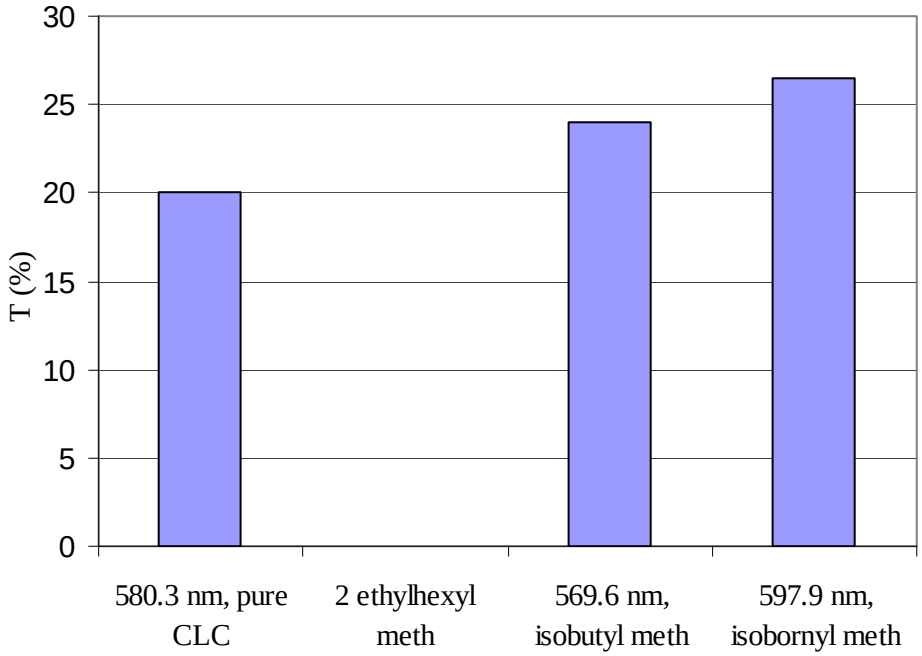

Figure 4.21. Comparison of normalized transmission intensity of PDCLC films made with branched methacrylates.

The reasons for these different results from these acrylate monomer and methacrylate monomers can be explained by applying two interfacial models that are used to explain the anchoring behavior of NLC at a polymer surface in PDLC films. One is the thermodynamic model [56 - 58] that has been used to explain the anchoring behavior of TL213 at the polymer surface in PDLC films. The other is side chain conformation model [59, 60]. In this model, if the side chain of polymer is long and linear, for example, poly(n-heptyl acrylate), the side chain will interdigitate with the aliphatic tail of NLC as shown in Figure 4.22, then the homeotropic anchoring of NLC will be formed at this polymer surface. If the side chain of polymer is branched, i.e. if there is a side group in this side chain and it is close to the polymer backbone, for example, poly(1-MHA), the side chain of this polymer will tilt due to the steric effect of

the 1-methyl side group. Therefore, interdigitation is not possible and for entropic reasons the nematic director will be planar. In this case, the planar anchoring of NLC will be formed at this polymer surface as schematically shown in Figure 4.22.

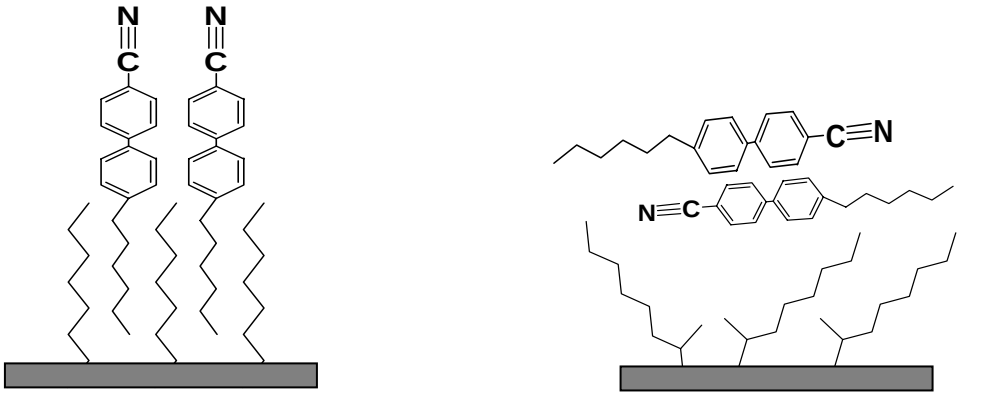

Poly (n-heptyl acrylate) Poly (1-methylheptyl acrylate)

Figure 4.22. Examples for the side chain conformation model at the polymer surfaces. Refer to [59, 60].

But the addition of CB15 in fabricating PDCLC films can affect these interactions. There are two reasons for this interruption. One is that CB15 has long aliphatic tail containing 15 carbon atoms [50], which will definitely change the interaction between side chain of polymers and aliphatic tail of NLC. The other is that there is a chiral center in the long aliphatic tail, which introduces a spiral structure to the nematic host, TL213, as shown from the small reflector in Figure 4.10. This intrinsic spiral structure of CLC will compete with the constraining from polymers that anchor NTL at their surface. What texture will be formed finally depends on the result of this competition. In the case of planar anchoring of TL213 in PDLC films, if helices are not slightly distorted and they orient randomly with respect to the polymer surface, then the focal conic texture of CLC can be formed in PDCLC films. For example, this occurs in the PDCLC film made with

n-butyl methacrylate, as also seen from the POM texture and the transmission spectrum. If, on the other hand, all helices are not distorted as a result of this competition, i.e. they remain perpendicular to the polymer surface, then the planar texture of CLC can be formed in PDCLC films, as seen in films made with n-hexyl methacrylate.

In the case of homeotropic anchoring of TL213 at a polymer surface in PDLC films, if helices are dramatically distorted, for example, they flip 90° with respect to the polymer surface, then the planar texture may be obtained. Actually for the PDCLC film made with isobornyl methacrylate, CLC does have the planar texture in some individual cells. However, if the competition results in only slight distortion of helices, which means that helices just slightly tilt with respect to the polymer surface, then the focal conic texture of CLC will be obtained in PDCLC films, like in the film made with 2-MHA. If helices are not distorted by this competition, then we should obtain the fingerprint texture. For the PDCLC films made with CLC having weight ratio of CB15 to TL213 to be 35/65, we did not observe this texture, but for the PDCLC film made with isobornyl mehtacrylate and CLC having this ratio to be 3/97, we do observe the fingerprint texture as shown in Figure 4.23. This is due to the balance between the size of individual cells and the pitch of CLC. Keeping all other UV curing conditions fixed, variation of the chiral dopant concentration results in the pitch changes from 0.36 μm (CB15/TL213 = 35/65) to 2.6 μm (CB15/Tl213 = 3/97). For the PDCLC film where CLC has bigger pitch, there is less freedom for helices to move around in the longitudinal direction, thus helices in this case are not easily distorted and the fingerprint texture of CLC for this PDCLC film is observed.

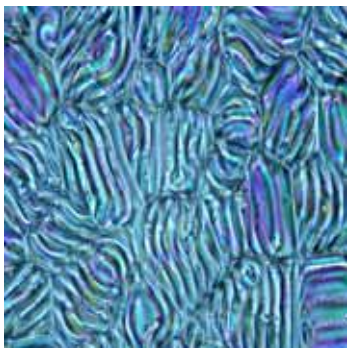

Figure 4.23. Fingerprint texture observed for the PDCLC film made with isobornyl methacrylate and CLC having weight ratio of CB15 and TL213 as 3/97.

Note: Other UV-curing conditions for above PDCLC films: curing intensity, 74 μW/cm^2; concentration of CLC, 90 wt%; spacer size, 10 μm.

4.4.2 Effect Of Dimensions Of Individual Cells In PDCLC Films

The diameter and thickness of individual cells have the different effect on the anchoring behavior of CLC at the polymer surface in PDCLC films, which can be controlled by UV-curing intensity and the spacer size, respectively.

4.4.2.1 Effect Of Diameter Of Individual Cells In PDCLC Films

The UV-curing intensity is adjusted to vary the diameter of the individual cell in PDCLC films. As shown in Table 4.14, the POM textures of CLC in these PDCLC films change from the planar texture to the focal conic texture as the cell diameter increases from 48.8 μm to 31.3 μm. However, further observation of their corresponding transmission spectra (Figure 4.24) show that CLC in these two films has the tendency to have the planar texture since there are transmission peaks in these PDCLC films. By comparison of the normalized transmission intensities of these three PDCLC films (Figure 4.25), it is found that the normalized transmission intensity increases with the diameter, which indicates that the tendency of CLC to have planar texture in these

PDCLC films increases with the diameter, i.e. the distortional degree of helices of CLC in these PDCLC films decreases with the diameter. The experimental result can be explained as followings. Since the thickness of the sample is fixed to be 10 μm and the pitch of CLC is fixed to be 0.36 μm, helices of CLC in the longitudinal direction have almost the same freedom to move around in all these PDCLC films. However, for the PDCLC film with larger individual cells, CLC molecules encapsulated by polymer matrices have more cross-sectional freedom to rotate perpendicular around their helices, i.e. helices of these CLC molecules are not easily to be distorted, then the planar texture of CLC in this PDCLC film is obtained and the focal conic texture of CLC is obtained for those PDCLC films having smaller individual cells.

Table 4.14 Effect of diameter of the individual cell

UV-curing intensity ($\mu W/cm^2$)	Diameter of individual cell (μm)	POM texture of PDCLC films
42	48.8	
74	35.0	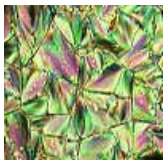
137	31.3	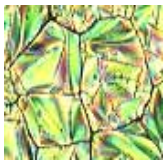

Note: other UV-curing conditions for above PDCLC films: monomer, 1-MHA; concentration of CLC, 90 wt%; pitch of CLC, 0.36 μm (CB15 / TL213 = 35 / 65, weight ratio); spacer size, 10 μm.

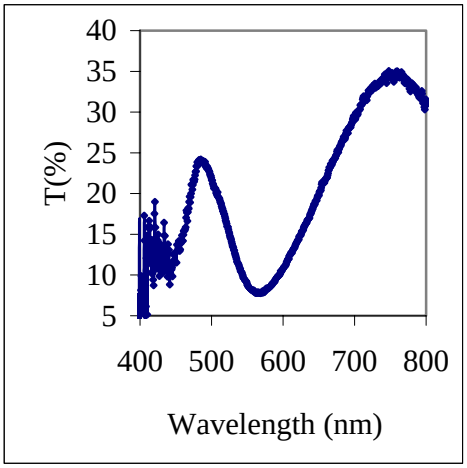

a. diameter: 48.8 μm

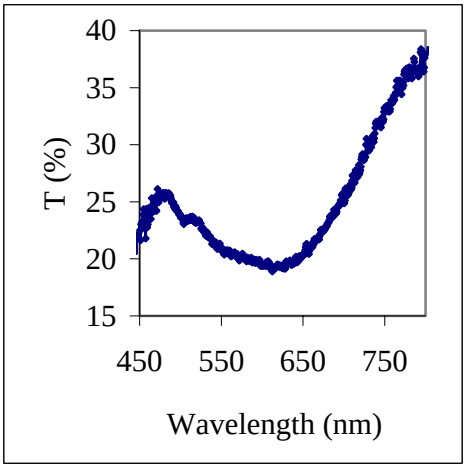

b. diameter: 35.0 μm

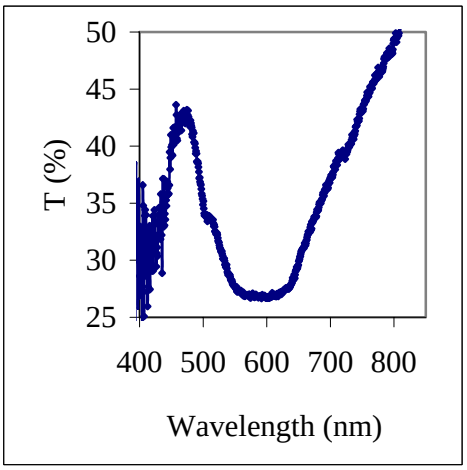

c. diameter: 31.3 μm

Figure 4.24. Transmission spectrum of PDCLC films with different diameter size of individual cells.

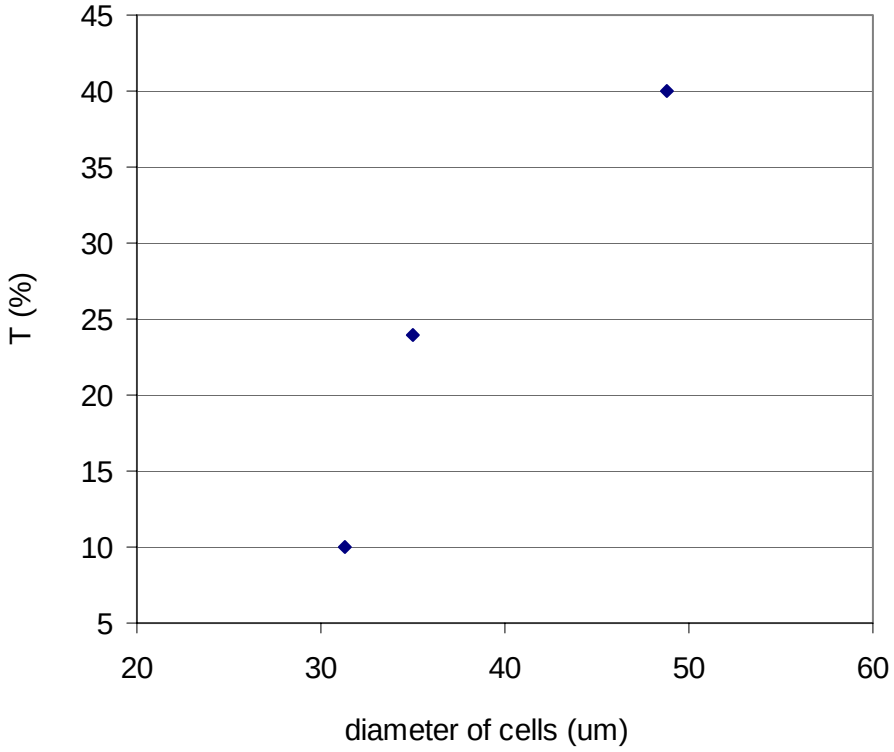

Figure 4.25. Comparison of normalized transmission intensity of PDCLC films with different diameter size of individual cells.

4.4.2.2 Effect Of The Thickness Of Individual Cells In PDCLC Films

The thickness of the individual cell is controlled by changing the spacer size. As shown in Table 4.15, the POM texture of the PDCLC film with thickness of 3 μm indicates that CLC has the planar texture in this PDCLC film. For the diameter of 5 and 10 μm, POM texture of CLC is focal conic, i.e. helices of CLC randomly orient with respect to the polymer surface in these two PDCLC films. However, further observation of their corresponding transmission spectra (Figure 4.26 b and c) show that CLC tends to have the planar texture in these two films. For the diameter of 15 μm, the POM texture and transmission spectrum indicate that the helices of CLC in this PDCLC film have random orientation. By comparison of the normalized transmission intensities of these

four PDCLC films (Figure 4.27), it is found that the normalized transmission intensity decreases with the thickness, which indicates the tendency of CLC to have the planar texture in these PDCLC films decreases with the thickness. We can explain it as follows. Since we fixed the UV curing intensity for each PDCLC film here and CLC molecules have the same size, then they have almost the same freedom to rotate around helices. But for the PDCLC film where the thickness is smaller, helices do not have much freedom to move around in the longitudinal direction. They are not easily distorted by the competition between the spiral structure of CLC and the constrain imposed by the anchoring of CLC molecules by the polymer. The planar texture of CLC in this PDCLC film is formed.

Table 4.15 Effect of thickness of the individual cell

Spacer size (μm)	Diameter of the cell (μm)	POM texture of PDCLC films
3	48.8	
5	42.5	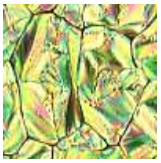
10	49.6	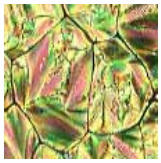
15	41.8	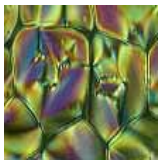

Note: Other UV-curing conditions for above PDCLC films: UV intensity, 42 μW/cm^2; monomer, 1-MHA; concentration of CLC, 90 wt%; pitch of CLC, 0.36 μm (CB15 / TL213 = 35 / 65, weight ratio).

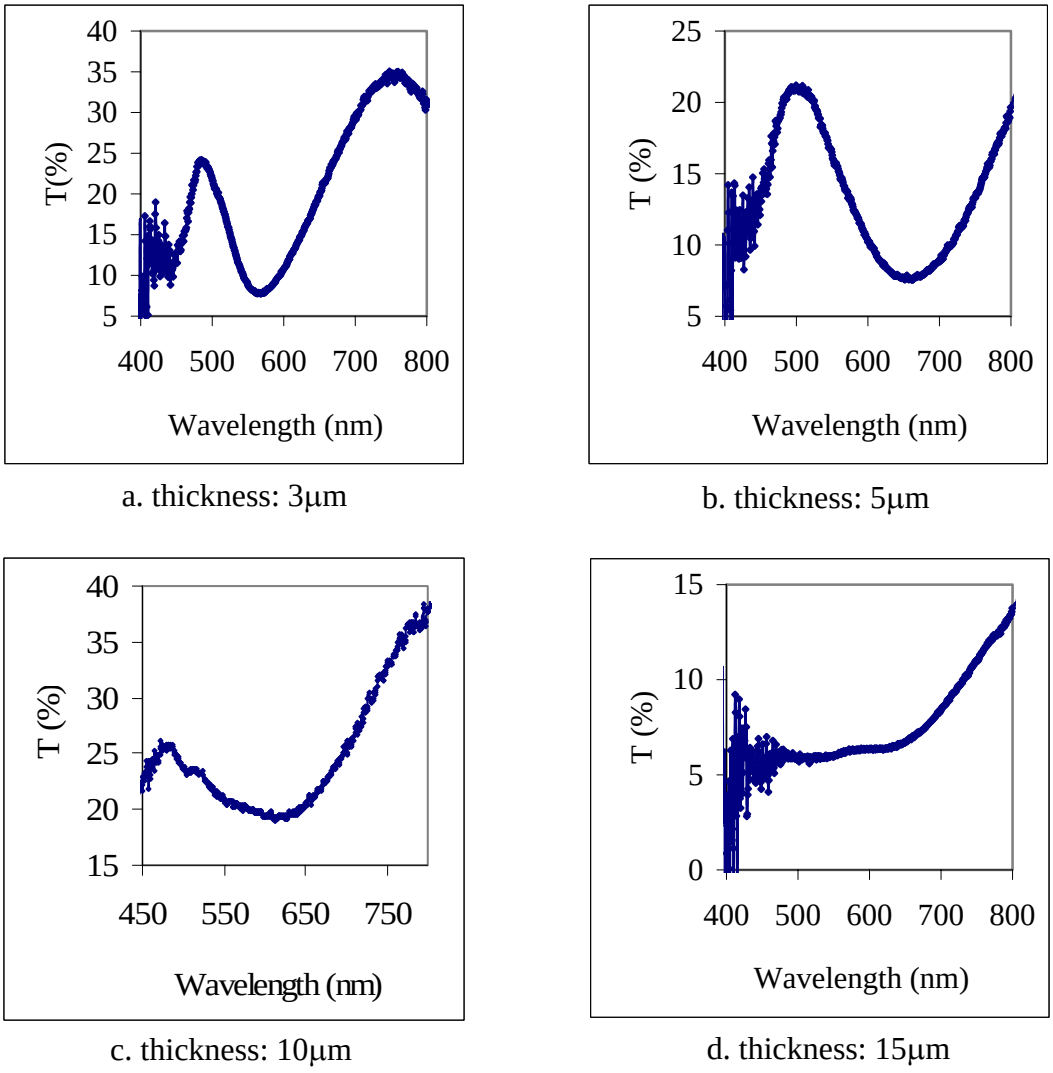

a. thickness: 3μm

b. thickness: 5μm

c. thickness: 10μm

d. thickness: 15μm

Figure 4.26. Transmission spectra of PDCLC films with different thickness of individual cells.

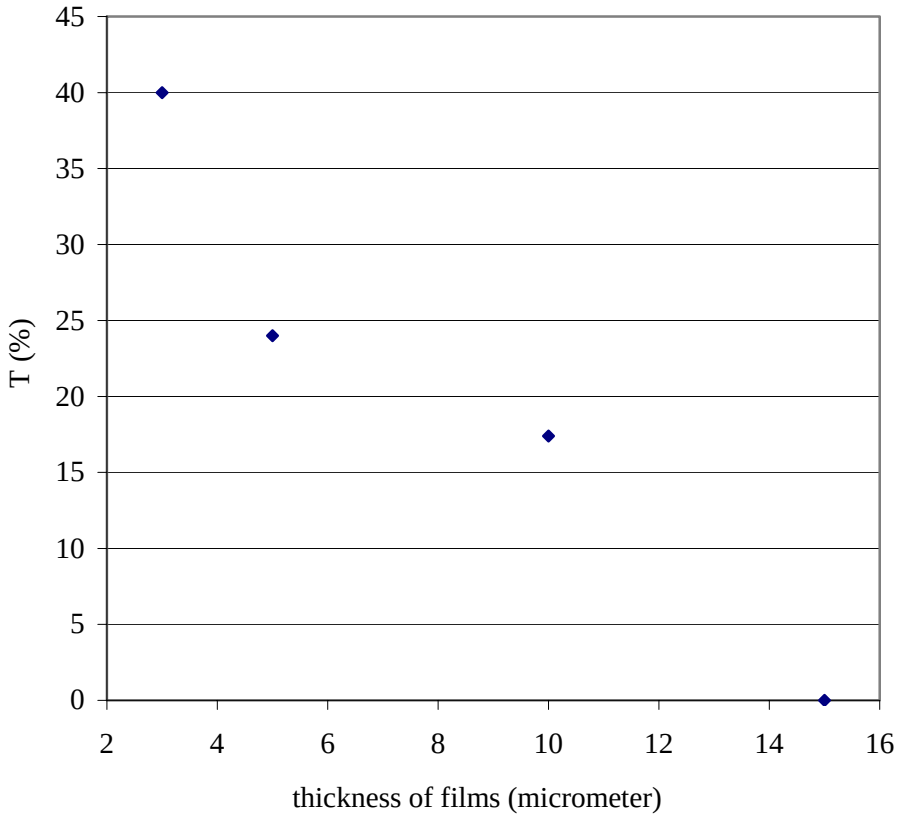

Figure 4.27. Comparison of normalized transmission intensity of PDCLC films with different thickness of individual cells.

4.4.3 Effect Of Temperature

One PDCLC sample made with n-hexyl methacrylate is selected since CLC has the perfect planar texture in this PDCLC films. As the temperature is increased from 24.0 °C, the planar texture of CLC begins to change to the focal conic texture around 69.1 °C and this transition is completed in the range of 2 °C (Figure 4.28). The system becomes isotropic phase at 84.1 °C, and the polymer wall is clearly observed without polarizers in POM as shown in Figure 4.28. Then the PDCLC film is cooled from the isotropic state at 0.5 °C/min and at each observation temperature the sample is annealed for about 10 min. The POM textures in the slow cooling process show that the focal conic texture is

maintained even at room temperature, without returning to the original planar texture. This is due to many defects existing in the focal conic texture, which cannot move away spontaneously to recover to the planar texture where there is no defect.

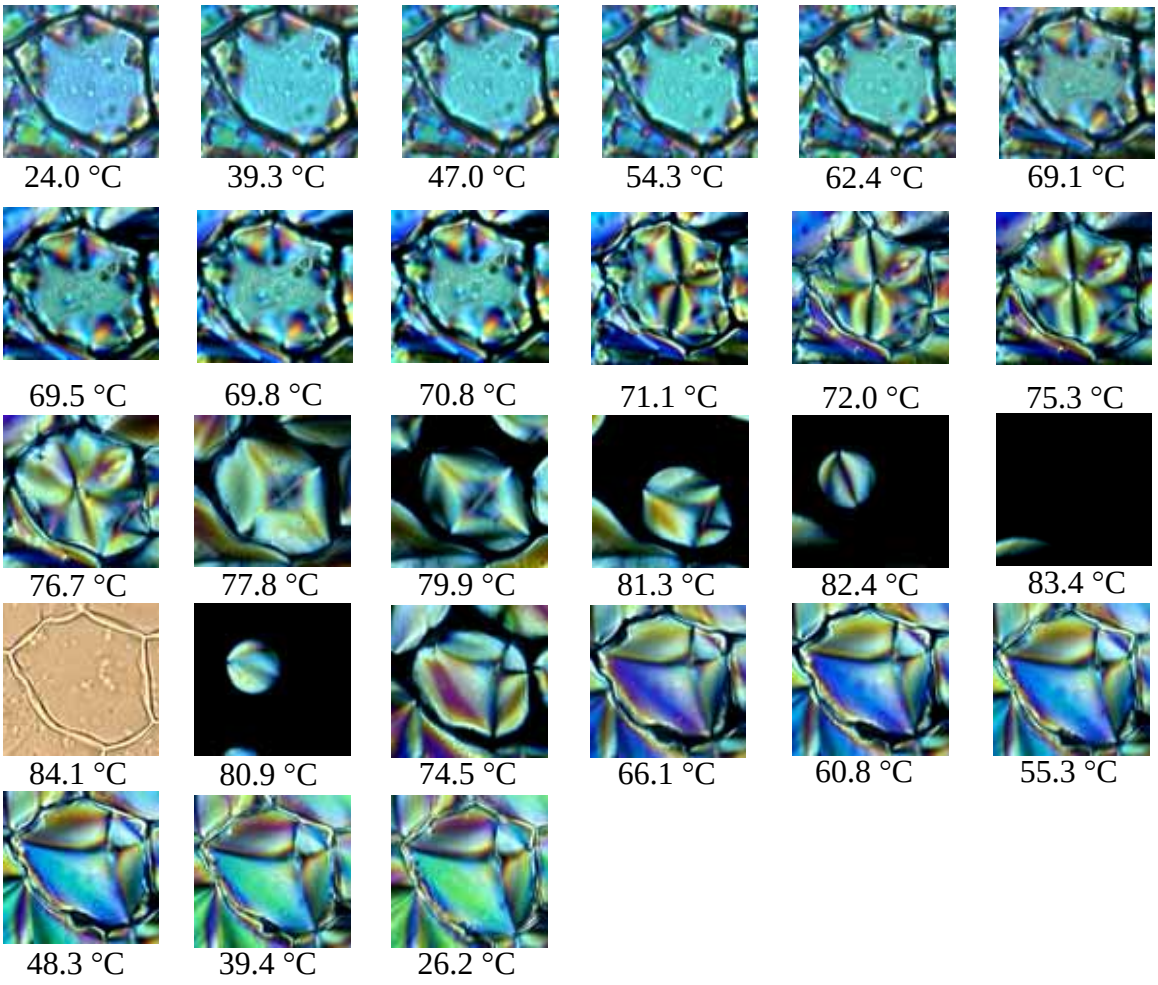

Figure 4.28. The texture variation of a PDCLC film with temperature.

Note: other UV-curing conditions for above PDCLC films: curing intensity, 74 μW/cm^2; concentration of CLC, 90 wt%; pitch of CLC, 0.36 μm (CB15 / TL213 = 35 / 65, weight ratio); spacer size, 10 μm. Images are taken with POM under crossed polarizers, except at 84.1 °C (without polarizers).

In the heating process, the pitch in PDCLC is found to increase with temperature as pure CLC does (Figure 4.29). The reason is the same, i.e. CLC changes to the nematic

phase with temperature. But the increasing rate of pitch for this PDCLC film is a little bit slower than that of pure CLC. Meanwhile, the normalized reflectance of the sample decreases with temperature, which also indicates that helices become random as temperature increases (Figure 4.30)

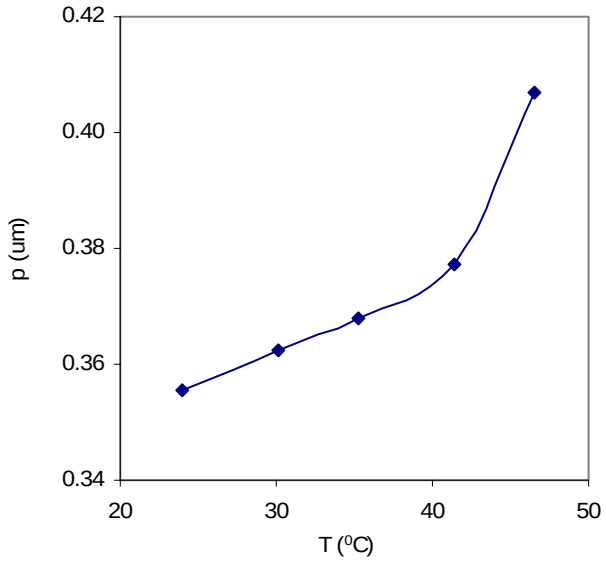

Figure 4.29. Pitch of CLC in the PDCLC film varies with temperature.

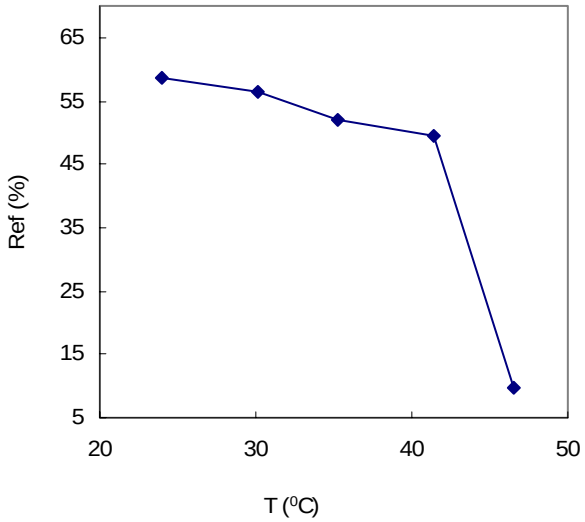

Figure 4.30. Reflectance of the PDCLC film varies with temperature.

4.4.4 Effect Of Surface Treatment

For the given choice of parameters, PDCLC films made from 1-MHA with coated and uncoated polyimide on the substrates all show the planar texture (Figure 4.31), but for different reasons. For the films coated with polyimide, the parallel alignment of the director of CLC was induced by the alignment of the rubbed polyimide film on the substrates. For the uncoated films, it resulted from the anchoring behavior of CLC at the polymer interface. The normalized transmission intensity for the PDCLC films made with these two methods is the same (Figure 4.32). But the process of prealignment of substrates is a complicated and expensive. With our simple and quick method, the PDCLC film can be made with the same reflectance as that of the prealignment method (Table 4.17).

Table 4.16 Normalized transmission intensity of PDCLC films with and without polyimide coating.

Polyimide	Average size of cells (μm)	Maximum wavelength at selective reflection (nm)	Normalized transmission intensity (%)
Coated and rubbed	20.2	615.5	30
uncoated	48.8	573.3	30

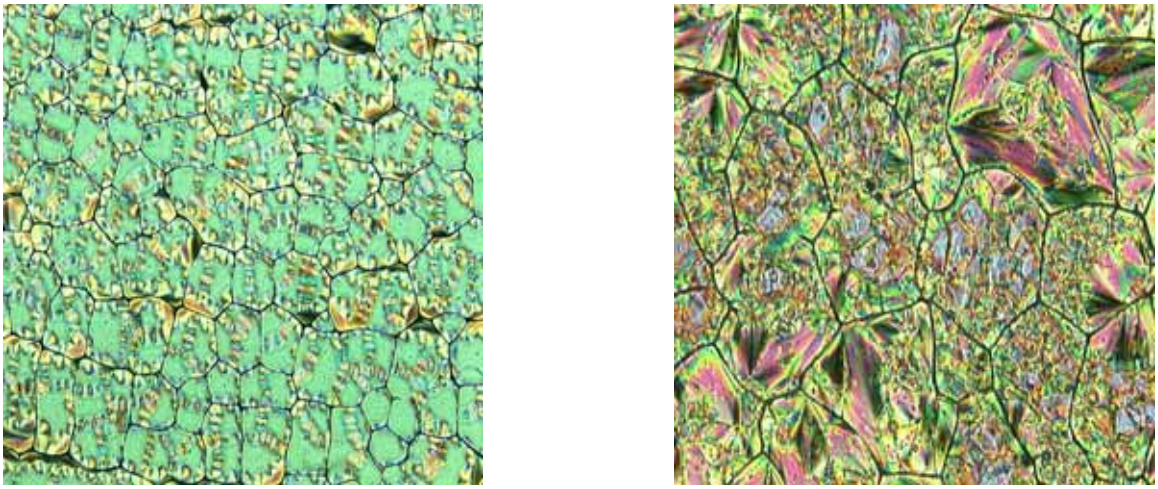

a. with polyimide coating b. without polyimide coating

Figure 4.31. The POM texture of PDCLC films with and without polyimide coating.
Notes: Other parameters were set to be as follows: monomer, 1-MHA; concentration of CLC, 90%; weight ratio of CB15 and TL213, 35 / 65; UV curing intensity, 42 μW / cm^2; spacer size, 3 μm.

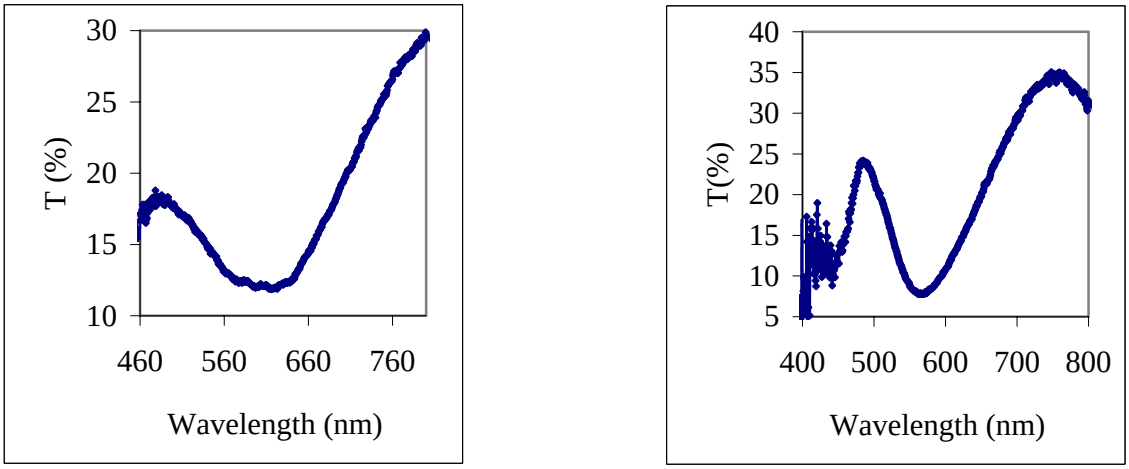

a. with polyimide coating b. without polyimide coating

Figure 4.32. The transmission spectra of PDCLC films with and without polyimide coating.
Notes: Other parameters were set to be as follows: monomer, 1-MHA; concentration of CLC, 90%; weight ratio of CB15 and TL213, 35 / 65; UV curing intensity, 42 μW / cm^2; spacer size, 3 μm.

CHAPTER 5

CONCLUSIONS

In this research work, the properties of CLC made from the mixture of TL213 and CB15 were characterized and the anchoring behavior of LC at a polymer surface in PDLC and PDCLC films was investigated. It is found that:

1. For CLC made with the mixture of TL213 and CB15, it is found that the reciprocal of pitch is linearly related to the reciprocal of concentration of CB15, and the value of its helical twisting power is 0.056 according to the equation, $1/p = (HTP)Xc$, suggested by De Gennes [7]. This value shows that CB15 is right-handed and has weak twisting power. The pitch of the CLC is the increasing function of temperature.

2. The anchoring behavior of nematic liquid crystal, TL213, at the polymer surface in PDLC films made with n-octyl methacrylate is neither typical homeotropic nor homogeneous. The director of TL213 has tilt angle with the polymer surface. This tilt angle may vary with temperature, which calls for further verification.

3. The best UV curing conditions for making PDCLC films with large enough cells for microscopic observation are found to be the concentration of CLC in the homogeneous solution, 90wt%; UV curing intensity, 42 and 74 $\mu W/cm^2$; and the spacer size, 3, 5, and 10 μm.

4. The anchoring behavior of CLC at the polymer surface in PDCLC films is affected by the following factors: the chemical structure of monomers, the dimensions of individual cells in PDCLC films, temperature, and surface treatment.

- For acrylate monomers, short linear tails and 1-position substituent tails tend to have the planar texture of CLC at polymer surface in PDCLC films. The bulkier the substituent, the larger tendency for CLC in PDCLC films to have the planar texture.
- For methacrylate monomers, long linear tails and short-branched tails tend to have the planar texture of CLC at polymer surface. Especially methacrylate with linear tail containing six carbon atoms gives the perfect planar texture of CLC in this PDCLC film. Its normalized transmission intensity is a little bit larger than that of pure CLC.
- The tendency to have the planar texture of CLC in PDCLC films increases with diameter of cells, which is controlled by UV curing intensity, and decreases with the thickness of cells, which is controlled by the spacer size.
- The anchoring behavior of CLC changes from the planar texture to the focal conic texture when temperature increases and on cooling this focal conic texture can not be recovered to the original planar texture. This is due to many defects existing in the focal conic texture, which can not move away spontaneously on time scale of experiments (cooling rate is 0.5 °C/min and holding time at each temperature is 10 min).

- The normalized transmission intensity of the PDCLC film made with our method is the same as that of the PDCLC film with the prealignment method. But the prealinging is complicated, expensive, not reproducible, and with low yield.

In our experimental result, the PDCLC film which reflects brilliant color can be fabricated without the prealignment of substrates and without application of external fields. This will greatly save time and cost to make the color display with this material. The problem that needs to be solved is the area which reflects brilliant color is only around 4 μm^2. If we want to apply this material to make color display, the size of active area must be increased. This can be accomplished only if we can make bigger cells in this photo polymerization induced phase separation.

REFERENCES

1. Collings, P. J., *Liquid Crystals, Nature's Delicate Phase of Matter*, 2nd edition, Princeton Universiy Press 1990

2. Kato, K., Tanaka, K., Tsuru, S. And Sakai, S., Characteristics of Right- and Left-Handed Polymer-Dispersed Cholesteric Liquid Crystals, *Jpn. J. Appl. Phys*. 1994 (33), 4946-4949

3. The web site: www.kth.se/fakulterter/TFY/kmf/lcd/lcd~/.html

4. Nwabunma, D. and Kyu, T., Phase Behavior, Photo polymerization, and Morphology Development in Mixtures of Eutectic Nematic Liquid Crystal and Photocurable Monomer, *Polymer* 2001 (42), 801-806

5. Collings, P. J. and Patel, J. S., *Handbook of liquid Crystal Research*, New York 1997

6. Kitzerow, H.-S. And Bahr C., *Chirality in Liquid Crystals*, Springer 1996, 160

7. De Gennes, P. G. and Prost, J., *The Physics of Liquid Crystals*, 2nd edition, Oxford, Clarendon Press 1973, 282

8 Bilnov, L., *Electro- and Magneto-Optical Properties of Liquid Crystals*, Chichester, John Wiley, 213

9. Drzaic, P. S., *Liquid Crystal Dispersions*, World Scientific, Singapore 1995

10. Frank, F. C., Liquid Crystals – On the Theory of Liquid Crystals, *Frans. Faraday Soc*. 1958 (25), 19-28

11. Chandrasekhar, S., *Liquid Crystals*, Cambridge University Press, 1977, 61

12. Candau, S., Roy, P. L. and Debeauvais, F., Magnetic-Field Effects in Nematic and Cholesteric Droplets Suspended in an Isotropic Liquid, *Mol. Cryst. Liq. Cryst*. 1973 (23), 283-297

13. Robinson, C. and Ward, J. C., Liquid-Crystalline Structures in Polypeptide, *Nature*, Lond. 1957 (180), 1183

14. Kurik, M. V. and Lavrentovich O. D., Negative-Positive Monopole Transitions in Cholesteric Liquid-Crystals, *Sov. Phys. JETP Lett*. 1982 (35), 445-447

15. Zhou, J., Collard, D. M., Park, J. O. and Srinivasarao, M., Control of the Anchoring Behavior of Polymer-Dispersed Liquid Crystals: Effect of Branching in the Side Chains of Polyacrylates, *J. Am. Chem. Soc*. 2002 (24), 9980-9981

16. Zhou, J., Study of anchoring behavior of nematic fluids at the interfaces of polymer dispersed liquid crystals, *Ph. D. thesis*, Georgia Tech, 2003

17. James, F., Polymer Encapsulated Nematic Liquid Crystals for Display and Light Control Applications, *SID Dig. Tech. Pap*. 1985 (16), 68

18. Doane, J. W., Vaz, N. and Wu, B. G., Field Controlled Light Scattering from Nematic Microdroplets, *Appl. Phys. Lett*. 1986 (48), 269-271

19. Doane, J. W., Golemme, A., West, J., Whitehead, J. and Wu, B. G., Polymer Dispersed Liquid-Crystals for Display Application, *Mol. Cryst. Liq. Cryst*. 1988 (165), 511-532

20. Noh, C. H., Jung, J. Y., Kim, D. S. and Choi, K. S., A Study on the Morphology and Electrooptic Properties of Liquid Crystal-Polymer Composite Films, *Mol. Cryst. Liq. Cryst. Sci. Tec. A* 1993 (237), 299-309

21. Amundson, K., Blaaderen, A. V. and Wiltzius, P., Morphology and Electro-Optic Properties of Polymer-Dispersed Liquid-Crystal Films, *Phys. Rev. E*, 1997 (55), 1646-1654

22. Margerum, J. D., Lackner, A. M., Ramos, E., Lim, K. C. and Smith, W. H., Effects of Off-State Alignment in Polymer Dispersed Liquid-Crystals, *Liq. Cryst*. 1989 (5), 1477-1478

23. Takatsu, H., Takeuchi, K. and Umezu, Y., A Novel Liquid-Crystal Display – a Randomly-Oriented Nematic Liquid-Crystal Display (RON-LCD), *Mol. Cryst. Liq. Cryst*. 1993 (225), 81-88

24. Lackner, A. M, Margerum, J. D., Ramos, E. and Lim, K. C. Stability Studies on Polymer Dispersed Liquid Crystal Films, *Proc. SPIE*., 1989 (1080), 53-61

25. Doane, J. W., Golemme, A. And West, J. L., Electrooptics of Polymer Dispersed Liquid-Crystals, *Ferroelectrics*, 1989 (91), 277

26. Yang, D. K., Chien, L. C. and Doane, J. W., Cholesteric Liquid Crystal/Polymer Dispersion for Haze-Free Light Shutters, *Appl. Phys. Lett*. 1992 (60), 3102-3104

27. Ma, R. Q. and Yang, D. K., Polymer-Stabilized Bistable Black-White Choleteric Reflective Display, *SID 97 Digest* 1997, 101-104

28. Held, G. A., Kosbar, L. L. and Miller, R. D., Confocal Microscopy Study of Texture Transitions in a Polymer Stabilized Cholesteric Liquid Crystals, *Phys. Rev. Lett.* 1997 (79), 3443-3446

29. Dierking, I., Kosbar, L. L. and Held, G. A., Two-Stage Switching Behavior of Polymer Stabilized Cholesteric Textures, *J. Appl. Phys.* 1997 (81), 3007-3014

30. Dierking, I., Kosbar, L. L. and Lowe, A. C., Polymer Network Structure and Electro-Optic Performance of Polymer Stabilized Cholesteric Textures: I. The Influence of Curing Temperature, *Liq. Cryst.* 1998 (24), 387-395

31. Dierking, I., Kosbar, L. L. and Lowe, A. C., Polymer Network Structure and Electro-Optic Performance of Polymer Stabilized Cholesteric Textures: II. The Effect of UV Curing Conditions, *Liq. Cryst.* 1998 (24), 397-406

32. Rajaram, C. V. and Hudson, S. D., Effect of Polymerization Temperature on the Morphology and Electrooptic Properties of Polymer-Stabilized Liquid Crystals, *Chem. Mater.* 1996 (8), 2451-2460

33. Okada, M., Hatano, T. and Hashimoto, K., Reflective Multicolor Display Using Cholesteric Liquid Crystals, *SID 97 Digest* 1997, 1019-1022

34. Chien, L. C., Muller, U., Nabor, M. F. and Doane, J. W., Multicolor Reflective Cholesteric Displays, *SID 95 Digest* 1995, 169-171

35. Pfeiffer, M., Yang, D. K. and Doane, J. W., A High-Information-Content Reflective Cholesteric Display, SID 95 Disgest 1995, 706-709

36. Yang, D. K. And Doane, J. W., Cholesteric Liquid Crystal/Polymer-Gel Dispersions: Reflective Display Applications, *SID 92 Digest* 1992, 759-761

37. Crooker, P. P. and Yang, D. K., Polymer-Dispersed Chiral Liquid Crystal Color Display, *Appl. Phys. Lett.* 1990 (57), 2529-2531

38. Kitzerow, H. S., Crooker, P. P. and Heppke, G., Chromaticity of Polymer-Dispersed Cholesteric Liquid Crystals, *Liq. Cryst.* 1992 (12), 49-58

39. Kitzerow, H. S. and Crooker, P. P., Behavior of Polymer Dispersed Cholesteric Droplets with Negative Dielectric Anisotropy in Electric-Fields, *Liq. Cryst.* 1992 (11), 561-568

40. Kitzerow, H. S. and Crooker, P. P., Polymer-Dispersed Cholesteric Liquid Crystals – Challenge for Research and Application, *Ferroelectrics* 1991 (122), 1-4

41. Magnaldo, A., Nourry, J., and Sixou, P., Annealing and Memory Effects in Polymer-Dispersed Chiral Liquid Crystals, *J. Appl. Phys*. 1996 (80), 2586-2588

42. Magnaldo, A., Nourry, J., and Sixou, P., High Memory Effects in Polymer Dispersed Chiral Liquid Crystals with Negative Dielectric Anisotropy, *J. Appl. Phys*. 1996 (79), 8193-8196

43. Kitzerow, H. S. and Crooker, P. P., UV-Cured Cholesteric Polymer-Dispersed Liquid Crystal Display, *J. Phys. II France* 1993 (3), 719-726

44. Kitzerow, H. S., Rand, J. and Crooker, P. P., Dynamics of Polymer-Dispersed Cholesteric Liquid Crystals, *J. Phys. II France* 1992 (2), 227-234

45. Kitzerow, H. S. and Crooker, P. P., Electro-Field Effects on the Droplet Structure in Polymer Dispersed Cholesteric Liquid Crystals, *Liq. Cryst*. 1993 (13), 31-43

46. Kitzerow, H. S. and Crooker, P. P., Behavior of Polymer Dispersed Cholesteric Droplets with Negative Dielectric Anisotropy in Electric-Fields, *Liq. Cryst*. 1992 (11), 561-568

47. Kato, K., Tanaka, K., Tsuru, S. and Sakai, S., Multipage Display Using Stacked Polymer-Dispersed Liquid Crystal Films, *Jpn. J. Appl. Phys*. 1993 (32), 4594-4599

48. Kato, K., Tanaka, K., Tsuru, S. And Sakai, S., Color Image Formation Using Polymer-Dispersed Cholesteric Liquid Crystal, *Jpn. J. Appl. Phys*. 1993 (32), 4600-4604

49. Kato, K., Tanaka, K., Tsuru, S. And Sakai, S., Reflective Color Display Using Polymer-Dispersed Cholesteric Liquid Crystal, *Jpn. J. Appl. Phys*. 1994 (33), 2635-2640

50. Private correspondence, Granzow, J., EM Chemicals

51. The web site: www.microscopyu.com/articles/polarized/polarizedintro.html

52. The web site: www.cs.ubc.ca/spider/ladic/images/optics.gif

53. The web stie: www.microscopyu.com/articles/polarized/michel-levy.html

54. Gay, P., *An Introduction to Crystal Optics*, Jarrold & Sons Ltd 1967, 212

55. Porte, G., Tilted Alignment of MBBA Induced by Short-chain Surfactants, *J. Phys. (France)* 1976 (37), 1245 –1252

56. Roussel, F., Canlet, C., and Fung, B. M., Morphology and Orientational Order of Nematic Liquid Crystal Droplets Confined in a Polymer Matrix, *Phys. Rev. E*. 2002 (65), 021701

57. Sharlow, M. F., and Gelbart, W. M. On the Parallel Perpendicular Transition for a Nematic Phase at a Wall, *Liq. Cryst.* 1992 (11), 25 – 30

58. Aliev, F. M. And Zgonnik, V. N., Thermo-Optics and Thermal Stability of Poly(alkyl methacrylates) in Porous Matrices, *Eur. Polym. J.* 1991 (27), 969-973

59. Walba D. M., Korblova, E., Shao, R. and Maclennan, J. E., A Ferroelectric Liquid Crystal Conglomerate Composed of Racemic Molecules, *Science* 2000 (288), 2181-2184

60. Collard, D. M. and Lillya, C. P., Structure-Property Relationships for the Thermal Phase Behavior of Discotic Liquid Crystals: the Effect of Branching and Unsaturation in the Side Chains of Disklike Molecules, *J. Am. Chem. Soc.* 1991 (113), 8577-8583